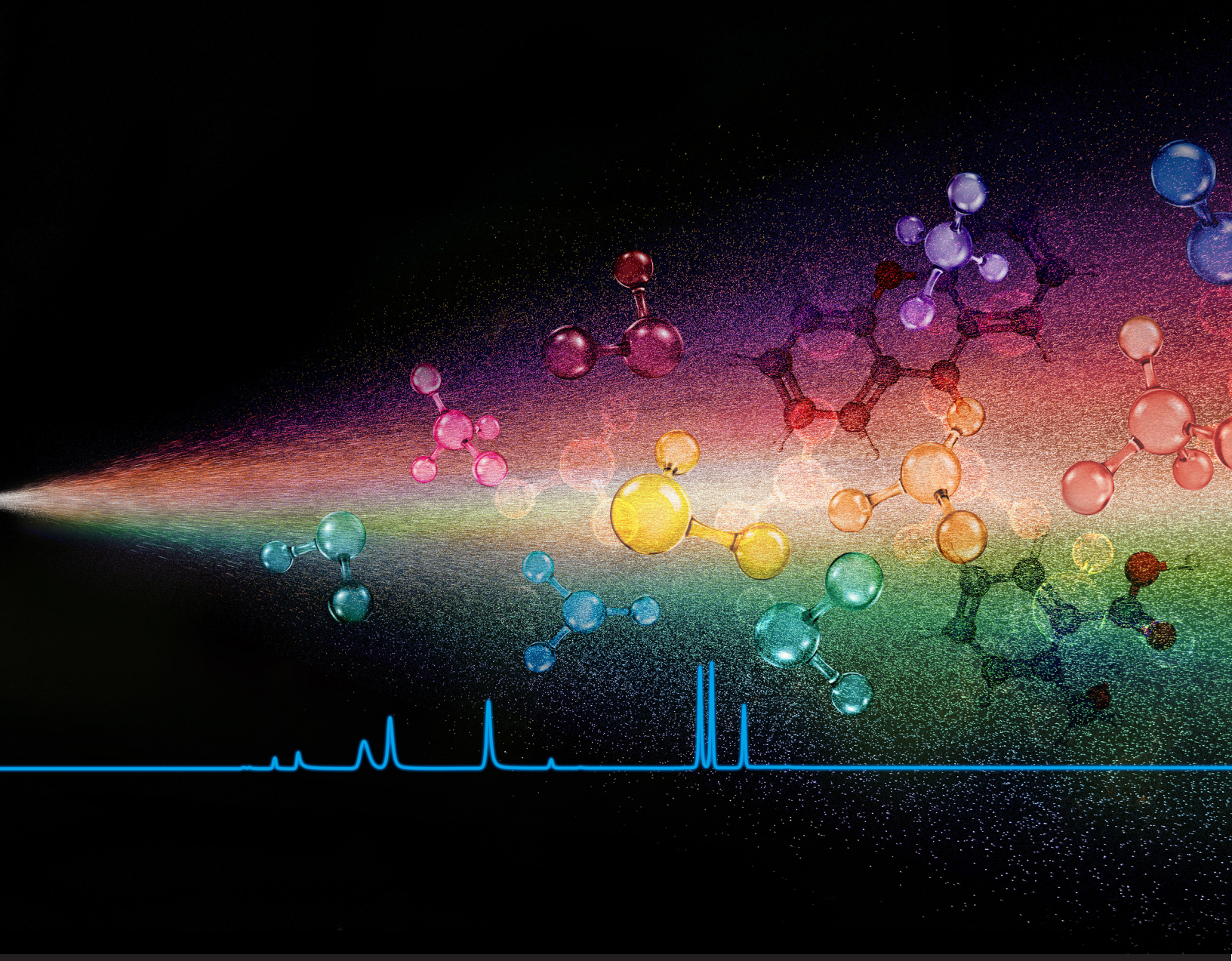

How Charged Aerosol Detection is Revolutionizing HPLC Analysis

ARTICLE COLLECTION

WILEY Analytical Science

Sponsored by:

ThermoFisher SCIENTIFIC

ThermoFisher SCIENTIFIC

Liquid chromatography

Take your science a step beyond

With Thermo Scientific™ Vanquish™ HPLC and UHPLC systems

- Enhanced, no-compromise performance keeps you ahead of future demands
- Improved system productivity and ease-of-use accelerates your vital work
- Platform versatility opens up new analytical opportunities
- Higher robustness and quality-of-results help maintain compliance
- Trade-in programs, CDS compatibility, training, and support make refreshing your outdated technology easier

Learn more at **thermofisher.com/liquidchromatography**

thermo scientific

Contents

FURTHER READING AND RESOURCES
(click below to learn more)

Charged Aerosol Detection Publications

Introduction

Traditional detection methods like UV-Vis and mass spectrometry (MS) have limited effectiveness in the analysis of complex compounds, such as compounds that lack a chromophore or cannot ionize. The Charged Aerosol Detector (CAD) response is independent of compound structure and overcomes this challenge by providing highly-sensitive, reliable detection for even the most complex separations.

The versatility of the CAD lies in the mechanism of detection. In brief, compounds that elute from the column are nebulized into droplets and subsequently dried into particles. In a mixing chamber, these particles collide with a stream of ionized nitrogen gas, which charges the particles. An electrometer measures the total particle charge and produces a signal that is directly proportional to the amount of analyte present. Bigger particles have a higher charge and thus generate a higher signal.

The CAD can detect all non-volatile and many semi-volatile compounds. With near-universal detection and standard-free quantitation, the CAD allows scientists to quantitatively measure compounds incompatible with UV-Vis or MS and determine the concentration of compounds when certified standards aren‘t available. This property makes the CAD an invaluable tool for scientists in the pharmaceutical and natural medicine industries.

As you will learn from the articles in this collection, the CAD enables scientists to extract valuable information about sample composition, which is not always possible with traditional detection methods.

The collection begins with a study by Kinsey et al. (2022) on a reversed-phase chromatographic method with CAD to analyze the identity and content of individual lipid components and associated impurities and degradants in lipid nanoparticles (LNPs). The method was optimized for lipids of interest and validated for linearity, accuracy, precision, and specificity to support process and formulation development for new drugs and vaccines.

Socia et al. (2020) describe the development and performance of a simple analytical method for accurately quantifying linear polyethylenimines, an excipient with many pharmaceutical applications, including gene therapy. The method, which uses UHPLC and either the CAD or a UV-Vis detector, is applied to both starting solution and formulated oligonucleotide/polyethylenimine polyplexes, with sample preparation by trifluoroacetic acid necessary for the latter. The method supports formulation development and monitoring the synthesis and purification of linear polyethylenimines.

Next, Zheng et al. (2022) report a study about the chemical components of *Crataegus pinnatifida* Bge. var *major* N.E.Br (hawthorn leaves) and the effects of harvest season on the quality of the leaves. Using UHPLC and quadrupole time-of-flight mass spectrometry, principal component analysis, and HPLC-CAD, they determined the chemical compositions of hawthorn leaves are significantly affected by harvest season, with the highest content of five key components present in autumn. This research emphasizes the importance of harvest time on the quality of medicinal plants and reveals autumn is the best time to harvest hawthorn leaves.

Finally, Granica (2015) discusses the authentication and standardization of *Polygonum aviculare L.* or common knotgrass. They used UHPLC-ESI(+)-MS and UHPLC-CAD methods to develop a procedure for the proper authentication and standardization of the herb. Twenty-five major constituents were detected, three of which were newly identified. Flavanol glucuronides were confirmed as major compounds, and the total flavonoid content varied among the nine samples. The developed procedure is useful for the routine standardization of common knotgrass, and it suggests that the pharmacopoeial approach to the authentication and standardization of the herb should be revised.

Through this article collection, we hope to educate you on the benefits of the CAD. For more information, we encourage you to visit Thermo Fisher Scientific to explore more all the analytical available to enhance your research.

Róisín Murtagh
Editor at Wiley Analytical Science

References

Kinsey, C., Lu, T., Deiss, A., Vuolo, K., Klein, L., Rustandi, R.R. and Loughney, J.W. (2022), Determination of lipid content and stability in lipid nanoparticles using ultra high-performance liquid chromatography in combination with a Corona Charged Aerosol Detector. *ELECTROPHORESIS*, 43: 1091-1100. https://doi.org/10.1002/elps.202100244

Socia, A, Liu, Y, Zhao, Y, Abend, A, Wuelfing, WP. Development of an ultra-high-performance liquid chromatography-charged aerosol detection/UV method for the quantitation of linear polyethylenimines in oligonucleotide polyplexes. *J Sep Sci*. 2020; 43: 3876– 3884. https://doi.org/10.1002/jssc.202000414

Zheng, W, Zhou, M, Chai, R, et al. Quality analysis of hawthorn leaves (the leaves of *Crataegus pinnatifida* Bge. var *major* N.E.Br) in different harvest time. *Phytochemical Analysis*. 2022; 33(7): 1147- 1155. doi:10.1002/pca.3166

Granica, S. (2015) Quantitative and qualitative investigations of pharmacopoeial plant material polygoni avicularis herba by UHPLC-CAD and UHPLC-ESI-MS methods. *Phytochem. Anal.*, 26: 374– 382. doi: 10.1002/pca.2572.

Electrophoresis 2022, *43*, 1091–1100

Caleb Kinsey
Tian Lu
Alyssa Deiss
Kim Vuolo
Lee Klein
Richard R. Rustandi
John W. Loughney

Vaccine Analytical Research & Development, Merck & Co. Inc., West Point, Pennsylvania, USA

Received August 11, 2021
Revised October 31, 2021
Accepted November 1, 2021

Research Article

Determination of lipid content and stability in lipid nanoparticles using ultra high-performance liquid chromatography in combination with a Corona Charged Aerosol Detector

For many years, lipid nanoparticles (LNPs) have been used as delivery vehicles for various payloads (especially various oligonucleotides and mRNA), finding numerous applications in drug and vaccine development. LNP stability and bilayer fluidity are determined by the identities and the amounts of the various lipids employed in the formulation and LNP efficacy is determined in large part by the lipid composition which usually contains a cationic lipid, a PEG-lipid conjugate, cholesterol, and a zwitterionic helper phospholipid. Analytical methods developed for LNP characterization must be able to determine not only the identity and content of each individual lipid component (i.e., the parent lipids), but also the associated impurities and degradants. In this work, we describe an efficient and sensitive reversed-phase chromatographic method with charged aerosol detection (CAD) suitable for this purpose. Sample preparation diluent and mobile phase pH conditions are critical and have been optimized for the lipids of interest. This method was validated for its linearity, accuracy, precision, and specificity for lipid analysis to support process and formulation development for new drugs and vaccines.

Keywords:
Cationic lipid / Charged aerosol detection (CAD) / Lipid degradation / Lipid nanoparticles (LNP) / Reverse-phase chromatography
DOI 10.1002/elps.202100244

1 Introduction

Lipid nanoparticles (LNPs) have been used for a variety of applications throughout the years such as therapeutics [1], delivery system [2], vaccines [3], and adjuvants [3]. Most recently, mRNA and LNP technology is being evaluated and approved by the Food and Drug Association (FDA) as a delivery vehicle for two of the leading vaccine candidates for SARS-CoV-2 global pandemic [4]. In the past, this technology was utilized for RSV vaccine candidates such as V171 (mRNA-1777) [5] and preclinical vaccine development for VZV (mRNA-1278) [6]. For any of these applications, the LNP formulation typically consists of multiple lipids.

In this paper, we consider LNPs for mRNA delivery formulated with four types of lipids: a cationic lipid with an amine functional group that interacts with mRNA via ionic interactions (Cationic Lipid 1 or Cationic Lipid 2), a PEG (Polyethylene glycol)-lipid conjugate (PEG-DMG (1,2-Dimyristoyl-rac-glycero-3-methylpolyoxyethylene) or PEG Lipid 2), cholesterol, and a zwitterionic helper phospholipid (1,2-Distearoyl-sn-glycero-3-phosphocholine (DSPC)). Quantitation of the individual lipids is required to support process and formulation development and are key quality attributes for manufacture. Chemical stability of each lipid is also important for clinical and safety studies and quality assurance. Lipid chemical degradation could lead to LNP aggregation and degradation during storage [7, 8]. Therefore, a robust, stability-indicating analytical tool was required to support clinical development and the following commercialization.

Previously, gas chromatography coupled with flame ionization detection (GC/FID) [9], LC/MS [10], high-performance liquid chromatography (HPLC), and ultra-high-performance liquid chromatography (UHPLC) coupled with an evaporative light scattering detector (ELSD) [11, 12] have been utilized for the analysis of lipids. However, GC–FID is rather laborious involving derivatization and is not able to analyze high molecular weight components. LC–MS is expensive and difficult for high sample throughput, and is better suited for investigational purposes instead of routine

Correspondence: Dr. Tian Lu, Vaccine Analytical Research & Development, Merck & Co. Inc., West Point, PA 19486, USA.
E-mail: tian.lu@merck.com

Abbreviations: **CAD**, charged aerosol detection; **DSPC**, 1,2-Distearoyl-sn-glycero-3-phosphocholine; **LNP**, lipid nanoparticles

Color online: See article online to view Figs. 2–4 in color.

testing. Finally, ELSD does not provide sufficient sensitivity for impurity detection.

Charged aerosol detection has become increasingly popular in the pharmaceutical industry due to its ability to detect analytes lacking chromophores that have low vapor pressure [13]. Previously at Merck & Co., Inc., Kenilworth, NJ, USA, a UHPLC coupled with charged aerosol detector (CAD) method was developed and used for lipid analysis for small interfering RNA (siRNA) LNP studies [14]. The CAD's high sensitivity makes it an ideal choice over the ELSD. Charged aerosol detection has been found to be up to six times more sensitive than the ELSD making integration and identification of low-level impurities better achievable [15, 16]. By utilizing reversed phase liquid chromatography coupled with a CAD, this method could even be modified for mass spectrometry for investigational impurity identification [17]. Finally, the CAD's ease of use and low maintenance is beneficial for transfer to QC labs.

For the aforementioned reasons, UHPLC combined with a CAD was chosen and evaluated to support various mRNA-LNP vaccine programs. In this article, we describe the development of a robust and efficient UHPLC-CAD method using commercially available materials and instrumentation is described for lipid analysis of mRNA loaded lipid nanoparticles used in vaccine candidates. Though three of the lipids mentioned in this article are proprietary and cannot be disclosed, this methodology is valuable to highlight in the growing field of mRNA-LNP technology. In addition to chromatography conditions, sample preparation diluent is also discussed due to its importance for accurate lipid quantitation. This method was validated using standard analytical parameters such as linearity, specificity, range, accuracy, and precision. Finally, an example lipid stability study is reported using the UHPLC-CAD method.

2 Materials and methods

2.1 Chemicals and reagents

Methanol (LCMS grade), 2-propanol (LCMS grade), and Triethylamine (HPLC grade) were purchased from Fisher (Fair Lawn, NJ). Acetic Acid (99.7%+) was purchased from Acros (West Chester, PA). Formic Acid: Triethylamine Complex (5:2), pure ethanol (200 proof), 1-tetradecanoic acid–myristic acid (99% grade), formamide (99% grade), 30% hydrogen peroxide, sodium hydroxide (10.0N) were purchased from Sigma-Aldrich (St. Louis, MO). Cholesterol (99%) was purchased from Minakem (Dunkerque, FR). 1,2-Distearoyl-sn-glycero-3-phosphocholine (DSPC) (>99%), 1-stearoyl-2-hydroxy-sn-glycero-3-phosphocholine (1-LysoPC), and 2-stearoyl-sn-glycero-3-phosphocholine (2-LysoPC) were purchased from Avanti Polar Lipids (Alabaster, AL). 1,2-Dimyristoyl-rac-glycero-3-methylpolyoxyethylene (PEG-DMG), was purchased from NOF (White Plains, NY). Water was dispensed using a MilliQ filter system from Millipore (Burlington, MA). Octadecanoic acid (referred to as stearic acid) was purchased from European Pharmacopeia (Strausburg, FR). Cationic Lipid 1, Cationic Lipid 2, and PEG Lipid 2 are proprietary products that were manufactured at Merck & Co., Inc., Kenilworth, NJ, USA which operates as MSD outside of the USA and Canada. The LNP vaccine samples were prepared as previously described [18]. In the LNP vaccine manufacture process, a lipid mixture was prepared by dissolving cationic lipid, cholesterol, phospholipid, and PEG-conjugate lipid (molar ratio of 50–58:30–39:10:1–2) in ethanol. Then lipid nanoparticles were produced by simultaneous T-mixing of the lipid mixture with an aqueous solution mRNA, followed by stepwise dia-filtration [19]. Both starting solutions are submitted for analysis along with samples post diafiltration. Each submitted sample has a targeted mRNA dose concentration and is used for sample preparation.

2.2 Assay stock standard and LNP sample preparation

Each lipid was individually dissolved in pure ethanol for stock standard preparation and then diluted with assay diluent (described below). Each LNP sample was treated with a diluent consisting of ethanol:formamide (85:15 %V/V) mixture. A minimum of four-fold dilution relative to the concentration of mRNA is required to fully recover all the lipids based on developmental data (see Section 3.1 for more sample preparation information).

When analyzing samples containing Cationic Lipid 1, 0.5% Formic Acid:Triethylamine Complex (5:2) was added to the assay diluent. When analyzing samples containing Cationic Lipid 2, 19.2mM glacial acetic acid and 16.2mM triethylamine were added to the assay diluent. Samples were diluted to final concentrations that were within the prepared calibration curves.

2.3 Mobile phase composition

When measuring LNP samples containing ionizable Cationic Lipid 1, the following mobile phase compositions were used: mobile phase A consisted of water:methanol (1:1 %V/V) with 0.5% Formic Acid:Triethylamine Complex (5:2) – a premixed, purchasable reagent from Sigma Aldrich – at pH of 3.5, and mobile phase B was composed of methanol with 0.5% Formic Acid:Triethylamine Complex (5:2). When measuring LNP samples containing Cationic Lipid 2, the following mobile phases were used: mobile phase A was composed of water:methanol (1:1 %V/V) with 19.2 mM glacial acetic acid and 16.2 mM triethylamine, and mobile phase B was composed of methanol with 19.2 mM glacial acetic acid and 16.2 mM triethylamine. The pH of both mobile phases was measured after mixing by adding 1mL of mobile phase and 9 mL water, and adjusted with their respective acid or triethylamine when necessary.

2.4 UHPLC-CAD conditions

Samples were analyzed on a Waters Acquity Classic binary UPLC system (Waters Corp, Willmington, DE). Strong needle wash was composed of 2-propanol. Weak needle wash composed of water:methanol (80:20 %V/V). Seal wash was composed of water:2-propanol (1:1 %V/V).

Samples were injected using a Waters Acquity Classic autosampler using a fixed loop injection at 5 μL with a 50 μL sample loop. Lipids were separated using a Waters BEH C18 1.7 μm particle size, 2.1 mm ID x 150 mm column heated to 50°C (Waters Corp, Willmington, DE). Using a flow rate of 0.3mL/min, the mobile phase composition began at 0% B with one-minute hold time, then %B increased to 79% as the first step gradient change. At 7.5 min, %B increased to 98% as the second step gradient change; at 17.5 min, the %B decreased to the initial condition, 0%, and equilibrated for 3.5 min before the next sample injection. Analytes were detected using a Corona VEO RS CAD from Thermo Scientific (Waltham, MA). Filtered nitrogen was used at a preset manufacture pressure of 60.7 psi; data collection rate of 5 Hz; power function of 1; nebulizer temperature set to 35°C. Data were processed using Waters Empower 3 software.

2.5 Theoretical Log D calculations

Advanced Chemistry Development (ACD/Labs) Software V11.02 (© 1994–2020 ACD/Labs) was used to predict the logarithm of the distribution coefficient, Log $D_{7.4}$ from the compound structures. The distribution coefficient (D) considers the partitioning of all ionic species of a compound. In order to calculate the Log $D_{7.4}$ value for a test compound, both the logarithms of the partition coefficient (Log P) and the acid dissociation constants (pKa) are needed for weak acids or bases. To perform these calculations, the test compound structure is drawn graphically, after which the computational program PrologD automatically calculates Log $D_{7.4}$. The pKa of cationic lipids were also theoretically calculated using this software.

2.6 Forced lipid degradation preparation

Oxidation of Cationic Lipid 2 was performed by adding 60 μL 30% H_2O_2 to 5 mL of 85 mg/mL Cationic Lipid 2 in pure ethanol. This sample was stirred for 4 h before it was injected at 1 μL along with an untreated Cationic Lipid 2. PEG Lipid 2 hydrolysis was performed by treating 2 mL of 0.7 mg/mL PEG Lipid 2 solution in ethanol with 0.1 mL of 0.01 N NaOH.

3 Results and discussion

3.1 Sample preparation diluent selection

In order to analyze lipid components in mRNA-LNP vaccines, the diluent selection is critical. The diluent ought to be able to dissolve each lipid component and dissociate any interactions between lipids and encapsulated mRNA. This is especially true for lipids with cationic functional groups that have strong ionic interactions with negatively charged mRNA molecules.

The first diluent evaluated was a 1:1 Ethanol:DMSO mixture. A sample of 0.05 mg/mL mRNA loaded LNP containing PEG-DMG, Cholesterol, Cationic Lipid 1 and DSPC was analyzed using four different dilutions - four, six, eight, and ten (Figure 1). All four lipid components were adequately recovered at a sixfold, eightfold, and tenfold dilutions with recovery greater than 95%. However, after a four-fold dilution, both Cationic Lipid 1 and DSPC were severely under recovered at $\leq$35%. In addition, the %molar fraction of each lipid was consistent with the targeted formulation ($\pm$1%), except for the fourfold dilution sample. The four-fold sample showed an increased molar fraction for PEG-DMG and cholesterol, and a decreased molar fraction for cation lipid 1 and DSPC. Both the decrease in lipid recovery and a decrease in molar ratio suggest that the LNP and mRNA were either not fully soluble or the not fully dissociated from each other. A new diluent was considered to achieve greater solubility of all lipid and mRNA components at a lower dilution.

When optimizing the new diluent, a similar dielectric solvent strength as ethanol:DMSO (1:1) was desired while also increasing the amount or strength of a nonpolar solvent for adequate solubility of all lipids. Linear combinations using the dielectric constants of the pure solvents and their volume were used to estimate solvent combinations with similar dielectric solvent strength as ethanol: DMSO (1:1). A diluent with a combination of ethanol and formamide at a 85:15 ratio was chosen.

Another dilution experiment measuring an LNP sample containing 0.05 mg/ml mRNA was analyzed using dilution factors of 4 and 10. The ethanol: formamide diluent showed all lipid components had greater than 93% recovery and the target molar fraction was observed in both dilutions tested (Figure 1b). These data suggest that the ethanol:formamide diluent was able to disrupt all non-covalent interactions between the mRNA and lipids and maintain solubility for both mRNA and lipids during analysis. Based on this data, ethanol: formamide (85:15) was chosen as the optimal diluent for mRNA-loaded LNP vaccine samples. Furthermore, when evaluating samples with various mRNA concentrations, samples were diluted based on the concentration of mRNA due to a fixed mRNA to lipid ratio. For example, a 0.05 mg/mL mRNA must be diluted 4-fold and a 0.1 mg/mL mRNA sample 8-fold for full recovery of lipids and be within the linear range.

3.2 Chromatographic separation

A UHPLC method that can quantitate neutral and cationic lipids was developed for the evaluation of LNPs containing mRNA. The final chromatographic conditions consisted of a step gradient with two isocratic holds after various

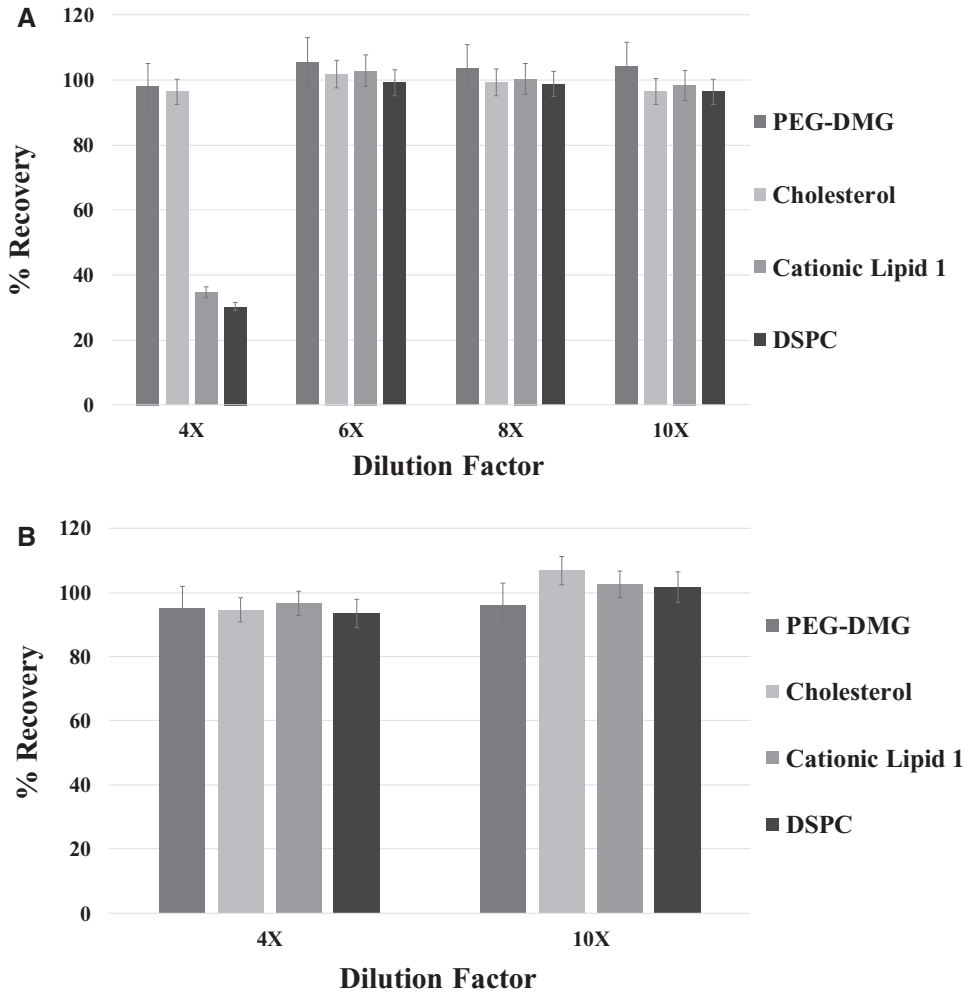

Figure 1. Recovery of the lipids (PEG-DMG, Cholesterol, Cationic Lipid 1 and DSPC) from mRNA-LNP samples at four-, six-, eight-, and tenfold dilutions with (A) 1:1 Ethanol: DMSO and four- and tenfold dilutions with (B) 85:15 ethanol:formamide.

chromatographic conditions were explored during method development.

Potential degradants such as myristic acid, lyso-PC 1 and 2, and stearic acid are more hydrophilic than their parent lipids and eluted in the first isocratic hold. The four main lipid components are highly hydrophobic and eluted in the second isocratic hold. Two isocratic holds were chosen to minimize the effect of each analytes response factor based on mobile phase composition [20]. Impurities or degradants were monitored by loss of four main lipid peaks and percent impurity analysis for any addition of new, unspecified peaks. Percent impurity analysis was performed by integrating any peaks apart from the void, system, and parent lipid peaks. This analysis was monitored and compared in stability studies to the zero time point. As previously mentioned, based on the relative response of each analyte, the universal response of both parent lipids and their degradants are not achievable with this method. It would be worth exploring this method with the use of an inverse gradient or another means to a more universal response for impurity analysis utilizing a CAD.

Figure 2A shows the separation of an mRNA-LNP sample containing PEG-DMG, Cholesterol, Cationic Lipid 1, and DSPC. These lipid components are separated in order of increasing retention time 9.60, 10.15, 12.00, and 13.40 min. Figure 2B illustrates the separation of an mRNA-LNP sample containing the four lipids PEG Lipid 2, Cholesterol, Cationic Lipid 2, and DSPC in order of increasing retention time at 9.25, 10.15, 11.75, and 13.40 min. In both formulations, the four main lipids were baseline resolved for identification and content analysis.

Of the four lipid analytes, three of them (PEG-DMG, Cholesterol, and DSPC) have an overall neutral charge and are not affected by mobile phase pH. These neutral and zwitterionic lipids were well separated prior to introducing a mobile phase pH modifier. Each analyte's calculated $LogD_{7.4}$ values helped predict their retention under reversed phased conditions, that is, retention increases with an increase in $LogD_{7.4}$ value. DSPC has the highest calculated $LogD_{7.4}$ value of 13.60 of the neutral lipids and as predicted eluted after cholesterol and both PEG-conjugates. Cholesterol's calculated value was 9.85 and eluted well before DSPC. The predicted $LogD_{7.4}$ value for the neutral and zwitterionic lipids correlated well with their retention times. Neither PEG Lipid 2 or PEG-DMG $LogD_{7.4}$ values were predicted for this

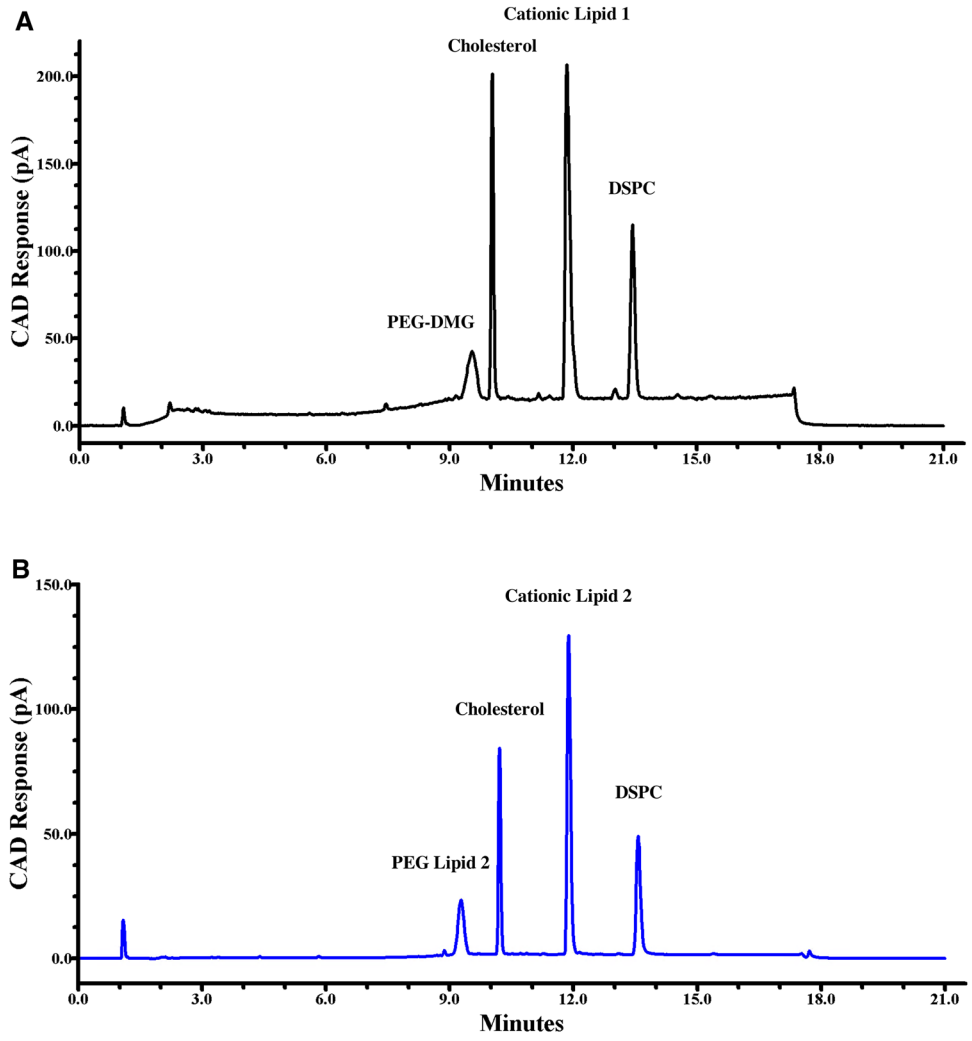

Figure 2. Chromatographic profile of (A) PEG-DMG, cholesterol, Cationic Lipid 1, and DSPC with the mobile phases of water and methanol containing formic acid and Triethylamine (pH 3.5); (B) PEG Lipid 2, cholesterol, Cationic Lipid 2, and DSPC with the mobile phases of water and methanol containing acetic acid and triethylamine (pH 5.4).

study due to the complexity of the polymer. It is conceivable that polyethyleneglycol's (PEG) large, hydrophilic head group plays an important role in reducing its hydrophobicity and retention in this method. Cationic Lipid 1 and Cationic Lipid 2's $LogD_{7.4}$ values were theoretically calculated to be 15.48 and 12.54, respectively. These values were somewhat helpful in predicting the strength of their hydrophobicity. Instead, their retention was greatly influenced from their ionizable amine funtional group.

The mobile phase pH was a crucial attribute that influenced the retention of the cationic lipids by controlling protonation of their amine functional groups. To start, triethylamine was chosen due to its volatility and its ability to prevent secondary interactions between the amine functional groups and silica base stationary phases thereby reducing tailing of the cationic lipid peaks (data not shown) [21,22].

When studying LNP samples containing Cationic Lipid 1, the mobile phase pH was adjusted to 3.5 by mixing formic acid at a 5:2 ratio with triethylamine – purchasable from Sigma Aldrich. Optimizing the pH to 3.5 controlled the elution of Cationic Lipid 1, with a theoretical pKa of 9.37 - between cholesterol and DSPC (Figure 2A). Doing so provided sufficient resolution for impurity and degradant analysis.

When analyzing LNP samples containing Cationic Lipid 2 at pH 3.5, it eluted prior to cholesterol. The Cationic lipid 2, with a theoretical p*K*a of 9.70, eluted between PEG Lipid 2 and cholesterol, further demonstrating the effect of mobile phase pH on cationic lipid separation (Figure 3A). The separation between Cationic Lipid 2 and PEG Lipid 2 was not optimal for quantitation or impurity analysis. So, a mobile phase pH of 3.5 was not used for analyzing Cationic Lipid 2, and a higher mobile phase pH was investigated.

To increase the pH above 3.5, acetic acid was substituted for formic acid. This substitution, after pH adjusting to 5.4, eluted Cationic Lipid 2 between cholesterol and DSPC providing comparable retentions as with the more acidic mobile phase. Similarly, a retention time shift was observed for Cationic Lipid 1 when using a pH 5.4 mobile phase (Figure 3B). At higher pH, there was less ionization of the amine functional group resulting in a more hydrophobic molecule. Consequently, causing Cationic Lipid 1 to elute after DSPC.

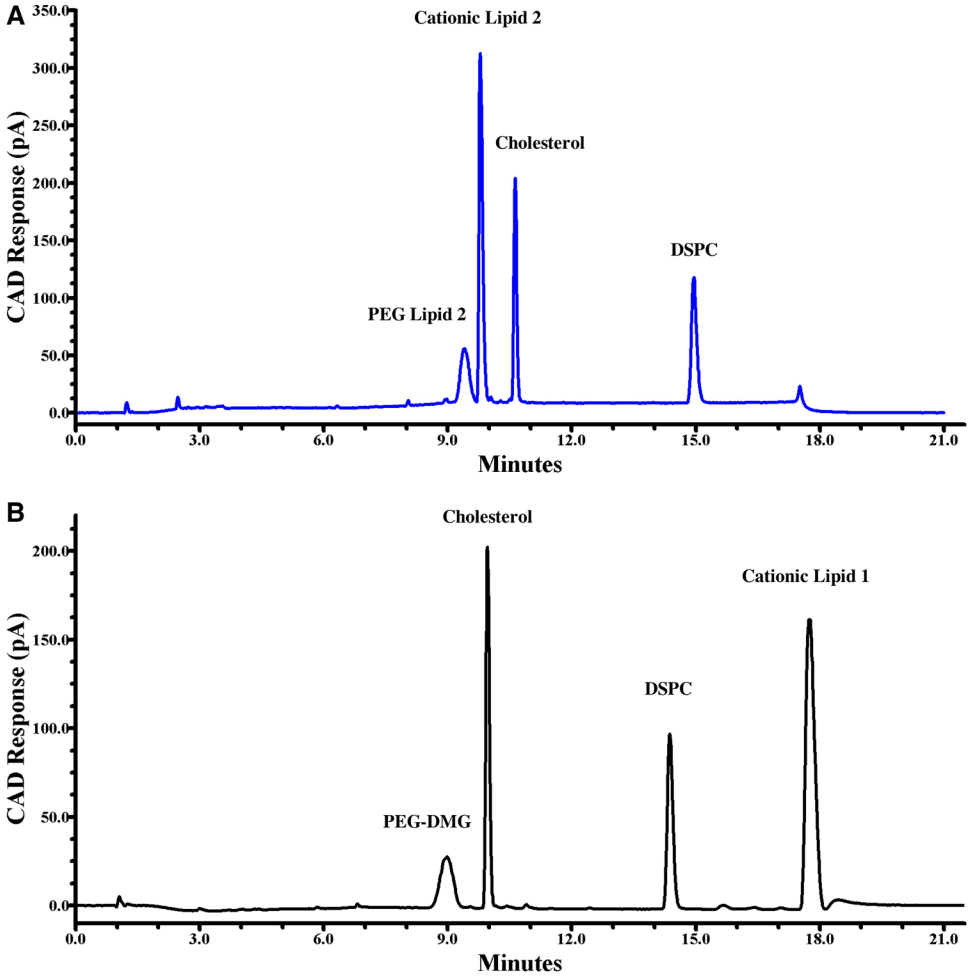

Figure 3. Mobile phase pH effects on cationic lipid separation (A) PEG Lipid 2, cholesterol, Cationic Lipid 2, and DSPC separation at pH 3.5 (B) PEG-DMG, cholesterol, DSPC, and Cationic Lipid 1 separation at pH 5.4.

3.3 Forced lipid degradation study

This method was optimized to capture potential degradation products of the four lipids measured in each method. An impurity reference standard was prepared using myristic acid, Lyso-PC1, Lyso-PC2, stearic acid, and a known degradant of Cationic Lipid 1 dissolved in pure ethanol. Myristic acid was used because it is a hydrolysis degradant of both PEG lipids. Lyso-PC1, Lyso-PC2, and stearic acid were chosen because they are hydrolysis degradants of DSPC. Cholesterol is known to be stable and therefore no suspected degradants of cholesterol were not used in this experiment [23].

Another degradant is the oxidation product of Cationic Lipid 2 that eluted between cholesterol and Cationic Lipid 2 at 10.6 min (Figure 4B) [24]. Forced degradation products of PEG Lipid 2 were determined by hydrolysis under basic conditions. Three degradation peaks were observed, see Figure 4C. Though mRNA-LNP vaccines would not likely be exposed to NaOH or high concentrations of H_20_2, these conditions were chosen in order to evaluate chromatographic selectivity of the analytes' degradants, especially when these samples were monitored for stability over 12 months.

Figure 4A features a chromatogram of the lipid hydrolysis degradants, myristic acid, lyso-PC1, lyso-PC2, and stearic acid. All were resolved in order of increasing retention times 3.5, 3.8, 4.0, and 7.5 min in the first isocratic hold of the gradient at 79% mobile phase B. From 5.0 min to 7.50 min, mobile phase B is ramped to 98% to elute the four main lipid components, Cationic Lipid 2 oxidation, and the known degradant of Cationic Lipid 1.

3.4 Method validation

The method's accuracy, repeatability (intra-assay precision), inter-assay precision, specificity, linearity, and range were all validated for this UHPLC-CAD method. Validation results are summarized in Table 1.

The accuracy of this method was determined by spike recovery using a spike of 20%, 50%, and 70% of each lipid. The intra-assay precision of six injections was between 1 and 7% for all lipids ($n = 6$). Inter-assay precision was determined by evaluating the same sample between three separate runs on three different days. The inter-assay precision results for all lipids were between 1% and 6% ($n = 3$).

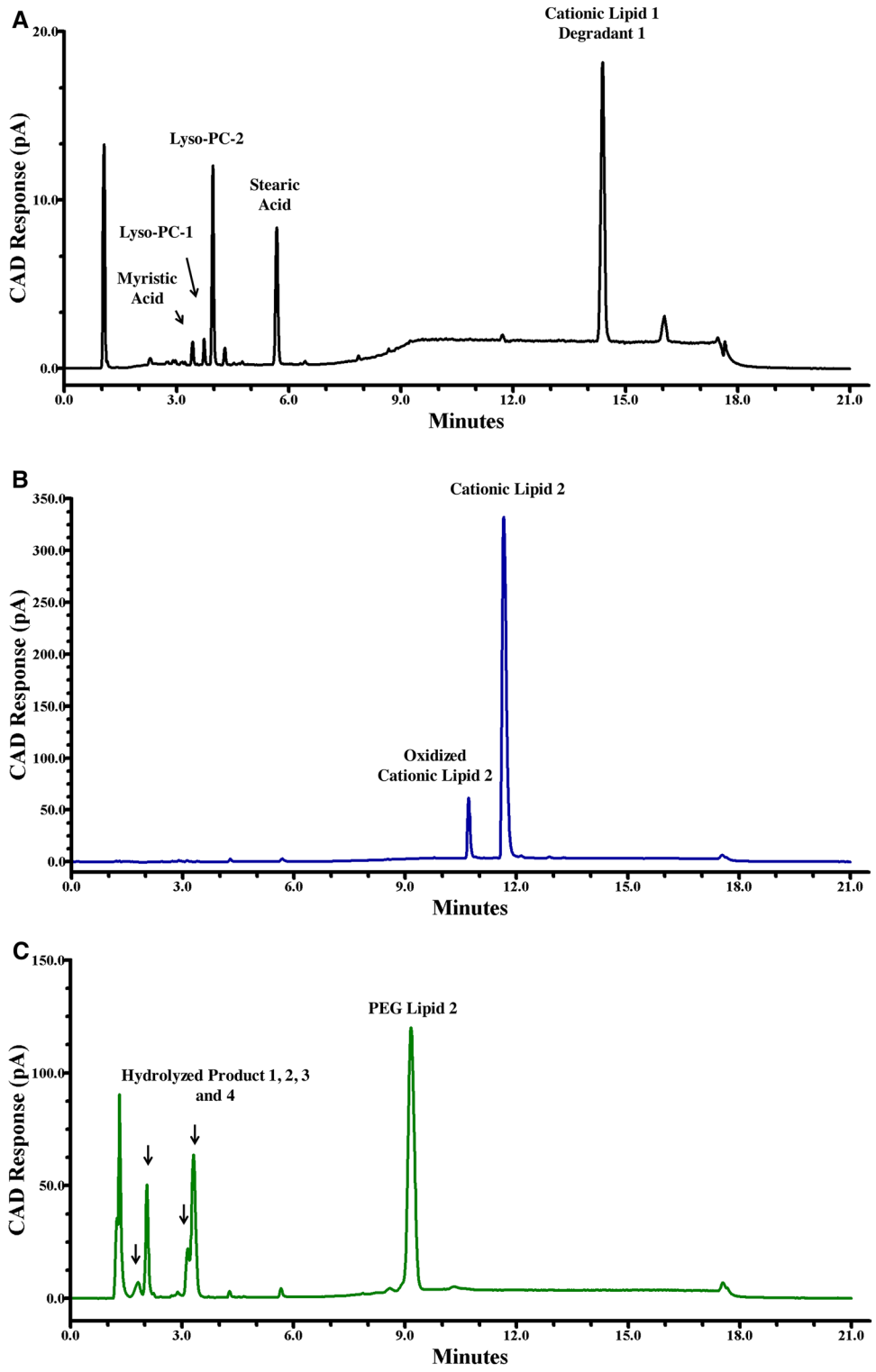

Figure 4. Selectivity of lipid degradation products of (A) myristic acid, lyso-PC-1, and lyso-PC-2, stearic acid, and a known degradant of Cationic Lipid 1 with mobile phase at pH 3.5 (B) oxidized Cationic Lipid 2 and Cationic Lipid 2 with mobile phase at pH 5.4 (C) hydrolyzed product 1, 2, 3, and 4 of PEG Lipid 2, and PEG Lipid 2 with mobile phase at pH 5.4.

Four independent preparations of a negative control sample were prepared, and each preparation was injected once. The negative control sample consisted of the formulation buffer without lipids or mRNA. The negative control chromatogram and blank chromatogram were compared. Peaks with the same retention time in the blank were disregarded when compared to the negative control to obtain the peaks that were only related to the negative control. No interfering peaks from the negative control sample were observed.

Table 1. Assay validation results

	PEG-DMG*	PEG Lipid 2**	Cholesterol*	Cationic Lipid 1*	Cationic Lipid 2**	DSPC*
Accuracy (%Recovery)	93–96%	98–102%	99–103%	95–97%	98–102%	96–99%
Intra-assay precision (%RSD)	1–7%	1–3%	1–3%	1–6%	1–3%	1–3%
Inter-assay precision (%RSD)	5–6%	1%	1–2%	5–6%	1%	1–2%
Linearity (R^2)	0.993–0.997	1.000	1.000	0.993–0.999	1.000	0.999
Linear range (mg/mL)***	0.007–0.019	0.017–0.027	0.036–0.056	0.067–0.163	0.086–0.130	0.025–0.038

*Mobile Phase Modifier: FA/TEA
**Mobile Phase Modifier: AA/TEA
***Lower limit of linear range indicates qualified LOQ of each lipid component. LOD was not determined.

Table 2. Positive control sample chart

mRNA Loaded LNP Control ($n = 80$)				
	PEG DMG	Cholesterol	Cationic Lipid 1	DSPC
%RSD	7.1	4.1	4.7	4.0
mRNA Loaded LNP Control ($n = 95$)				
	PEG Lipid 2	Cholesterol	Cationic Lipid 2	DSPC
%RSD	5.8	3.5	4.1	3.5

The previously mentioned oxidation study of Cationic Lipid 2 was performed to demonstrate specificity for this method. Linearity was evaluated using a quadratic fitting between three independent runs using the concentration ranges listed in Table 1. The correlation coefficient (R^2) of each quadratic fit was 0.993–1.000 for all lipids.

Assay performance was monitored using a control chart and a positive control sample. The performance was monitored over the course of 28 months with an mRNA-LNP sample containing Cationic lipid 1, and 15 months with an mRNA-LNP sample containing Cationic Lipid 2. Their results are listed in Table 2. All lipid concentration measurements had a % RSD of < 5% with the exception of PEG-DMG and PEG Lipid 2. Both PEG-lipid conjugates had a % RSD <10%. This is likely because each of the two PEG-conjugate lipids is the lowest concentrated relative to the other lipids. Their broad peak shape also likely contributes to this variability.

Finally, the LOQ of this method is listed as the lowest range of lipids in Table 1. LOD was not determined in this paper.

3.5 Lipid stability

This lipid assay was used to monitor lipid stability at four temperatures –70°C, –20°C, 4°C, and 25°C and wsd pulled for analysis at the following time points: initial (time zero), 1 month, 3 months, 6 months, and 10 months. The stability data are illustrated in Figure 5 for the following four main lipids: PEG-DMG, cholesterol, Cationic Lipid 1, and DSPC. It is a relative comparison of each time point with the initial –70°C time zero measurement. Each sample from each time-point was prepared in duplicate, and each timepoint sample submission was tested once. PEG-DMG showed 0% change at –70°C, 4°C, and 25°C in 1 M, –20°C, and 4°C in 3 M and 4°C in 6 M. The stability study at elevated temperature, 25°C, was run for 6 months and discontinued due to significant mRNA degradation. The decrease of the lipid concentration was approximately 10–15% at 6-month time point under –70°C storage temperature, which was the most significant change among all the time points at all the temperatures. The trend of the stability data across the temperatures indicates it may be due to sample handling, variability from sample pull date to time of testing, or assay variability instead of chemical degradation. Samples stored at higher temperatures for longer times would be expected to show more lipid concentration decrease if it was caused by chemical degradations, which was not observed in the stability study. Therefore, the stability results demonstrated all four lipids were chemically stable in the mRNA vaccine product at all the evaluated temperatures.

4 Concluding remarks

An efficient and sensitive reverse-phase UHPLC-CAD method was developed for the analysis of lipid components of mRNA encapsulated lipid nanoparticles (LNPs) in order to support process and formulation development studies and clinical material release and stability testing. The sample preparation and chromatographic conditions were optimized to fully recover and separate the main lipids and their potential degradants. This method was validated to be linear, precise, accurate, and specific for two LNP formulations: PEG-DMG, cholesterol, Cationic Lipid 1 and DSPC, and PEG Lipid 2, Cholesterol, Cationic Lipid 2, and DSPC.

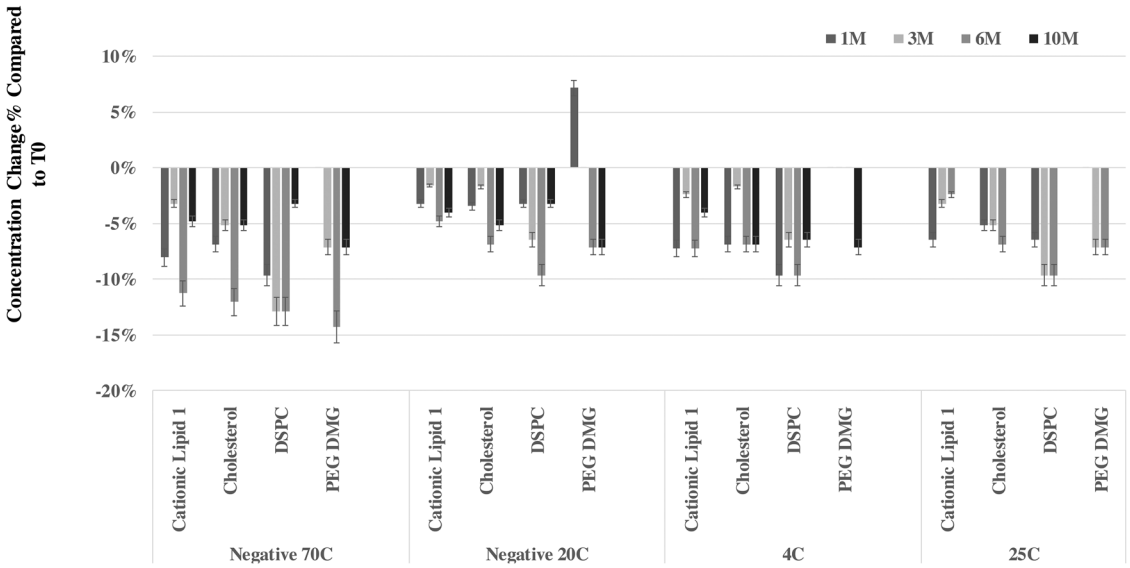

Figure 5. Stability data of a 10-month stability study for lipids PEG-DMG, Cholesterol, Cationic Lipid 1, and DSPC at –70°C, –20°C, 4°C, and 25°C storage conditions.

This robust separation makes the method ideal for future work to support mRNA-LNP vaccines or other LNP containing drug candidate development for measuring lipid content and identity as well as monitoring the stability of LNP formulations. With optimization of the mobile phase pH other amine-containing lipids can be controlled to elute in-between cholesterol and DSPC and main reasonable run times. We think this method will be a beneficial contribution to the growing interest LNP technologies – not only in vaccines, but also therapeutics and there drug candidates utilizing this technology.

We would like to extend our gratitude to Dr Adam Socia and Dr Ping Zhuang for providing critical review to the manuscript. We also would like to extend our gratitude to our colleagues at Merck & Co., Inc., Kenilworth, NJ, USA Vaccine Process Development and Vaccine Drug Product Development MRL for providing us with all of the LNP materials used for this study.

The authors have declared no conflict of interest.

Data availability statement

The data that support the findings of this study are available from the corresponding author upon reasonable request.

5 References

[1] Cullis, P. R., Hope, M. J., *Mol. Ther.* 2017, *25*, 1467–1475.

[2] Lian, T., Ho, R. J. Y., *J. Pharm. Sci.* 2001, *90*, 667–680.

[3] Swaminathan, G., Thoryk, E. A., Cox, K. S., Meschino, S., Dubey, S. A., Vora, K. A., Celano, R., Gindy, M., Casimiro, D. R., Bett, A. J., *Vaccine* 2016, *34*, 110–119.

[4] Krammer, F., *Nature* 2020, *586*, 516–527.

[5] Aliprantis, A. O., Shaw, C. A., Griffin, P., Farinola, N., Railkar, R. A., Cao, X., Liu, W., Sachs, J. R., Swenson, C. J., Lee, H., Cox, K. S., Spellman, D. S., Winstead, C. J., Smolenov, I., Lai, E., Zaks, T., Espeseth, A. S., Panther, L., *Hum. Vaccines Immunother.* 2020, *17*, 1248–1261.

[6] Monslow, M. A., Elbashir, S., Sullivan, N. L., Thiriot, D. S., Ahl, P., Smith, J., Miller, E., Cook, J., Cosmi, S., Thoryk, E., Citron, M., Thambi, N., Shaw, C., Hazuda, D., Vora, K. A., *Vaccine* 2020, *38*, 5793–5802.

[7] Mehnert, W., Mäder, K., *Adv. Drug Delivery Rev.* 2012, *64*, 83–101.

[8] Grit, M., Crommelin, D. J. A., *Chem. Phys. Lipids* 1993, *64*, 3–18.

[9] Radomska-Soukharev, A., *Adv. Drug Delivery Rev.* 2007, *59*, 411–418.

[10] Sommer, U., Herscovitz, H., Welty, F. K., Costello, C. E., *J. Lipid Res.* 2006, *47*, 804–814.

[11] Zhong, Z., Ji, Q., Zhang, J. A., *J. Pharm. Biomed. Anal.* 2010, *51*, 947–951.

[12] McLaren, D. G., Miller, P. L., Lassman, M. E., Castro-Perez, J. M., Hubbard, B. K., Roddy, T. P., *Anal. Biochem.* 2011, *414*, 266–272.

[13] Baertschi, S. W., *TrAC Trends Anal. Chem.* 2006, *25*, 758–767.

[14] Li, Z., Schariter, J. A., Zhang, J., Davis, J. C., Leone, A. M., *Am. Pharm. Rev.* 2010, *13*, 102.

[15] Vervoort, N., Daemen, D., Török, G., *J. Chromatogr. A* 2008, *1189*, 92–100.

[16] Vehovec, T., Obreza, A., *J. Chromatogr. A* 2010, *1217*, 1549–1556.

[17] Chesnut, S. M., Salisbury, J. J., *J. Sep. Sci.* 2007, *30*, 1183–1190.

[18] Loughney, J. W., Minsker, K., Ha, S., Rustandi, R. R., *Electrophoresis* 2019, *40*, 2602–2609.

[19] Abrams, M. T., Koser, M. L., Seitzer, J., Williams, S. C., DiPietro, M. A., Wang, W., Shaw, A. W., Mao, X., Jadhav, V., Davide, J. P., Burke, P. A., Sachs, A. B., Stirdivant, S. M., Sepp-Lorenzino, L., *Mol. Ther.* 2010, *18*, 171–180.

[20] Almeling, S., Ilko, D., Holzgrabe, U., *J. Pharm. Biomed. Anal.* 2012, *69*, 50–63.

[21] Roos, R. W., Lau-Cam, C. A., *J. Chromatogr. A* 1986, *370*, 403–418.

[22] Kiel, J. S., Morgan, S. L., Abramson, R. K., *J. Chromatogr. A* 1985, *320*, 313–323.

[23] Engel, L. L., Brooks, P., *Steroids* 1971, *17*, 531–539.

[24] Hoh, G., Barlow, D., Chadwick, A., Lake, D., Sheeran, S., *J. Am. Oil Chem. Soc.* 1963, *40*, 268–271.

Received: 10 April 2020 | Revised: 5 August 2020 | Accepted: 9 August 2020

DOI: 10.1002/jssc.202000414

RESEARCH ARTICLE

JOURNAL OF SEPARATION SCIENCE

Development of an ultra-high-performance liquid chromatography-charged aerosol detection/UV method for the quantitation of linear polyethylenimines in oligonucleotide polyplexes

Adam Socia | **Yong Liu** | **Yuejie Zhao** | **Andreas Abend** | **W. Peter Wuelfing**

Merck & Co., Inc., Kenilworth, NJ, USA

Correspondence
Adam Socia, Mailstop WPB46-3243E
770 Sumneytown Pike West Point,
PA 19486, USA.
Email: Adam_Socia@merck.com

Linear polyethylenimines are polycationic excipients that have found many pharmaceutical applications, including as a delivery vehicle for gene therapy through formation of polyplexes with oligonucleotides. Accurate quantitation of linear polyethylenimines in both starting solution and formulation containing oligonucleotide/polyethylenimine polyplexes is critical. Existing methods using spectroscopy, matrix-assisted laser desorption/ionization mass spectrometry time-of-flight, or nuclear magnetic resonance are either complex or suffer from low selectivity. Here, the development and performance of a simple analytical method is described whereby linear polyethylenimines are resolved by ultra-high-performance liquid chromatography and quantified using either a charged aerosol detector or an ultraviolet detector. For formulated oligonucleotide/polyethylenimine polyplexes, sample preparation through decomplexation/digestion by trifluoroacetic acid was necessary to eliminate separation interference. The method can be used not only to support formulation development but also to monitor the synthesis/purification and characterization of linear polyethylenimines.

KEYWORDS
charged aerosol detection, decomplexation, oligonucleotides, polyethylenimines, reversed-phase high-performance liquid chromatography

1 | INTRODUCTION

Linear polyethylenimines (PEIs) are cationic polymers with repeating units composed of amine and a [-CH_2CH_2-] spacer [1]. The synthesis of linear PEIs was first reported by Saegusa through polymerization of 2-oxazoline and subsequent hydrolysis of the poly(2-ethyl-2-oxazoline) (PEOx) [2]. When protonated in acidic aqueous solution, PEIs possess high solubility and a high positive charge density. This property enables important industrial applications including chelating reagent for metal ions in wastewater treatment [3], flocculation of negatively charged fibers in paper industry [4], and pretreatment of fibers in the textile industry [5].

In recent years, linear PEIs have become one of the key in vitro and in vivo nonviral gene delivery vehicles in the pharmaceutical industry [6–8]. Through the formation of nanoparticles (polyplexes) by electrostatic interaction

Article Related Abbreviations: CAD, charged aerosol detection; PEI, polyethylenimines; PEOx, Poly(2-ethyl-2-oxazoline); *p*TSA, *p*-toluene sulfonic acid; WFI, water for injection

between the negatively charged phosphodiester backbone of the oligonucleotide and the positively charged nitrogen atoms of PEIs, the oligonucleotides are encapsulated. Such delivery systems not only provide good transfection efficiency, but also stability from enzymatic degradation of the oligonucleotides [9–11]. Different nanoparticles with various transfection efficiencies and physical stabilities can be formed by changing the molar ratio (N/P ratio) of amine (N; from PEI) to oligonucleotide phosphodiester backbone (P; from oligonucleotides) [12,13].

Therefore, during formulation development, N/P ratio is an important parameter to explore for optimum transfection efficiency and stability of formulated oligonucleotides. Accurate quantitation of PEI in both starting solution and formulation containing the oligonucleotide/PEI complex is critical to achieve and determine the desired N/P ratio. MALDI-TOF and size exclusion chromatography coupled with refractive index detector have been used to monitor the synthesis and characterization of PEIs [14] while spectrophotometry has been used to analyze PEIs in the presence of copper (II) ions, which forms a dark blue cuprammonium complex [15]. Wang and colleagues previously reported quantification of free PEIs in formulated PEI/oligonucleotide solution by NMR [16]. However, these methods are either relatively complex, or suffer from low sensitivity and/or selectivity, as nitrogenous buffers commonly used in sterile formulations, such as histidine or tris(hydroxymethyl)aminomethane (TRIS), can cause significant interference in spectrophotometric methods using copper complexation. Thus, there is a strong demand to develop a simple sensitive method to resolve and quantify PEIs for N/P determination to guide formulation development and provide accurate characterization of those polyplex nanoparticles. Furthermore, current reaction monitoring of the synthesis and characterization of the isolated PEIs are performed via NMR, which is inconvenient in a manufacturing setting. Herein, we report the development of a RP HPLC method with charged aerosol detection (CAD)/UV detection for linear PEI analysis in starting solution and formulated drug product. Additionally, we report its validation as a "quantitative measurement of the major component(s) in the drug substance," according to current guidance ICH Q2B(R1) and USP < 1225 > [17,18].

2 | MATERIALS AND METHODS

2.1 | Chemicals and reagents

All PEI samples used for this work are linear PEIs. In vivo jetPEI™ (98.9% pure as HCl salt, average molecular weight of poly(2-ethyl-2-oxazoline) intermediate ~50 kD, and polydispersity (Mw/Mn) was 1.1, according to its certificate of analysis) was purchased from ChemCon (Freiburg, Germany). Additional 10 and 20 kD PEI HCl salts were purchased from Sigma Aldrich (St. Louis, MO). PEOx (5 kD) was obtained from Alfa Aesar (Haverhill, MA). TRIS, trehalose dihydrate, TFA and deionized water for injection (WFI) were purchased from Fisher Scientific (Norristown, PA). Single-strand oligonucleotides (antisense and sense) composed of 24 nucleotides were synthesized, annealed, purified, and lyophilized in-house (Merck & Co., Inc., Rahway, NJ, USA).

2.2 | Instrumentation

The UHPLC system consisted of an Agilent 1290 (Santa Clara, CA) equipped with a quaternary pump, a photodiode array detector set at 234 nm, and a Thermo Corona VEO RS Charged Aerosol Detector (Waltham, MA). Data acquisition was performed at a sampling rate of 10 Hz by Empower 3 software for both detectors. Analysis was carried out with a 100 mm × 2.1 mm id Waters HSS T3 column, and 1.8 μm particle size at a column temperature of 60°C. The mobile phase was a gradient of 0.2% (v/v) TFA in water as "mobile phase A" and 0.2% (v/v) TFA in acetonitrile as "mobile phase B," starting at 5% "B" over 1 minute for 1 min, then ramping up to 53% "B" over 7 min, up to 95% "B" for 1 min, and then re-equilibration at 5% "B" for 3 min. The flow rate was set at 0.6 mL/min. Injection volume was 10 μL.

2.3 | Preparation of solutions

2.3.1 | PEI stock solution

A stock solution of PEI was prepared by dissolving an accurately weighed amount of in vivo jetPEI in WFI to reach ~0.58 mg/mL concentration as an HCl salt. An accurate concentration of 0.5640 mg/mL was then determined by application of a correction factor based on the moisture level in the solid material by Karl Fisher titration.

2.3.2 | Starting PEI solution

A starting PEI sample solution was prepared by dissolving an accurately weighed amount of in vivo jetPEI in WFI containing 300 mM trehalose to reach ~0.58 mg/mL concentration as an HCl salt.

2.3.3 | Starting oligonucleotide solution

A starting oligonucleotide sample solution was prepared by dissolving an accurately weighed amount of oligonucleotide in a solution of 5 mM phosphoric acid, 2.5 mM TRIS, and 300 mM trehalose in WFI to reach ~0.40 mg/mL oligonucleotide concentration.

2.3.4 | PEI/oligonucleotide drug product solution

The PEI/oligonucleotide sample solution was prepared by mixing equal portions of the starting PEI solution and the starting oligonucleotide solutions to form the active polyplex species. The final solution contained 2.5 mM phosphoric acid, 1.25 mM TRIS, and 300 mM trehalose in WFI to reach ~0.20 mg/mL concentration of oligonucleotide and ~0.29 mg/mL PEI as an HCl salt.

2.3.5 | Preparation of starting PEI sample solution for analysis

A portion of the starting PEI solution was diluted 1:1 with WFI to a concentration of ~0.29 mg/mL PEI as an HCl salt.

2.3.6 | Preparation of formulated PEI/oligonucleotide polyplex sample solution for analysis

A portion of the PEI/oligonucleotide drug product solution is diluted in a ratio of 4:1 with concentrated TFA, sealed, mixed well, and incubated for at least 3 h at room temperature to decomplex the polyplex, digest the oligonucleotide, and liberate the PEI. The concentration of PEI is ~0.23 mg/mL as an HCl salt.

2.4 | Method validation

2.4.1 | Linearity

The linearity and calibration curves were constructed at five concentrations prepared in duplicate and injected in triplicate, ranging from ~0.025 to ~0.50 mg/mL PEI according to Supporting Information Figure S1 by serial dilution of the PEI stock solution (from Section 2.3.1) with WFI. The linearity for the CAD of these solutions was evaluated by the second-order polynomial regression analysis, while the UV234 nm detection was evaluated by linear regression analysis. These levels were selected to cover the target analytical concentrations expected from both the polyplex formulation and the starting PEI solution levels in routine analysis.

2.4.2 | System suitability

The system suitability was assessed by the six analyses of the above "linearity solution" at a target concentration of ~0.25 mg/mL PEI. The acceptance criterion was ±3.0% for the percent RSD (%RSD) for both the peak area and retention times for PEI.

2.4.3 | Accuracy and precision

Accuracy and precision of the assay method was determined using the triplicate injections of the duplicate sample preparations of the "starting polyethylenimine solution" and the "formulated polyethylenimine/oligonucleotide polyplex sample solution." The resulting recoveries were calculated against the theoretical concentrations of PEIs, as mentioned in Sections 2.3.4 and 2.3.5.

3 | RESULTS AND DISCUSSION

3.1 | Method development and optimization

3.1.1 | Chromatographic mode of analysis

As a literature search failed to show any chromatographic method for the rapid determination of PEIs, chromatographic method development was initiated. PEIs are large polycations with a range of molecular weights (polydisperse) possessing high hydrophilicity at acidic pH. TFA was selected as a mobile phase additive for its ability to interact with these polycations forming ion pairs and thus promote hydrophobic interaction with the stationary phase in RPLC. TFA was also selected for the decomplexation of the polyplex samples, as discussed in Section 3.1.4. Furthermore, TFA was chosen due to its compatibility with aerosol-based detection [19], which will be discussed in the following section. Therefore, the use of TFA in the mobile phase would be prudent. As the analyte is polydisperse, a gradient containing acetonitrile as the strong solvent was selected to resolve, compress, and sharpen the peak. A column temperature of 60°C was selected to reduce system pressure and increase mass transfer of the polymer. The

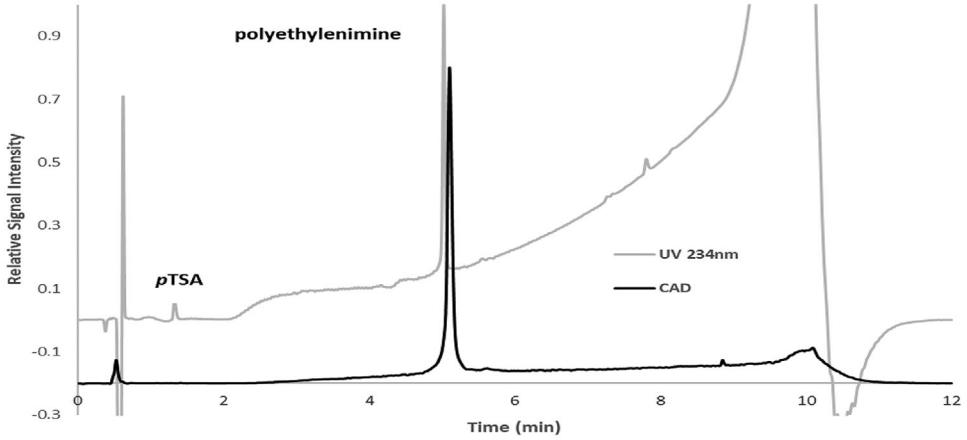

FIGURE 1 Chromatographic overlays of UV234 nm and CAD signals for polyethylenimine standard solution, absorbance scaled relative to polyethylenimine peak height. Method parameters as listed in Section 2.2

pore size of the column used was 100 Å, which is sufficient for an analyte of its molecular weight [20].

3.1.2 | Detection

Based on its chemical structure, linear PEI should possess low or no UV absorbance and therefore alternative detectors such as a mass spectrometer and aerosol-based detection were explored. Our previous work had shown good detection of volatile amines with CAD when TFA was used as a mobile phase modifier [21]. We chose to use CAD for this work due to its robustness, ease of use, and availability in manufacturing settings over mass spectrometers. Default CAD settings were utilized for this work without further exploration as they were adequate to meet method validation requirements (filter = medium, nebulization temperature = 35°C, range = 100 pA).

Interestingly, when UV spectra were acquired from 200 to 400 nm along with the CAD signal, we observed slight absorbance from 220 to 250 nm at the retention time of the linear PEI from the CAD signal (e.g., UV234 nm; Figure 1). Various other linear PEIs (e.g., UV234 nm; Supporting Information Figure S2) were also examined and they all showed a similar UV spectral feature from 220 to 250 nm as jetPEI (Supporting Information Figure S3). The linear PEI synthetic precursor, PEOx, however does not possess this spectral absorbance when analyzed using this method, but rather has a high nonspecific absorbance spectrum with an apex at 205 nm, decreasing in absorbance down to 240 nm. The exact reason for the UV response in linear PEI is unknown and is still being investigated in our laboratory. Despite the unknowns regarding the exact reason responsible for UV absorbance for PEI, validation work with UV detector was carried in subsequent section to evaluate its feasibility as simpler in-process method for laboratories that may not be equipped with a CAD.

Additionally, a small peak eluted at ~1.5 min (Figure 1) in the jetPEI sample when using UV detection, and was identified through retention time and spectral matching from the analysis of authentic material as *p*-toluene sulfonic acid (*p*TSA), a by-product during the synthesis of linear PEI. This peak was only seen with the jetPEI material and not with the other linear PEIs tested. No *p*TSA peak was seen for any PEI sample when using the mass-based CAD due to the relatively low mass fraction of the *p*TSA relative to jetPEI.

3.1.3 | TFA modifier level

The TFA level in the starting mobile phase was observed to affect the ability of the method to elute the PEI in a single, well-retained peak. For example, when the mobile phase TFA levels are less than 0.15%, a main PEI peak was seen at the expected retention time (ion-paired) and a secondary peak was seen eluting in the void volume. Note that 0.2% TFA in both mobile phase A and B was found enough to ensure that all the PEI injected is retained in a single peak resolved from other components.

3.1.4 | Development sample preparation procedure for the analysis of PEIs in the drug product

Once the method conditions for PEI starting solution were finalized, the sample preparation of the oligonucleotide-containing drug product was investigated. Neat injections of these samples showed a large peak in the region of the PEI peak well above the theoretical amount of PEI

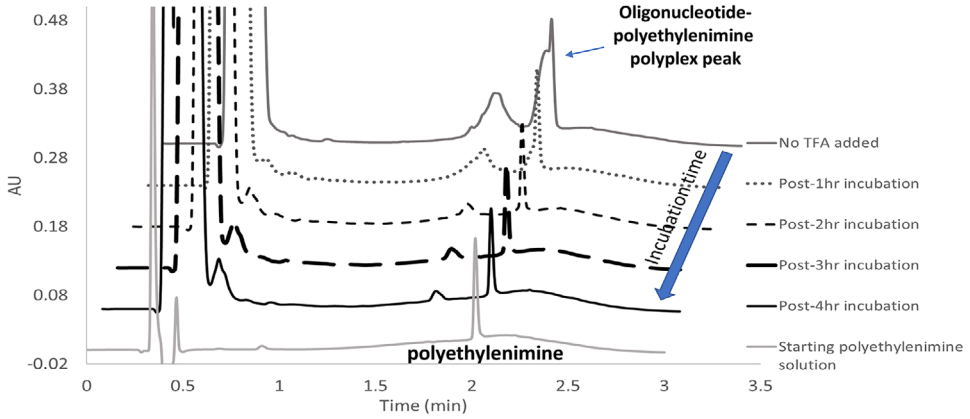

FIGURE 2 Overlaid and offset UV234 nm chromatograms showing incubation time effect of 1:4 TFA addition on liberation of polyethylenimines from oligonucleotide-containing polyplexes. Method parameters as listed in Figure 1 but with a gradient that was approximately sixfold steeper

added. The spectral data of that peak showed significant UV absorbance at 200–310 nm, with an apex at 260 nm, a characteristic of nucleic acids (Supporting Information Figure S4). Since the oligonucleotide elutes close to the void volume upon injection of a pure oligonucleotide sample, this indicated that the oligonucleotide-PEI polyplex was coeluted with PEI. Consequently, the oligonucleotide-PEI polyplex is required to be fully decomplexed through the sample preparation procedure before injection into the system to ensure accurate recoveries of PEI. The use of 1 M $CuSO_4$, 8 M urea, 6 M guanidine, 6 N HCl, formamide, DMSO, DMF, and concentrated TFA were explored based on a literature search of reagents used to decomplex the polyplex and liberate the PEI [22–27]. These procedures showed various levels of decomplexation effectiveness, both with and without heating, as determined by how close the peak shape and area matched that of the PEI standard at the same theoretical concentration of PEI. Ultimately, the use of concentrated TFA in a ratio of 1 volume of TFA per 4 volumes of drug product solution was selected as it was the only reagent that resulted in full decomplexation, hydrolysis of the oligonucleotide, and liberation of free PEIs after 3 h incubation at room temperature, as shown in the kinetic study in Figure 2. It should be noted that failure to fully decomplex resulted in an increase in the apparent recoveries due to the presence of additional mass (CAD) or absorbance (UV) from the oligonucleotide. For example, the peak area for the UV detection was almost four times as large for the untreated sample as that of the 3-h incubation sample. It should also be noted that this experiment was performed using an earlier developmental method that was similar to the final method described in Section 2.2, but with a gradient that was approximately sixfold steeper.

3.1.5 | Method optimization to support reaction monitoring during synthesis of linear PEIs

According to Supporting Information Figure S5, linear PEIs are manufactured by the polymerization of 2-oxazoline to PEOx, resulting in the formation of the by-product *p*TSA, and then the subsequent hydrolysis of the PEOx to afford linear PEIs. Currently, reaction monitoring for the synthesis of linear PEIs is mainly carried out by NMR or MALDI-TOF, as referenced previously, which are not easily accessible for analytical scientists in a manufacturing setting. We explored the application of our HPLC-UV/CAD method for reaction monitoring. As shown in Figure 3, *p*TSA, linear PEIs, and PEOx can readily be resolved within 10 min through simple optimization of the validated method gradient and detection by UV. This was performed by removing the 53% "B" step in the gradient (Section 2.2), resulting in a slightly stronger gradient to elute the PEOx before the wash-off step. This sample was generated by spiking the linear jetPEI starting solution containing 0.4% residual *p*TSA, with the PEI precursor molecule, PEOx. Due to the low CAD response for *p*TSA, we recommend using UV detection to monitor this reaction process, while using CAD for the conversion of PEOx to PEI and yield calculations. Although the modified method used for reaction monitoring was not validated here, it could be explored further by others, as needed.

3.2 | Method validation

Calibration curves were generated from the calibration standards using CAD and UV 234 nm detection to satisfy

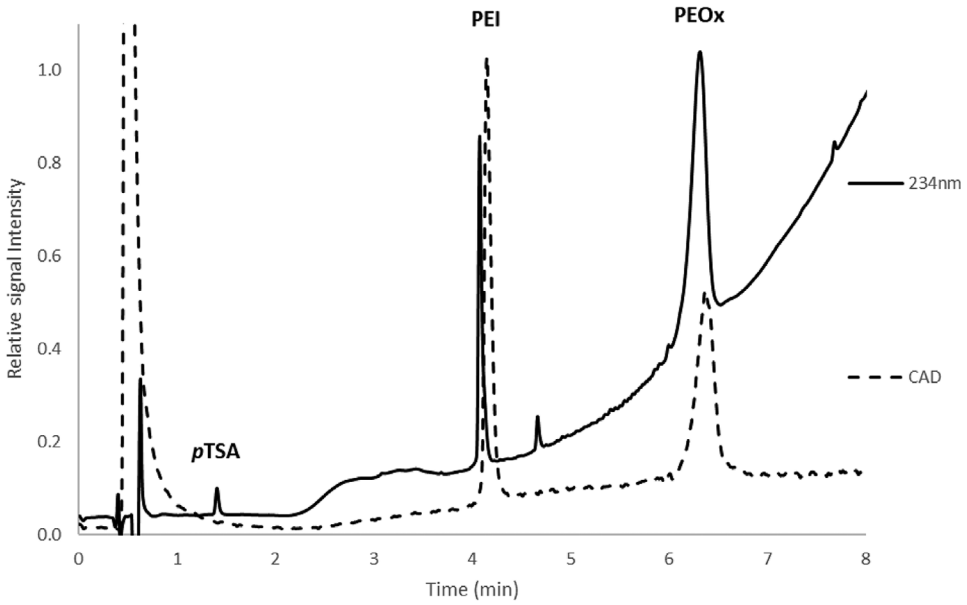

FIGURE 3 Chromatographic overlays of UV234 and CAD signals for reaction monitoring for the synthesis of linear polyethylenimine using *p*TSA and PEOx spiked polyethylenimine solution. Method parameters as listed in Figure 1 while removing the 53% "B" step in the gradient, resulting in a slightly stronger gradient to elute the PEOx before the wash-off step

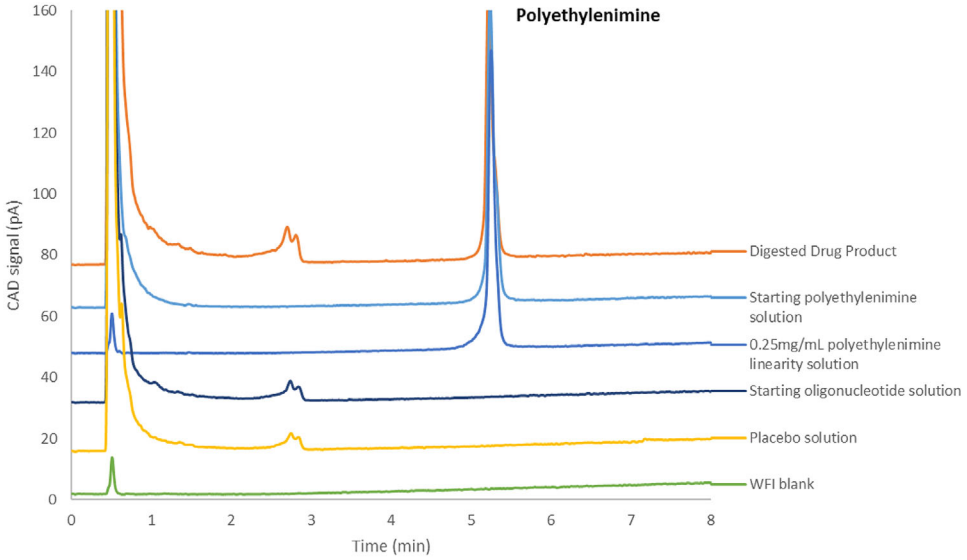

FIGURE 4 Chromatographic overlays of CAD signals for specificity. Method parameters as listed in Figure 1

the requirements for assay of a drug substance or finished product based on USP < 1225 > and ICH Q2B(R1). Calibration standard solutions and samples were analyzed by duplicate preparations with triplicate injections. None of the solution components (oligonucleotide, placebo, or WFI blank) interfered with the PEI peak, as seen in Figure 4.

As shown in Table 1 and Supporting Information Figure S6, the HPLC-CAD method developed is linear (when applying a second-order polynomial fitting [28]), accurate, reproducible, and specific for the quantitative determination of PEIs in both starting solution and oligonucleotide-containing drug product. The LOD was calculated to be 0.2 μg/mL and the LOD was calculated to be 0.7 μg/mL. This is the preferred method to accurately analyze PEIs.

Likewise, the response of the same solutions from above when analyzed by UV detection at 234 nm (Table 2 and Supporting Information Figure S6) is also linear (least-squares fitting), reproducible, and specific for the

TABLE 1 Results for validation and sample analysis using HPLC-CAD and analysis by the second-order polynomial regression

Linearity of calibration standards		
Range (mg/mL)	**Correlation coefficient (*R*)**	
0.02504–0.5008	0.9996	
Repeatability (%RSD; *n* = 6) of triplicate injections of duplicate preparations for PEI determination		
	Area counts	**Retention time**
Standard 0.02504 mg/mL	3.4%	0.2%
Standard 0.05008 mg/mL	1.6%	0.2%
Standard 0.1002 mg/mL	1.8%	0.2%
Standard 0.2504 mg/mL	0.8%	0.2%
Standard 0.4006 mg/mL	1.2%	0.2%
Standard 0.5008 mg/mL	0.7%	0.2%
Starting solution (without oligonucleotide)	2.6%	0.2%
Drug product (with oligonucleotide)	1.2%	0.2%
Accuracy/recovery		
Concentration in sample (mg/mL)	**% Recovery**	
Starting solution (without oligonucleotide)	97.5 ± 3.6%	
Drug product (with oligonucleotide)	100.4 ± 1.6%	

TABLE 2 Results for validation and sample analysis using HPLC-UV234 nm and analysis by least squares linear regression

Linearity of calibration standards		
Range (mg/mL)	**Correlation coefficient (*R*)**	
0.02504–0.5008	1.000	
Repeatability (%RSD; n = 6) of triplicate injections of duplicate preparations for PEI determination		
	Area counts	**Retention time**
Standard 0.02504 mg/mL	3.6%	0.2%
Standard 0.05008 mg/mL	2.6%	0.2%
Standard 0.1002 mg/mL	0.8%	0.2%
Standard 0.2504 mg/mL	1.0%	0.2%
Standard 0.4006 mg/mL	0.6%	0.2%
Standard 0.5008 mg/mL	0.3%	0.2%
Starting solution (without oligonucleotide)	2.4%	0.2%
Drug product (with oligonucleotide)	4.5%	0.2%
Accuracy/recovery		
Concentration in sample (mg/mL)	**% Recovery**	
Starting solution (without oligonucleotide)	90.0 ± 2.3%	
Drug product (with oligonucleotide)	93.7 ± 4.3%	

quantitative determination of PEIs in both starting solution and oligonucleotide-containing drug product. The LOD was calculated to be 0.4 μg/mL and the LOQ was calculated to be 1.4 μg/mL. However, the accuracy was lower than expected compared to CAD, at only 90% for the starting solution and 94% for the formulated drug product. While investigating these lower recoveries, it was discovered that the different batches of PEI material used showed slightly different linear coefficients (slopes and *Y*-intercepts). Since the exact source of 234 nm absorbance is not well understood for linear PEIs, it is therefore recommended to generate PEI batch-specific calibration curves, ensuring that the batch of PEI used for preparing standards match that of the samples to ensure accuracy, when CAD is not an option.

Finally, the decomplexation step was tested for intermediate precision by a second analyst including the re-preparation of all solutions, digestion of the oligonucleotide-containing drug product, and use of a second chromatographic system at a different site.

Analysis was performed using only UV234 nm detection, which is the worst-case scenario for demonstrating interference with any intact oligonucleotide polyplexes. This analysis yielded an average recovery of 92.9 ± 1.9%, comparable to the data in Table 2 (93.7 ± 4.3%), showing satisfactory robustness of the decomplexation step of the oligonucleotide-containing drug product.

4 | CONCLUDING REMARKS

A rapid, specific, gradient UHPLC method using a CAD and/or a UV detector has been developed for the determination of pure linear PEI in solution or in a polyplex with oligonucleotide in formulation matrix. The sample preparation procedure using TFA to decomplex PEI/oligonucleotide polyplexes is simple and comprehensive. The method with both CAD and UV detection demonstrated acceptable specificity, accuracy, precision, and linearity for in-process control, with CAD being the preferred method to guide oligonucleotide polyplex formulation development. Furthermore, the method could be used to monitor the synthesis/purification and characterization of linear PEI.

ACKNOWLEDGMENTS

We wish to thank Cory Bottone, Eric Kemp, and Katelyn Smith for their invaluable discussions.

CONFLICT OF INTEREST

The authors have declared no conflict of interest.

ORCID

Adam Socia https://orcid.org/0000-0003-4754-4948

REFERENCES

1. Jäger, M., Schubert, S., Ochrimenko, S., Fischer, D., Schubert, U. S., Branched and linear poly(ethylene imine)-based conjugates: Synthetic modification, characterization, and application. Chem Soc Rev. 2012;41:4755–4767.
2. Saegusa, T., Ikeda, H., Fujii, H., Crystalline polyethylenimine. Macromolecules. 1972;5:108.
3. Bolto, B. A., Soluble polymers in water purification. Prog Polym Sci. 1995;20:987–1041.
4. Horn, D., Linhart, F., in: Roberts, J. C. (Ed.), Paper Chemistry, Springer, Dordrecht 1991, pp. 44–62.
5. Ramos-Tejada, M. M., Ontiveros-Ortega, A., Giménez-Martín, E., Espinosa-Jiménez, M., Molina Díaz, A., Effect of polyethyleneimine ion on the sorption of a reactive dye onto Leacril fabric: Electrokinetic properties and surface free energy of the system. J Colloid Interface Sci. 2006;297:317–321.
6. Bandyopadhyay, P., Ma, X., Linehan-Stieers, C., Kren, B. T., Steer, C. J., Nucleotide exchange in genomic DNA of rat hepatocytes using RNA/DNA oligonucleotides. Targeted delivery of liposomes and polyethyleneimine to the asialoglycoprotein receptor. J Biol Chem. 1999;274:10163–10172.
7. Kren, B. T., Bandyopadhyay, P., Steer, C. J., In vivo site-directed mutagenesis of the factor IX gene by chimeric RNA/DNA oligonucleotides. Nat Med. 1998;4:285–290.
8. Brissault, B., Kichler, A., Guis, C., Leborgne, C., Danos, O., Cheradame, H., Synthesis of linear polyethylenimine derivatives for DNA transfection. Bioconjugate Chem. 2003;14:581–587.
9. Prevette, L. E., Kodger, T. E., Reineke, T. M., Lynch, M. L., Deciphering the role of hydrogen bonding in enhancing pDNA-polycation interactions. Langmuir. 2007;23:9773–9784.
10. Prevette, L. E., Lynch, M. L., Kizjakina, K., Reineke, T. M., Correlation of amine number and pDNA binding mechanism for trehalose-based polycations. Langmuir. 2008;24:8090–8101.
11. Remy, J.-S., Behr, J.-P., Gene transfer with multivalent synthetic vectors. J Liposome Res. 1996;6:535–544.
12. Dai, Z., Gjetting, T., Mattebjerg, M. A., Wu, C., Andresen, T. L., Elucidating the interplay between DNA-condensing and free polycations in gene transfection through a mechanistic study of linear and branched PEI. Biomaterials. 2011;32:8626–8634.
13. Grayson, A. C., Doody, A. M., Putnam, D., Biophysical and structural characterization of polyethylenimine-mediated siRNA delivery in vitro. Pharm Res. 2006;23:1868–1876.
14. Lambermont-Thijs, H. M. L., van der Woerdt, F. S., Baumgaertel, A., Bonami, L., Du Prez, F. E., Schubert, U. S., Hoogenboom, R., Linear poly(ethylene imine)s by acidic hydrolysis of poly(2-oxazoline)s: Kinetic screening, thermal properties, and temperature-induced solubility transitions. Macromolecules. 2010;43:927–933.
15. Ungaro, F., De Rosa, G., Miro, A., Quaglia, F., Spectrophotometric determination of polyethylenimine in the presence of an oligonucleotide for the characterization of controlled release formulations. J Pharm Biomed Anal. 2003;31:143–149.
16. Wang, X., Kelkar, S. S., Hudson, A. G., Moore, R. B., Reineke, T. M., Madsen, L. A., Quantitation of complexed versus free polymers in interpolyelectrolyte polyplex formulations. ACS Macro Lett. 2013;2:1038–1041.
17. Center for Drug Evaluation and Research (CDER), ICH harmonised tripartite guideline for validation of analytical procedures: Text and methodology Q2(R1), Center for Drug Evaluation and Research (CDER), Rockville, MD 2005.
18. The United States Pharmacopeial Convention, United States Pharmacopeia and National Formulary (USP 42-NF 37) validation of compendial procedures <1225>, The United States Pharmacopeial Convention, Rockville, MD 2019.
19. Cohen, R. D., Liu, Y., Advances in aerosol-based detectors. Adv Chromatogr. 2014;52:1–53.
20. Kakui, T., Nanoparticle Technology Handbook, Elsevier, Amsterdam, The Netherlands 2018.
21. Cohen, R. D., Liu, Y., Gong, X., Analysis of volatile bases by high performance liquid chromatography with aerosol-based detection. J Chromatogr A. 2012;1229:172–179.
22. Blake, R. D., Delcourt, S. G., Thermodynamic effects of formamide on DNA stability. Nucleic Acids Res. 1996;24:2095–2103.
23. Levine, L., Gordon, J. A., Jencks, W. P., The relationship of structure to the effectiveness of denaturing agents for deoxyribonucleic acid. Biochemistry. 1963;2:168–175.

24. Marmur, J., Ts'o, P. O. P., Denaturation of deoxyribonucleic acid by formamide. Biochim Biophys Acta. 1961;51:32–36.
25. Moelbert, S., Normand, B., De Los Rios, P., Kosmotropes and chaotropes: Modelling preferential exclusion, binding and aggregate stability. Biophys Chem. 2004;112:45–57.
26. Wang, X., Lim, H. J., Son, A., Characterization of denaturation and renaturation of DNA for DNA hybridization. Environ Anal Health Toxicol. 2014;29:e2014007.
27. Wen, T., Qu, F., Li, N. B., Luo, H. Q., A facile, sensitive, and rapid spectrophotometric method for copper(II) ion detection in aqueous media using polyethyleneimine. Arabian J Chem. 2017;10:S1680–S1685.
28. Fibigr, J., Šatínský, D., Solich, P., A UHPLC method for the rapid separation and quantification of phytosterols using tandem UV/charged aerosol detection—A comparison of both detection techniques. J Pharm Biomed Anal. 2017;140:274–280.

SUPPORTING INFORMATION

Additional supporting information may be found online in the Supporting Information section at the end of the article.

Received: 14 March 2022 | Revised: 16 June 2022 | Accepted: 8 July 2022

DOI: 10.1002/pca.3166

RESEARCH ARTICLE

Phytochemical Analysis WILEY

Quality analysis of hawthorn leaves (the leaves of *Crataegus pinnatifida* Bge. var *major* N.E.Br) in different harvest time

Wei Zheng[1] | **Ming Zhou**[1] | **Rui-ping Chai**[2] | **Hai-zhen Liang**[1] | **Jie Zhang**[1] | **Ye Zhao**[3] | **Xiao-hui Zheng**[3] | **Yan Jin**[2] | **Bao-lin Guo**[4] | **Bai-ping Ma**[1]

[1]Beijing Institute of Radiation Medicine, Beijing, China

[2]Thermo Fisher Scientific (China), Shanghai, China

[3]College of Life Sciences, Northwest University, Xi'an, China

[4]Institute of Medicinal Plant Development, Chinese Academy of Medical Sciences, Peking Union Medical College, Beijing, China

Correspondence
Baiping Ma, PhD, Beijing Institute of Radiation Medicine, No.27 Taiping Road, Haidian District, Beijing 100850, China.
Email: mabaiping@sina.com

Funding information
Project of Key Research and Development Plan of Shaanxi, Grant/Award Number: 2017ZDCXL-SF-01-02-01; The Key Project of Research and Development Plan of Shaanxi, Grant/Award Number: 2017ZDXM-SF-017; Programme for Changjiang Scholars and Innovative Research in University, Grant/Award Number: IRT_15R55; National Natural Science Foundation of China, Grant/Award Number: 82074008

Abstract

Introduction: Harvest time plays an important role on the quality of medicinal plants. The leaves of *Crataegus pinnatifida* Bge. var *major* N.E.Br (hawthorn leaves) could be harvested in summer and autumn according to the Pharmacopoeia of the People's Republic of China (Pharmacopoeia). However, little is known about the difference of the chemical constituents in hawthorn leaves with the harvest seasonal variations.

Objective: The chemical constituents of hawthorn leaves in different months were comprehensively analysed to determine the best harvest time.

Methods: Initially, the chemical information of the hawthorn leaves were obtained by ultra-high-performance liquid chromatography and quadrupole time-of-flight mass spectrometry (UHPLC-Q-TOF-MS). Subsequently, principal component analysis (PCA) was applied to compare the chemical compositions of hawthorn leaves harvested in different months. Then, an absolute quantitation method was established using high-performance liquid chromatography-charged aerosol detector (HPLC-CAD) to determine the contents of five compounds and clarify the changes of these components with the harvest seasonal variations. Meanwhile, a semi-quantitative method by integrating HPLC-CAD with inverse gradient compensation was also established and verified.

Results: Fifty-eight compounds were identified through UHPLC-Q-TOF-MS. PCA revealed that the harvest season of hawthorn leaves had a significant effect on the chemical compositions. The contents of five components were relatively high in autumn. Other four main components without reference standards were further analysed through the semi-quantitative method, which also showed a high content in autumn.

Conclusions: This work emphasised the effect of harvest time on the chemical constituents of hawthorn leaves and autumn is recommended to ensure the quality.

KEYWORDS

harvest time, hawthorn leaves, inverse gradient compensation, quality control, quantitative method

1 | INTRODUCTION

Medicinal plants have been used as health food or medicine for a long time, and they also have a marked influence on the discovery and development of the final drug entity. For example, from 1980s to the September 2019, 33.5% of the 185 small molecule of cancer drugs were either medicinal plants or directly derived therefrom.[1] The chemical compositions of medicinal plants are complex. For instance, more than 200 chemical components including saponins, flavonoids and cyclopeptides, have been isolated from *Panax notoginseng* (Burk.) F.H. Chen.[2] Furthermore, the biosynthesis of chemical components is affected by the growth and development of the plant, thus the quality of plants which are harvested in different months might be discrepant.[3] For example, the taxoid content of *Taxus wallichiana* var. *mairei* is highest in January, while the lowest value is in autumn, and the total flavonoids is observed highest in August, compared to the lower level in March.[4] Due to the complexity and diversity of the compositions, the content changes of different types of compounds of medicinal plants collected at different harvest time are obviously varied, thus the more enriched knowledge about the harvest time of medicinal plants could help us establish a comprehensive quality control method to ensure their stable clinical efficacy.

Hawthorn, which has been reported to encompass over 200 species, are widely distributed in the northern hemisphere, mostly in China, Europe, and North America.[5,6] The composition of hawthorn is intricate and over 150 chemical constituents, including 49 flavonoids, five hydroxycinnamic acids, six sugars, 10 organic or phenolic acids, 26 terpenes, and 56 essential oil constituents have been reported.[5,7,8] In Europe, the fruits, leaves, and flowers of hawthorn are traditionally used in the treatment of heart problems.[9] In China, only leaves and fruits of two species of hawthorn, *Crataegus pinnatifida* Bge. and *C. pinnatifida* Bge. var *major* N.E.Br are used in tradition Chinese medicine. The leaves can be both harvested in summer and autumn according to the Pharmacopoeia of the People's Republic of China (Pharmacopoeia). Meanwhile, immense medicinal applications have been reported in hawthorn leaves, such as antihypertensive activity,[10] anti-arrhythmic activity,[11] antiviral activity[12] and so on. Flavonoids in the hawthorn leaves were found to significantly reduce atherosclerotic lesion areas; two triterpenoid acids (oleanolic acid and ursolic acid) can reduce very low-density lipoprotein (VLDL) and low-density lipoprotein (LDL) cholesterol levels with the ability to inhibit the acyl-coA-cholesterol acyltransferase (ACAT) enzyme.[13] Not only that, Mexican hawthorn (*Crataegus gracilior* J. B. Phipps) stems and leaves induced cell death on breast cancer cells.[14] The different types of chemical composition has led to the diversity in the activity of medicinal plants. However, in the 2020-edition of the Pharmacopoeia, only total flavonoids and hyperoside are considered the markers of quality control without other components. Existing studies have only focused on the plant development changes of flavonoids,[15] while, there is no available report concerning the comprehensive analysis of all types of components in hawthorn leaves which are collected in different harvest time. Therefore, it is necessary to develop a specific method to comprehensively analyse the chemical constitution of hawthorn leaves harvested at different development stages.

Owing to high resolution and sensitivity, ultra-high-performance liquid chromatography and quadrupole time-of-flight mass spectrometry (UHPLC-Q-TOF-MS) has been used to analyse the complex samples, including medicinal plants and their prescriptions.[16,17] In addition, in order to achieve the in-depth and automatic understanding of the medicinal plants, more and more chemical composition databases have been built and used for the analysis of the complicated components of medicinal plants.[18,19] For the quality control of medicinal plants, we should not only understand the composition of medicinal plants, but also discuss the changes of their contents. In recent years, the charged aerosol detector (CAD) has become a valuable tool for fast and efficient quantitative chromatographic analysis of drug substances with weak ultraviolet absorption. Compared with other aerosol-based universal detectors, the CAD is more sensitive than the evaporative light scattering detector (ELSD), and more widespread than the condensation nucleation light scattering detector (CNLSD).[20,21] Since the response of the CAD varies as a function of the mobile-phase composition, an increase in the organic content of the mobile phase leads to an increase in the transport efficiency of the nebuliser, which results in a greater number of particles reaching the detector chamber and in a higher signal. The inverse gradient compensation method, providing the detector with a constant composition of the mobile phase for a uniform response at all times,[22] was established to conduct the fast quantitative or semi-quantitative analysis of analytes without standards.[23] Due to the uniform response with gradient compensation, when the relative correction factor of every compound reaches 1, the absolute quantitative result of one component can be used to define other components in the sample, so as to establish a more convenient quantitative method to determine the components without reference substance.

In this study, a comprehensive qualitative analysis of the chemical constituents based on UHPLC-Q-TOF-MS and quantitative analysis of main components by HPLC-CAD were performed to evaluate the quality of leaves of *C. pinnatifida* var. *major* in different harvest time. Firstly, a multicomponent identification workflow based on the hawthorn self-built database was built and then used to identified the hawthorn leaves by UHPLC-Q-TOF-MS. Secondly, the chemome of hawthorn leaves harvested in different time were clarified by principal component analysis (PCA). Subsequently, five representative primary components (caffeic acid, vitexin-2″-*O*-rhamnoside, hyperoside, euscaphic acid, and ursolic acid) in hawthorn leaves were selected for the absolute quantitative analysis by HPLC-CAD. Relying on the inverse gradient compensation method of CAD and adjusting the power function value to 0.7, a semi-quantitative method was established to reflect the content difference of all kinds of components of hawthorn leaves intuitively, which was verified by the earlier absolute quantitation. This research comparatively analyses the phytochemicals of hawthorn leaves in different harvest time, and these results will support the

exploration of collecting time of hawthorn leaves of *C. pinnatifida* var. *major*.

2 | EXPERIMENTAL

2.1 | Chemicals and materials

HPLC grade acetonitrile (ACN) and UPLC grade formic acid (FA) were obtained from Fisher Scientific (Loughborough, UK). Distilled water was purchased from Watson's Food & Beverage Co., Ltd (Guangzhou, China). The other reagents were obtained in analytical grade from commercially (Beijing, China). Five standards, caffeic acid, vitexin-2″-*O*-rhamnoside, hyperoside, euscaphic acid, ursolic acid, for quantitative analysis were purchased from Chengdu DeSiTe Biological Technology Co., Ltd (Sichuan, China), the purity of these compounds was greater than 98%. The other 15 standards were isolated in our laboratory and their structures were confirmed by comparing their MS and nuclear magnetic resonance (NMR) spectral data, including chlorogenic acid, epicatechin, procyanidin B2, (6*S*,7*E*,9*R*)-6,9-dihydroxy-4,7-megastigmadien-3-one-9-*O*-β-D-glucopyranoside, nikoenoside, vitexin, vitexin-4″-*O*-glucoside, quercetin-3-*O*-β-D-glucoside, epicatechin-(4$\beta \rightarrow$ 8)-epiafzelechin, icariside B_6, linalyl rutinoside, 2α,3β,19α-trihydroxyursolic acid, 19α-hydroxyursolic acid, crataegolic acid, and corosolic acid. The purity of these compounds was greater than 95%, as determined by HPLC-CAD analysis.

Twenty-one batches of leaves of *C. pinnatifida* Bge. var *major* N.E. Br were collected from Beijing Haidian district, China. Detailed information of all samples was shown in Supporting Information Table S1. The identity of the plant was authenticated by Prof. Bao-lin Guo of the Institute of Medicinal Plant Development, Chinese Academy of Medical Sciences & Peking Union.

2.2 | Standard and sample preparation

Stock solutions of five standard references of quantitative analysis were prepared in methanol at a final concentration of 1.0 mg/mL. The other 15 references were also dissolved into methanol of 0.3 mg/mL for UHPLC-Q-TOF-MS analysis. All the solutions were stored at 4°C for further study.

An aliquot of 0.2 g fine powder (< 40 mesh) of each sample was accurately weighed, and added into 10 mL of 70% aqueous ethanol, tightly plugged, shaken, and then weighed. After sonication for 30 min, the sample was cooled down to room temperature and made up for weight loss with 70% aqueous ethanol. All the solutions were filtered through a 0.22 μm filter membrane before analysis, and then, 2 μL was injected for UHPLC-Q-TOF-MS analysis, and 10 μL was injected into HPLC-CAD for quantitative analysis. Twenty-one batches of sample solution were blended equivalently as a quality control (QC) sample, which was inserted in every five injections during the UHPLC-Q-TOF-MS analysis to monitor the system stability and to minimise the analytical variation.

2.3 | Qualitative analysis of hawthorn leaves by UHPLC-Q-TOF-MS

UHPLC-Q-TOF-MS analysis was performed using a Waters ACQUITY I-Class system (Waters Corp., Milford, MA, USA) coupled with a VION-IMS-QTOF system (Waters Corp., Wilmslow, UK). A Waters ACQUITY UPLC HSS T3 column (100 mm × 2.1 mm, 1.8 μm) was used at a column temperature of 40°C. The mobile phases included water with 0.1% FA (A) and ACN (B). The gradient used was as follows: 0-6 min, 5–16% B; 6–8 min, 16% B; 8–12 min, 16–47% B; 12–15 min, 47–48% B; 15–17 min, 48–49% B; 17–18 min, 49–54% B; 18–20 min, 54–56% B; 20–22 min, 56–78% B; 22–23 min, 78–95% B. The flow rate was 0.5 mL/min. The data acquisition mode was MS^E. Each sample was injected both for positive electrospray ionisation (ESI^+) analysis and negative electrospray ionisation (ESI^-) analysis, and the data were acquired from 50 to 1500 Da. For MS, the conditions were as follows: the source temperature was 110°C, and the desolvation temperature was set at 450°C, with desolvation gas flow of 850 L/h. The capillary voltages were 3 kV (ESI^+) and 2.5 kV (ESI^-). The collision energy (CE) was 4 eV. At high CE scan, the CE was 20–40 eV ramp for ESI^+ analysis and 30–50 eV ramp for ESI^- analysis, respectively. The leucine-enkephalin was used as the lock mass. The instrument was controlled by UNIFI 1.9.4 software (Waters Corp., Milford, MA, USA).

2.4 | Multivariate statistical analysis

All data acquisition in MS^E mode was in continuum mode, and the raw data was processed by UNIFI 1.9.4 and Umetrics Ezinfo 3.0. The data analysis included deconvolution, alignment and data reduction to provide a list of mass and retention time (RT) pairs along with corresponding peak areas for all the detected peaks from each file in the data set. The processed data list was then imported by PCA. All test groups were discriminated in the PCA to investigate whether different groups can be separated. The parameters used in the analysis were 0–24 min for RT range, 100–1500 Da for mass range, 0.02 Da for mass tolerance and 0.10 min for RT tolerance. Meanwhile, the isotopic peaks were excluded for analysis.

2.5 | Quantitative analysis of main components by HPLC-CAD

The quantitative analysis was performed on Vanquish Core system (Thermo Fisher Scientific, Germering, Germany) equipped with dual pump C, autosampler C, column compartment C and charged aerosol detector H. A Thermo Accucore Phenyl-X column (150 mm × 4.6 mm, 2.6 μm) was used at a column temperature of 40°C. The mobile phases included water with 0.2% FA (A) and ACN (B). The gradient used was as follows: 0–3 min, 10–15% B; 3–10 min, 15–20% B; 10–13 min, 20% B; 13–23 min, 20–30% B; 23–55 min, 30–65% B; 55–65 min, 65–85% B; 65–70 min, 85–95% B. The flow rate was 0.7 mL/min. CAD evaporator temperature was set at 35°C, and the

nitrogen gas pressure for the nebuliser was set at 0.6 MPa. Data collection rate was set at 5 Hz, using a filter constant of 5 s. Chromeleon 7 software (Thermo Fisher Scientific) was used for data acquisition and analysis. A Thermo Acclaim 120 C18 (150 mm × 2.1 mm, 3 μm) was used for gradient compensation trials, the power function value was 0.7, and the inverse gradient was calculated automatically through Chromeleon 7 software.

3 | RESULTS AND DISCUSSION

3.1 | Characterisation of various components

A components database of hawthorn was established through literatures and databases, including name, formula, major fragment ions, and the mol. files of compound structures. Moreover, the reference standards were classified according to their structural types, and their characteristic fragments were obtained by MS/MS scanning of quasi-molecular ions in both positive and negative ion modes and supplemented into the database. Each sample was analysed under the ESI^+ and ESI^- mode with the same LC mobile phase to obtain the comprehensive information on the fragmentations and chromatography patterns of various components. Based on the fragment ions and RTs, 58 components including organic acids, flavonoids, triterpenoid acids, monoterpenes and sesquiterpenoids were identified or tentatively identified (Figure 1 and Table S2), and for the detailed identification process of components refer to our published work.[24]

3.2 | The discrimination of hawthorn leaves in different harvest time by PCA

All the UHPLC-Q-TOF-MS data of hawthorn leaves collected within 0–24 min were analysed by using UNIFI 1.9.4 software to obtain PCA score plots, so as to more intuitively understand the differences between hawthorn leaves samples from different months. According to the PCA (Figure 2), the change of chemical composition in the whole growth cycle of hawthorn leaves could be roughly divided into three stages. Stage I is the rapid growth period (April and May), stage II is the relatively stable growth period (June to September), and stage III is the recession period (October).

3.3 | Quantitative analysis of different samples by HPLC-CAD

Various components in hawthorn leaves contribute to its activity together, for instance, flavonoids could reduce atherosclerotic lesion

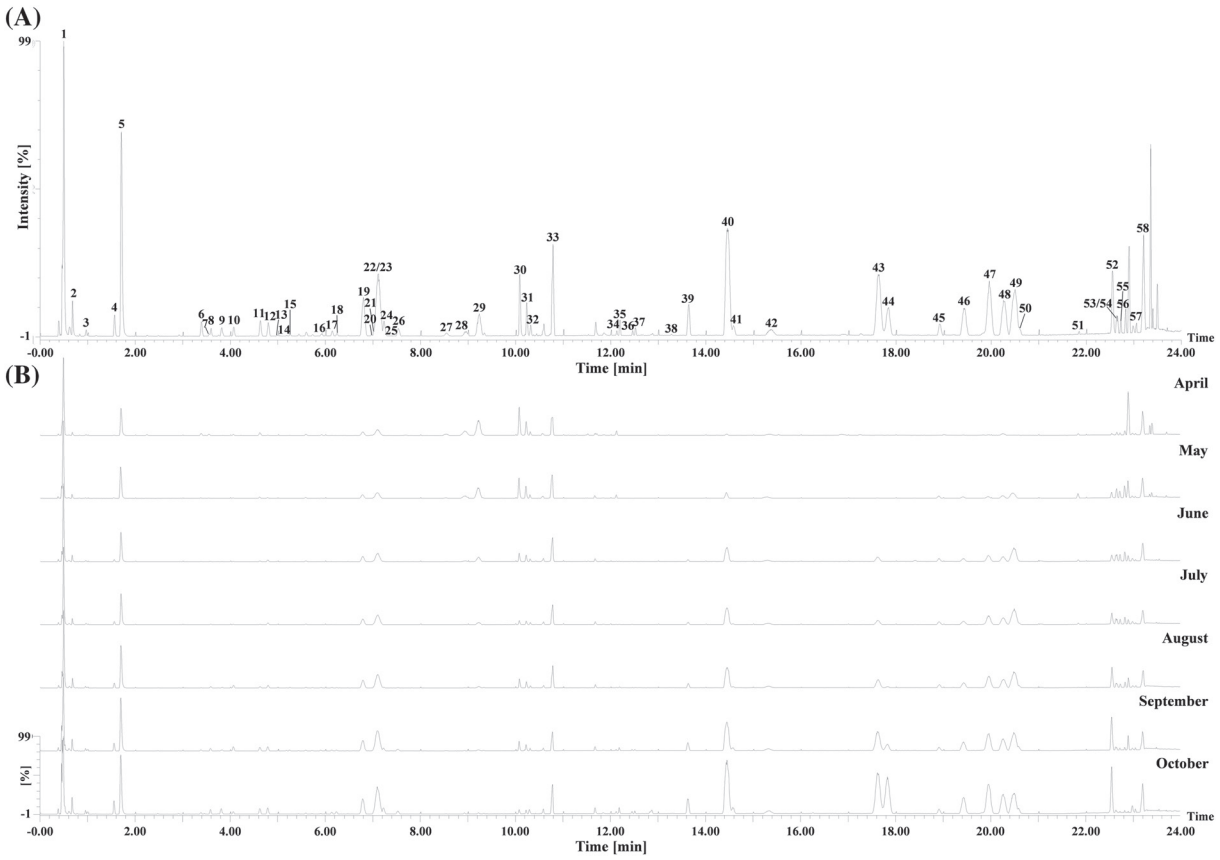

FIGURE 1 Base peak intensity (BPI) chromatograms of QC sample (A) and samples in different harvest time (B) of hawthorn leaves in negative ion mode by UHPLC-Q-TOF-MS^E analysis. The peak numbers are consistent with those in Supporting Information Table S2.

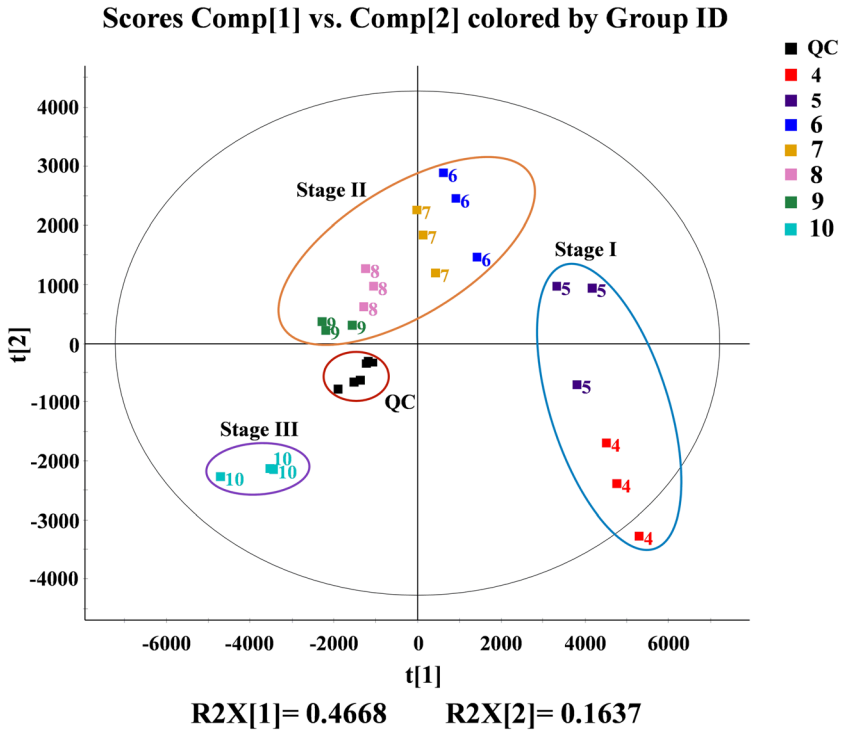

FIGURE 2 PCA score plots of hawthorn leaves in different harvest time. QC represents the quality control sample, and numbers 4–10 represent different months.

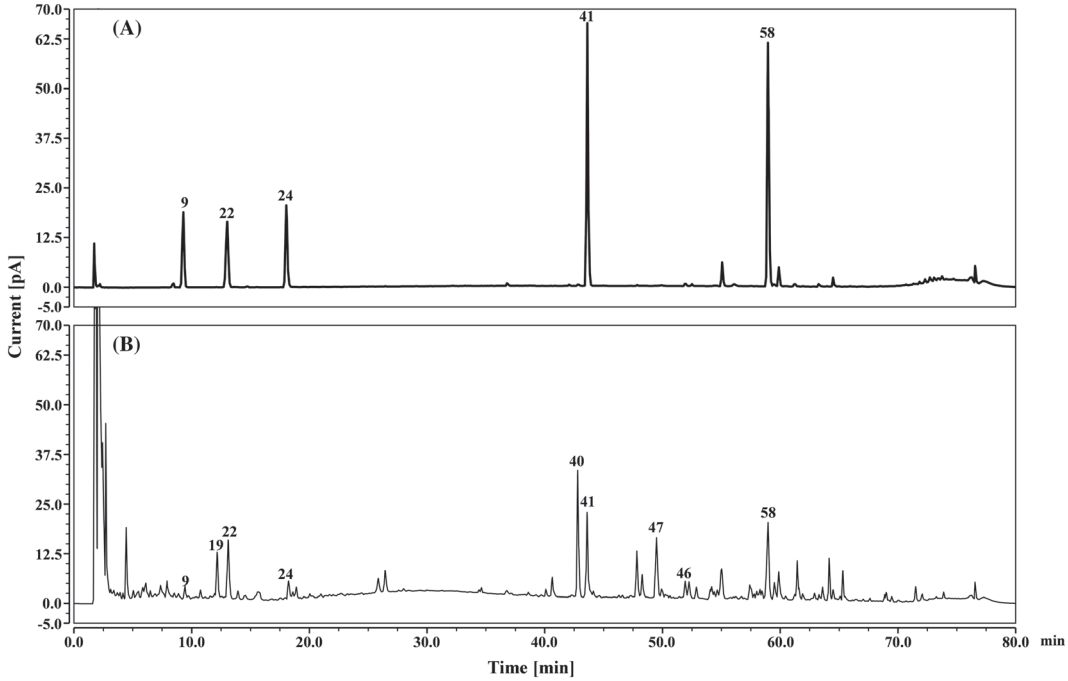

FIGURE 3 The typical chromatograms of reference standards (A) and QC sample (B) by HPLC-CAD analysis. Peak 9 (caffeic acid), peak 22 (vitexin-2″-*O*-rhamnoside), peak 24 (hyperoside), peak 41 (euscaphic acid), and peak 58 (ursolic acid), were used for quantitative analysis, as well as peak 19 (vitexin-4″-*O*-glucoside), peak 40 (2α,3β,19α-trihydroxyursolic acid), peak 46 (19α-hydroxyursolic acid), and peak 47 (crataegolic acid) were used for semi-quantitative analysis.

areas; two triterpenoid acids (oleanolic acid and ursolic acid) could reduce LDL and VLDL by inhibiting the ACAT enzyme, flavonoids and organic acids had synergetic effects for lipid lowering effects.[7,13] To further understand the variation in the contents of the main components harvested from different time, a HPLC-CAD approach was developed for absolute quantitative analysis of three types of

components of organic acids (caffeic acid, peak 9), flavonoids (vitexin-2″-*O*-rhamnoside, peak 22 and hyperoside, peak 24) and triterpenoid acids (euscaphic acid, peak 41 and ursolic acid, peak 58) in 21 samples.

Linear regression analysis of caffeic acid, vitexin-2″-*O*-rhamnoside, hyperoside, euscaphic acid, and ursolic acid were performed by the external standard method. The square of all the correlation coefficients (R^2) of these calibration curves were higher than 0.999. The limit of detection (LOD) and limit of quantification (LOQ) were determined at a signal-to-noise ratio (*S/N*) of 3 and 10, respectively. The results are shown in Table S3. The mixed standard solutions were analysed six times for precision. In addition, in order to confirm the repeatability, six different working solutions prepared from the same sample were analysed, one of them was also tested after 4, 8, 12, 24, and 48 h at room temperature for stability. The relative standard deviation (RSD) was taken as a measure of precision, repeatability, and stability. The results proved that the samples were stable and this assay has good precision and reproducibility with RSD less than 4.0% ($n = 6$) for the five analytes. Besides, recovery test was used to evaluate the accuracy of this method. Accurate amounts of five analytes were added to approximate 0.1 g of sample, which was then analysed as described earlier. The overall recoveries ranging from 96.97% to 102.76%, with RSD ranging from 1.91 to 4.13%. All results are given in Table S3. In summary, the HPLC-CAD method was precise, accurate and sensitive enough for simultaneously quantitative evaluation of these components in hawthorn leaves. A typical chromatogram of reference standards and sample is shown in Figure 3.

All 21 batches of samples were analysed by the established method, and the result was listed in Table S4. The contents of these components were averaged at each time, and the change trend graph of the content was draw according to the average value. As shown in Figure 4, the contents of caffeic acid and hyperoside were relatively low, which decreased first and then increased from August, while the content decreased slightly in October. Vitexin-2″-*O*-rhamnoside is a representative main flavonoid in hawthorn leaves, and the content gradually increased to a stable level with the change of months. Euscaphic acid is one of the main triterpenoid acids, where the content was lowest in spring, and gradually accumulated until reached the highest level in October. Although ursolic acid is also a triterpenoid acid, its content gradually decreased. While, compared with caffeic acid and hyperoside, the content of ursolic acid was also relatively high in autumn. According to the content and change trend of these five components, it is one-sided to only detect the contents of hyperoside and total flavonoids in the quality control of hawthorn leaves. Although the contents of different types of components varied with the different harvest time, the autumn harvest can ensure that the contents of these five components were relatively high.

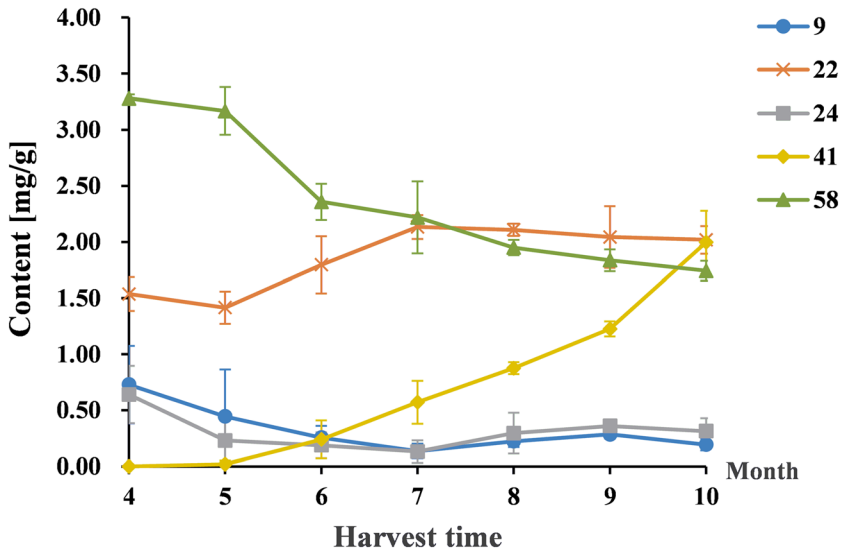

FIGURE 4 The change trends of the contents of five analytes in different harvest time. Peak 9 (caffeic acid), peak 22 (vitexin-2″-*O*-rhamnoside), peak 24 (hyperoside), peak 41 (euscaphic acid), and peak 58 (ursolic acid).

TABLE 1 The response factors of five analytes before and after the inverse gradient compensation. Peak 9 (caffeic acid), peak 22 (vitexin-2″-*O*-rhamnoside), peak 24 (hyperoside), peak 41 (euscaphic acid), and peak 58 (ursolic acid)

	Peak 9	Peak 22	Peak 24	Peak 41	Peak 58	Relative standard deviation (%)
Peak area (before gradient compensation)	3.097 4	2.903 5	3.170 6	7.270 3	6.740 9	
Peak area (after gradient compensation)	3.529 3	3.026 1	3.076 7	3.896 2	3.268 8	
Concentration (μg/mL)	50	50	50	50	50	
Response factor (before gradient compensation)	0.061 9	0.058 1	0.063 4	0.145 4	0.134 8	46.87
Response factor (after gradient compensation)	0.070 6	0.060 5	0.061 5	0.077 9	0.065 3	10.69

3.4 | A semi-quantitative method with the power function value as 0.7

CAD combined with inverse gradient compensation method was established to analyse hawthorn leaves. In order to evaluate the feasibility of this semi-quantitative method, the response factors (equation 1) and the relative correction factors (f_{si}, equation 2) of five quantitative analytes were compared before and after the inverse gradient compensation. Because hyperoside is the quality control marker in the Pharmacopoeia, it was used as an internal standard to calculate the relative correction factor. As shown in Table 1, the RSD (46.87%) of the response factors of these five components were significantly reduced after inverse gradient compensation (RSD: 10.69%), indicating that their response tended to be more consistent after inverse gradient compensation by CAD. However, due to the high response of euscaphic acid, the relative correction factor was not 1, as shown in Tables 1 and 2, so the semi-quantitative method relying on inverse gradient compensation was not feasible for this compound.

$$\text{response factor} = A_i / C_i \quad (1)$$

$$f_{si} = (A_s / C_s) / (A_i / C_i) \quad (2)$$

where A_i and A_s are the peak area of the other four analytes and hyperoside; C_i and C_s are the concentration of the other four analytes and hyperoside.

The influencing factors of the inverse gradient compensation method contain power function value (PFV), inverse gradient offset, and so on. Among them, PFV could increase the signal and extend the linear dynamic range of CAD. Therefore, in recent years, attention has been paid to the optimisation of PFV in the establishment of quantitative methods.[25] Normally, PFV was set as 1. Taking 0.1 as a gradient, the effects of PFV = 0.7–1.5 on the response factor of 50 μg/mL of these five analytes were investigated respectively (Table 3). With the PFV decreasing, their responses were gradually approaching. The electrospray of CAD would encapsulate the positive charge on the detected component and hydroxyl groups exist in the form of negatively charged ions (OH^-). Therefore, it was speculated that euscaphic acid could attract more positive charges to have higher response because of three hydroxyl groups. PFV will not only improve the linearity, but also affect the response of every chromatographic peak and the accuracy of determination. Therefore, the determination of PFV

TABLE 2 The relative correction factors (f_{si}) of other four analytes with hypericum as internal standard. Peak 9 (caffeic acid), peak 22 (vitexin-2″-*O*-rhamnoside), peak 24 (hyperoside), peak 41 (euscaphic acid), and peak 58 (ursolic acid)

Concentration (μg/mL)	$f_{24/9}$	$f_{24/22}$	$f_{24/41}$	$f_{24/58}$
10	1.228	1.042	0.712	0.907
25	1.027	1.016	0.735	0.904
50	0.919	1.009	0.754	0.915
75	0.917	1.008	0.773	0.921
100	0.885	0.998	0.760	0.910
Mean	0.995	1.014	0.747	0.912

TABLE 3 The response factors of five analytes with different power function value (PFV) after the inverse gradient compensation. Peak 9 (caffeic acid), peak 22 (vitexin-2″-*O*-rhamnoside), peak 24 (hyperoside), peak 41 (euscaphic acid), and peak 58 (ursolic acid)

PFV		Peak 9	Peak 22	Peak 24	Peak 41	Peak 58	Relative standard deviation (%)
0.7	Peak area	9.663 5	8.742 3	8.679 0	10.163 3	9.453 0	
	Response factor	0.193 3	0.174 8	0.173 6	0.203 3	0.189 1	6.75
0.8	Peak area	6.270 3	5.626 1	5.368 4	6.762 4	6.237 3	
	Response factor	0.125 4	0.112 5	0.107 4	0.135 2	0.124 7	9.18
0.9	Peak area	4.216 0	3.834 1	3.570 3	4.847 9	4.284 4	
	Response factor	0.084 3	0.076 7	0.071 4	0.097 0	0.085 7	11.71
1.0	Peak area	3.199 0	2.629 1	2.646 5	3.451 6	3.096 3	
	Response factor	0.064 0	0.052 6	0.052 9	0.069 0	0.061 9	11.95
1.1	Peak area	2.318 9	1.853 6	1.784 9	2.464 9	2.160 3	
	Response factor	0.046 4	0.037 1	0.035 7	0.049 3	0.043 2	13.84
1.2	Peak area	1.493 1	1.256 5	1.212 9	1.775 1	1.549 4	
	Response factor	0.029 9	0.025 1	0.024 3	0.035 5	0.031 0	15.75
1.3	Peak area	1.029 6	0.861 0	0.859 6	1.268 9	1.046 7	
	Response factor	0.020 6	0.017 2	0.017 2	0.025 4	0.020 9	16.63
1.4	Peak area	0.753 3	0.579 1	0.578 6	0.896 2	0.725 2	
	Response factor	0.015 1	0.011 6	0.011 6	0.017 9	0.014 5	18.87
1.5	Peak area	0.523 8	0.392 3	0.404 2	0.647 9	0.519 3	
	Response factor	0.010 5	0.007 8	0.008 1	0.013 0	0.010 4	20.98

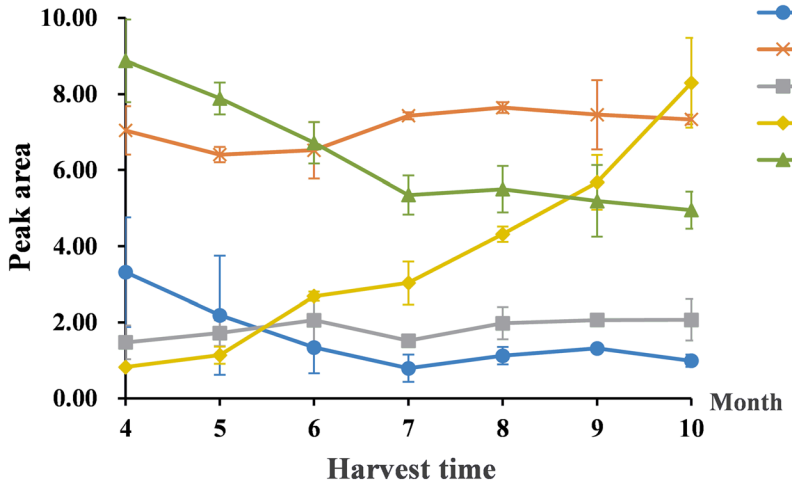

FIGURE 5 The changes in the peak areas of five analytes in different harvest time after inverse gradient compensation by CAD. Peak 9 (caffeic acid), peak 22 (vitexin-2″-*O*-rhamnoside), peak 24 (hyperoside), peak 41 (euscaphic acid), and peak 58 (ursolic acid).

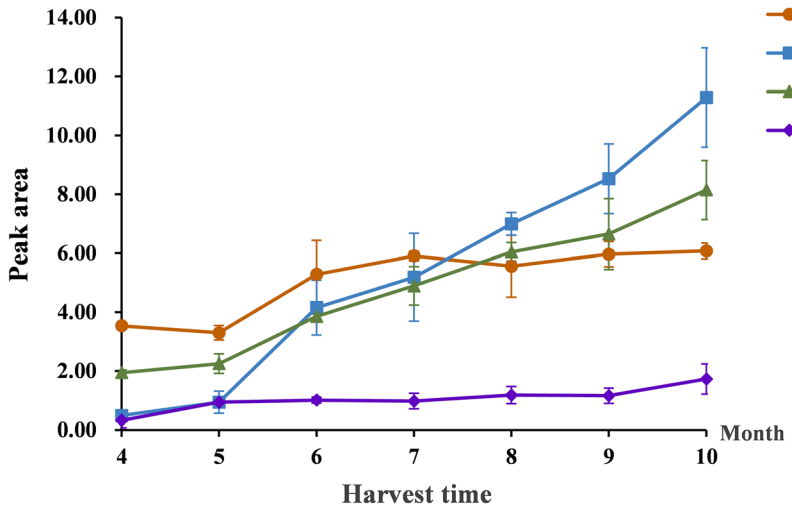

FIGURE 6 The changes in the peak areas of the other four analytes without reference in different harvest time after inverse gradient compensation by CAD. Peak 19 (vitexin-4″-*O*-rhamnoside), peak 40 (2α,3β,19α-trihydroxyursolic acid), peak 46 (19α-hydroxyursolic acid), and peak 47 (crataegolic acid).

needs to be further optimised, not just fixed as 1 directly. In this experiment, 0.7 was set as PFV, and the semi-quantitative method was established to analyse hawthorn leaves in different harvest time after inverse gradient compensation by CAD. The peak areas of five components (Table S5) were averaged at each time, and the change trends of peak areas were drawn according to the average value with different month. As shown in Figure 5, the change trends of the peak areas of five analytes were consistent with their contents, indicating that the semi-quantitative method is successful and validated through CAD combined with inverse gradient compensation. We also used the established semi-quantitative method to analyse other four main components without standards (Table S5), including one flavonoid (vitexin-4″-*O*-glucoside) and three triterpenoid acids (2α,3β,19α-trihydroxyursolic acid, 19α-hydroxyursolic acid and crataegolic acid). As shown in Figure 6, these four components showed an increasing trend as spring to autumn. Vitexin-4″-*O*-glucoside (peak 19) is another major flavonoid in hawthorn leaves. With plant development variation, its content fluctuated. It rose to the highest in July, decreased slightly in August, and then increased slowly from September to October. Compared with Figure 5, 2α,3β,19α-trihydroxyursolic acid (peak 40) is the largest amount of triterpenoid acid in hawthorn leaves, and its change trend was also consistent with peak 41. The content of peak 47 (crataegolic acid) was slightly lower than peak 41, and also showed a steady upward trend. The content and the increasing trend of 19α-hydroxyursolic acid (peak 46) were the lowest. Because the relative correction factor was not 1, the absolute quantification of unknown components cannot be realised using the peak area. However, due to the response of every component was closer after the inverse gradient compensation, the content relationship of corresponding components could be directly reflected by the peak area.

ACKNOWLEDGEMENTS

This work is financially supported by the National Natural Science Foundation of China (82074008), Programme for Changjiang Scholars and Innovative Research in University (IRT_15R55), Project of Key Research and Development Plan of Shaanxi (No.2017ZDCXL-SF-01-02-01) and The Key Project of Research and Development Plan of Shaanxi (2017ZDXM-SF-017).

CONFLICTS OF INTEREST

The authors declare no conflict in relation to this work.

DATA AVAILABILITY STATEMENT

The data that support the findings of this study are openly available in [repository name e.g "figshare"] at https://doi.org/[doi], reference number [reference number].

ORCID

Bai-ping Ma https://orcid.org/0000-0002-0810-0466

REFERENCES

1. Newman DJ, Cragg GM. Natural products as sources of new drugs over the nearly four decades from 01/1981 to 09/2019. *J Nat Prod*. 2020;83(3):770-803.
2. Wang T, Guo R, Zhou G, et al. Traditional uses, botany, phytochemistry, pharmacology and toxicology of *Panax notoginseng* (Burk.) F.H. Chen: a review. *J Ethnopharmacol*. 2016;188:234-258.
3. Pacifico S, Galasso S, Piccolella S, et al. Seasonal variation in phenolic composition and antioxidant and anti-inflammatory activities of *Calamintha nepeta* (L.) Savi. *Food Res Int*. 2015;69:121-132.
4. Yang L, Zheng ZS, Cheng F, et al. Seasonal dynamics of metabolites in needles of *Taxus wallichiana* var. *mairei*. *Molecules*. 2016;21(10):1403.
5. Edwards JE, Brown PN, Talent N, Dickinson TA, Shipley PR. A review of the chemistry of the genus *Crataegus*. *Phytochemistry*. 2012;79:5-26.
6. Lund JA, Brown PN, Shipley PR. Differentiation of *Crataegus* Spp Guided by Nuclear Magnetic Resonance Spectrometry with Chemometric Analyses. *Phytochemistry*. 2017;141:11-19.
7. Wu J, Peng W, Qin R, Zhou H. *Crataegus pinnatifida*: chemical constituents, pharmacology, and potential applications. *Molecules*. 2014;19(2):1685-1712.
8. Li CR, Hou XH, Xu YY, Gao W, Li P, Yang H. Manual annotation combined with untargeted metabolomics for chemical characterization and discrimination of two major *Crataegus* species based on liquid chromatography quadrupole time-of-flight mass spectrometry. *J Chromatogr A*. 1612;2020:460628.
9. Chang Q, Zuo Z, Harrison F, Chow MS. Hawthorn. *J Clin Pharmacol*. 2002;42(6):605-612.
10. Koçyildiz ZC, Birman H, Olgaç V, Akgün-Dar K, Melikoğlu G, Meriçli AH. *Crataegus tanacetifolia* leaf extract prevents L-NAME-induced hypertension in rats: a morphological study. *Phytother Res*. 2006;20(1):66-70.
11. Long SR, Carey RA, Crofoot KM, Proteau PJ, Filtz TM. Effect of hawthorn (*Crataegus oxycantha*) crude extract and chromatographic fractions on multiple activities in a cultured cardiomyocyte assay. *Phytomedicine*. 2006;13(9-10):643-650.
12. Shahat AA, Ismail SI, Hammouda FM, et al. Anti-HIV activity of flavonoids and proanthocyanidins from *Crataegus sinaica*. *Phytomedicine*. 1998;5(2):133-136.
13. Dehghani S, Mehri S, Hosseinzadeh H. The effects of *Crataegus pinnatifida* (Chinese hawthorn) on metabolic syndrome: a review. *Iran J Basic Med Sci*. 2019;22(5):460-468.
14. Maldonado CJ, Albores MEM, San ME, Quiroz-Reyes CN, González-Córdova GE, Casañas-Pimentel RG. Mexican hawthorn (*Crataegus gracilior* J. B. Phipps) stems and leaves induce cell death on breast cancer cells. *Nutr Cancer*. 2020;72(8):1411-1421.
15. Guo YP, Yang H, Wang YL, et al. Determination of flavonoids compounds of three species and different harvesting periods in *Crataegi folium* based on LC-MS/MS. *Molecules*. 2021;26(6):1602-1618.
16. Zhou M, Zheng W, Sun X, et al. Comparative analysis of chemical components in different parts of Epimedium herb. *J Pharm Biomed Anal*. 2021;198:113984.
17. Lin P, Wang Q, Liu Y, et al. Characterization of chemical profile and quantification of representative components of DanLou tablet, a traditional Chinese medicine prescription, by UHPLC-Q/TOF-MS combined with UHPLC-TQ-MS. *J Pharm Biomed Anal*. 2020;180:113070.
18. Pan J, Zheng W, Pang X, et al. Comprehensive investigation on ginsenosides in different parts of a garden-cultivated ginseng root and rhizome. *Molecules*. 2021;26(6):1696-1718.
19. Zhang Z, Tang Y, Yu B, et al. Chemical composition database establishment and metabolite profiling analysis of Yangyin Qingfei decoction. *Biomed Chromatogr*. 2019;33(9):e4581.
20. Xie M, Yu Y, Zhu Z, Deng L, Ren B, Zhang M. Simultaneous determination of six main components in Bushen Huoxue prescription by HPLC-CAD. *J Pharm Biomed Anal*. 2021;201:114087.
21. Schilling K, Holzgrabe U. Recent applications of the charged aerosol detector for liquid chromatography in drug quality control. *J Chromatogr A*. 1619;2020:460911.
22. Lísa M, Lynen F, Holcapek M, Sandra P. Quantitation of triacylglycerols from plant oils using charged aerosol detection with gradient compensation. *J Chromatogr A*. 2007;1176(1-2):135-142.
23. Górecki T, Lynen F, Szucs R, Sandra P. Universal response in liquid chromatography using charged aerosol detection. *Anal Chem*. 2006;78(9):3186-3192.
24. Zheng W, Zhou M, Wang SY, et al. Comparative analysis of chemical constituents in hawthorn leaves from different sources. *Acta Pharm Sin*. 2021;56(12):3526-3539.
25. Haidar AI, Blasko A, Tam J, et al. Revealing the inner workings of the power function algorithm in charged aerosol detection: a simple and effective approach to optimizing power function value for quantitative analysis. *J Chromatogr A*. 1603;2019:1-7.

SUPPORTING INFORMATION

Additional supporting information can be found online in the Supporting Information section at the end of this article.

Research article

Phytochemical Analysis

Received: 18 December 2014, Revised: 27 April 2015, Accepted: 29 April 2015 Published online in Wiley Online Library: 5 June 2015

(wileyonlinelibrary.com) DOI 10.1002/pca.2572

Quantitative and qualitative investigations of pharmacopoeial plant material polygoni avicularis herba by UHPLC-CAD and UHPLC-ESI-MS methods

Sebastian Granica*

ABSTRACT:

Introduction – *Polygonum aviculare* L. also known as common knotgrass is an annual herbaceous weed occurring all over the world in the temperate regions. Recent studies report that flavonol glucuronides are major constituents of common knotgrass. There is no comprehensive analytical procedure for the standardisation of Polygoni Avicularis Herba available on the European market.

Objective – To develop a method for the proper authentication and standardisation of Polygoni Avicularis Herba and to preliminary evaluate variability in qualitative and quantitative composition among commercial samples and samples from wild harvesting defined as *Polygonum aviculare sensu lato*.

Methodology – The UHPLC-ESI(+)-MS method was used for the qualitative screening of nine independent samples of *Polygonum aviculare* herb. The UHPLC-CAD method was developed for the quantitation of the major compounds in an extract using quercetin-3-*O*-glucuronide as a standard.

Results – Twenty-five major constituents were detected and characterised. Among them three new natural products were tentatively identified. Twelve compounds were quantitated using a validated UHPLC-CAD method. In all nine samples flavonol glucuronides were confirmed as major compounds. The total flavonoid content was estimated for all samples and varied from 0.70 to 2.20%.

Conclusion – The developed procedure may be used for the routine standardisation of common knotgrass. The results indicate that the pharmacopoeial approach to the authentication and standardisation of *Polygonum aviculare* herb should be revised.

Keywords: Flavonoids; UHPLC-CAD/ESI-MS; *Polygonum aviculare*; charged aerosol detector; standardisation

Introduction

Polygonum aviculare L., also known as common knotgrass, birdweed, pigweed or lowgrass, is an annual herbaceous weed occurring all over the world in the temperate climate zones. The plant has a semi-erect stem with hairless and short-stalked leaves (Strzelecka and Kowalski, 2000; van Wyk and Wink, 2004). The aerial parts of *P. aviculare* have been traditionally used in folk medicine, thus the monograph for this plant drug was introduced into the European Pharmacopoeia (2013). The plant material is used in the form of an infusion in the treatment of renal diseases, urinary bladder inflammations, as well as an expectorant and secretolitic agent for coughs and bronchial catarrh. The infusion may also be used externally for the treatment of skin affections and oral cavity inflammations (Hansel *et al.,* 1994; Wichtl, 2004). However, proper scientific validation of the bioactivity of *P. aviculare* extracts is still required.

The monograph of common knotgrass defines the pharmacopoeial drug as "whole or fragmented, dried flowering aerial parts of *P. aviculare sensu lato*" (European Pharmacopoeia, 2013). The current botanical approach describes *Polygonum aviculare sensu lato* as a group of at least seven separate taxa in the rank of subspecies or species (Rutkowski, 2014; The Plant List, 2014). All taxa are valid as pharmacopoeial plant materials according to the common knotgrass monograph. However, the data on phytochemical diversity among the specified taxa are lacking. The pharmacopoeial chemical authentication of *P. aviculare* is based on thin layer chromatography (TLC) using chlorogenic and caffeic acids and hyperoside as standards. A positive verification is achieved when the presence of spots corresponding to chlorogenic and caffeic acids is confirmed together with eliminating the presence of hyperoside. The monograph also mentions the presence of other flavonoids in the prepared extract but their identification remains unresolved. The standardisation of *P. aviculare* herb is based on the quantitation of total flavonoid content using hyperoside as a standard and should be not less than 0.3%. This method gives no information on the content of individual constituents occurring in this plant material.

Most available textbooks and scientific papers report that *Polygonum aviculare* herb contains mucilage, tannins, silicic acid deriva-

* Correspondence to: Sebastian Granica, Department of Pharmacognosy and Molecular Basis of Phytotherapy, Faculty of Pharmacy, Medical University of Warsaw, ul. Banacha 1, 02-097 Warsaw, Poland.
Email: sgranica@wum.edu.pl; sgranica@gmail.com

Department of Pharmacognosy and Molecular Basis of Phytotherapy, Faculty of Pharmacy, Medical University of Warsaw, Poland

tives and flavonoids as dominating compounds. Among the flavonoids, quercetin, kaempferol and myricetin glycosides are mentioned with avicularin as major flavonoid constituents occurring in aerial parts (Hansel *et al.,* 1994; Smolarz, 2002; Wichtl, 2004; Nikolaeva *et al.,* 2009; Nugroho *et al.,* 2014). Recent studies confirmed that common knotgrass contains flavonoids as major compounds and that the presence of most had not previously been reported (Granica *et al.,* 2013c). Further research led to the isolation of 11 flavonol glucuronides among which three new and one rare natural products were characterised (Granica *et al.,* 2013b).

Table 1. The list of plant material samples used in the present study

Sample symbol	Origin	Batch/voucher number
A	commercial/Flos, Mokrsko, Poland	1023/02.2014
B	wild harvesting/Warsaw, near Banacha St.	20140725_PA
C	commercial/Ervanario de Augusto Coutinho, Porto, Portugal	71336/09.2016
D	commercial/Kawon, Krajewice, Poland	620.2014/07.2015
E	wild harvesting/mazowieckie, near Ojrzanów	20140720_A
F	wild harvesting/experimental field, Warsaw University of Life Sciences – SGGW	20140822_B
G	wild harvestng/Warsaw, Bielany, near Vistula river	20140911_D
H	wild harvesting/warmińsko-mazurskie, near Koty	20140922_A
I	commercial/Kotlas, Wien, Austria	W13204172/03.2016

In the recent literature there is one paper reporting the quantitation of flavonoid glycosides in *Polygonum aviculare* using an HPLC-UV method. The authors used one sample of common knotgrass from wild harvesting in Korea. The study led to the isolation and quantitation of major constituents, namely nine flavonols including quercetin, myricetin, kaempferol and their glycosides (Nugroho *et al.,* 2014). However, no flavonol glucuronides, found in European samples of *P. aviculare* (Granica *et al.,* 2013b, 2013c), were detected.

The corona charged aerosol detector (CAD) is reported as a universal response device suitable for the HPLC systems (Górecki *et al.,* 2006). Previous studies have showed that CAD may be successfully used for the quantitation of plant polyphenols (Granica *et al.,* 2013a, 2014, 2015). It has been also demonstrated that in the case of flavonoid monoglycosides the response of the corona device may be assumed as universal no matter what the molecular weight or chemical structure of the analysed compound (Granica *et al.,* 2013a).

Compared to the evaporative light scattering detector (ELSD), another type of universal response device, CAD is less commonly used in analytical laboratories. However, it has been shown that CAD has several advantages over ELSD. The CAD has a better

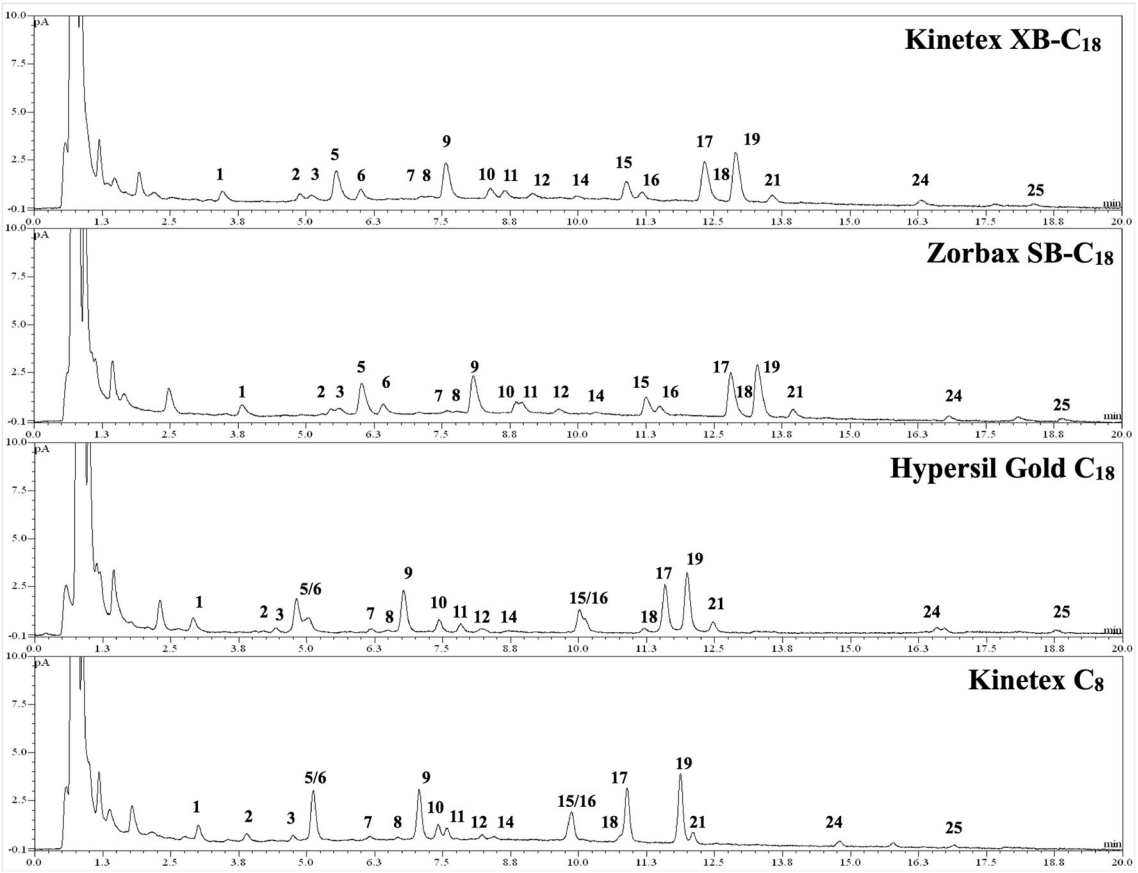

Figure 1. UHPLC-CAD chromatograms of sample F obtained using different UHPLC columns.

linearity over a wide range of concentrations of standard used in the calibration process than ELSD. It also has better sensitivity and reproducibility. Furthermore, the CAD response is less affected by physical properties of analysed compounds (Eom *et al.,* 2010; Thomas *et al.,* 2014). In addition, a major advantage in routine analyses is that CAD is easy to operate since the only parameter that needs to be adjusted is the output range and the data filtration mode (Eom *et al.,* 2010).

Diode array detectors (DADs) or more simple UV-vis detectors are the most popular devices used together with HPLC in the analysis of natural products. These can offer good selectivity, sensitivity and linearity (Wolfender, 2009). However, UV-vis absorbance detectors require analytes with suitable chromophores and thus the response can depend upon the structure. Therefore, confident quantitation requires an authenticated standard for each compound, in contrast to CAD which is a universal response device.

The aim of this present study was to develop ultra-high performance liquid chromatography electrospray ionization mass spectrometry (UHPLC-ESI-MS) and UHPLC-CAD methods for the standardisation of Polygoni Avicularis Herba available on the European market. As the current European pharmacopoeia

Table 2. The MS^2 data of compounds detected in *Polygonum aviculare* herb

	Compound name	Retention time (min)	$[M+H]^+$ *m/z*	MS^2 ions	MS^3 ions	NL detected (amu)
1	myricetin-3-*O*-glucuronide[a]	3.45	495	477, 343, **319b**, 301	301, 291, 283, 273b, 263, 245, 229, 165, 153, 109	176
2	unknown compound	4.87	333	283, 273, 207, 151, 123b	—	—
3	quercetin-3-*O*-galactoside[a]	5.05	465	447, 330, **303b**	275, 257b, 183, 165, 109	162
4	quercetin-3-*O*-glucoside[a]	5.42	465	447, 330, **303b**	285, 257b, 229, 165	162
5	quercetin-3-*O*-glucuronide[a]	5.53	477	345, **303b**, 257	285, 257b, 247, 229, 165, 153, 109	176
6	mearsetin-3-*O*-glucuronide[a]	5.98	503	491, 429, 411, **333b**, 318	318b, 301, 277, 259, 179	176
7	quercetin-3-*O*-arabofuranoside[a]	7.13	435	417, **303b**, 273, 267, 155	285b, 257, 247, 195	132
8	kaempferol-3-*O*-glucoside[a]	7.28	449	**287b**	197, 165b	162
9	kaempferol-3-*O*-glucuronide[a]	7.56	463	**287b**	197, 165b	176
10	isorhamnetin-3-*O*-glucuronide[a]	8.39	493	**317b**	302b, 285	176
11	myricetin-X″-*O*-acetyl-3-*O*-glucuronide	8.64	537	**319b**, 219, 201	283, 273b, 207, 165, 153	218
12	kaempferol-*O*-pentoside	9.14	419	**287b**	257b, 231	132
13	kaempferol-*O*-rhamnoside	9.61	433	**287b**	257b, 231	146
14	quercetin-3″-*O*-acetyl-3-*O*-glucuronide[a]	9.97	521	**303b**	257b, 165	218
15	quercetin-2″-*O*-acetyl-3-*O*-glucuronide[a]	10.86	521	**303b**	285, 257b, 165	218
16	mearsetin-X″-*O*-acetyl-3-O-glucuronide	11.15	551	**333b**, 219, 201	318b, 301, 273	218
17	kaempferide-3-*O*-glucuronide[a]	12.30	477	**301b**, 159	286, 258, 241, 165, 139b	176
18	kaempferol-3″-*O*-acetyl-3-*O*-glucuronide[a]	12.40	505	440, 369, **287b**	257b	218
19	kaempferol-2″-*O*-acetyl-3-*O*-glucuronide[a]	12.89	505	428, **287b**, 219, 201	257b, 231	218
20	unknown compound	13.28	795	763b, 672, 640, 601, 461, 449, 399	—	—
21	isorhamnetin-2″-*O*-acetyl-3-*O*-glucuronide[a]	13.55	535	401, **317b**, 219	302b, 261, 201, 153	218
22	quercetin derivative	14.10	515	497, **303b**, 285, 177, 145	257b, 195	—
23	unknown compound	15.22	807	775b, 684, 645, 613, 490, 461	—	—
24	unknown compound	16.30	351	333b, 281, 253, 195	—	—
25	kaempferide-X″-*O*-acetyl-3-*O*-glucuronide	18.37	519	**301b**, 219, 159	286, 272, 258, 241, 165, 139b	218

Note: b, base peak (the most abundant ion in recorded spectrum); values in bold, ions subjected to MS^3 fragmentation.
[a]Comparisons with chemical standard have been made.

monograph does not indicate which specific taxa within *Polygonum aviculare s. l.* should be used as medicinal plant material, the additional task was to evaluate variability in qualitative and quantitative composition among commercial samples and samples from wild harvesting defined as *P. aviculare s. l.*

Experimental

Reagents and materials

Chromatographic grade acetonitrile (MeCN) was purchased from Merck (Darmstadt, Germany). Water was purified with the Millipore Simplicity System (Bedford, MA, USA). Formic acid (HCOOH), trifluoroacetic acid (TFA) and methanol were purchased from POCh (Gliwice, Poland). Chemical standards of flavonoids used in this study were either isolated in the Department of Pharmacognosy and Molecular Basis of Phytotherapy (Warsaw, Poland) or purchased from Carl Roth (Karlsruhe, Germany), all of them were of > 95% HPLC purity.

Plant material

Aerial parts of *Polygonum aviculare* L. were either from wild harvesting in different regions of Poland in the period of blooming and dried in the shade at room temperature or purchased as commercial drug material from different manufacturers in Poland, Austria and Portugal. The plant material from wild harvesting was authenticated based on morphological characters as *P. aviculare s. l.* according to Rutkowski (2014) by Sebastian Granica. Samples bought as commercial drugs available on the European market were authenticated according to the monograph found in European Pharmacopoeia (2013). Voucher specimens of each plant material are available in the drug collection of the Department of Pharmacognosy and Molecular Basis of Phytotherapy, Medical University of Warsaw (Poland) (Table 1).

Table 3. Parameters calculated for linearity, limit of detection (LOD) and limit of quantitation (LOQ)

Linear range (ng per injection)	50–700
Linear regression $y = ax + b$	$y = 0.001824x + 0.0.0054$
Correlation coefficient for liner fit (r)	0.9991
F-Test value for linear fit[a]	2272.30
LOD (ng per injection)[b]	6.63
LOQ (ng per injection)[b]	50.00

[a]Critical F-value for $\alpha = 0.99$ and $n = 6$ is 21.20.
[b]Calculated for linear fit.

Isolation and purification of quercetin-3-*O*-glucuronide

Quercetin-3-*O*-glucuronide, used for quantitation, was isolated previously from *Polygonum aviculare* (Granica *et al.,* 2013b). In order to obtain chemical standard of high purity, the fraction obtained from water residue (Granica *et al.,* 2013b) by chromatography on Diaion HP-20 W and Toyopearl HW-40 F (50 mg) was subjected to preparative HPLC using Shimadzu LC-10 system equipped with two pumps, autosampler, column oven, UV detector and fraction collector. Using a Zorbax SB-C_{18} column (150 × 22.1 mm × 5 μm) (Agilent Technologies, Palo Alto, CA, USA) the components were eluted using (A) 0.1% HCOOH in H_2O; (B) 0.1% HCOOH in MeCN; 0–60 min, 5–26% B; flow 9.999 mL/min; and column temperature 25 °C. The fraction containing quercetin-3-*O*-glucuronide was collected between 37.2–39.2 min to yield 36 mg of the standard compound. The purity (>99%) and identity was confirmed by NMR and chromatographic methods (Granica *et al.,* 2013b). ^{1}H NMR (300 MHz, CD_3OD) δ 7.65–7.60 (m, 2H, H-2′ and H-6′), 6.83 (d, J = 9.2 Hz, 1H, H-5), 6.39 (d, J = 2.0 Hz, 1H, H-8), 6.20 (d, J = 2.0 Hz, 1H, H-6), 5.35 (d, J = 7.4 Hz, 1H, H-1″), 3.76 (d, J = 9.6 Hz, 1H, H-5″), 3.65 – 3.40 (m, 3H, H2″, H3″ and H4″).

Sample preparation

An accurately weighed aliquot (ca. 250 mg) of dried, powdered and sieved (sieve diameter 1 mm) aerial parts of plant material was placed in a conical tube with water:methanol mixture (10 mL, 7:3, v/v). Each sample was sonicated for 15 min at 40 °C. A sample was centrifuged at 3000 rpm for 10 min and the supernatant was carefully transferred to a 25 mL volumetric flask. The extraction procedure was repeated two more times with 10 mL and 5 mL of solvent in order to extract plant material exhaustively. The extraction using more steps did not result in higher yields. Finally, combined extracts were diluted up to 25 mL with water:methanol (7:3, v/v and filtrated through a 0.45 μm Chromafil polyester membrane (Macherey-Nagel, Duren, Germany). For better UHPLC separation 0.1% TFA (100 μL) was added to an aliquot of the extract (900 μL). The solution was stored in darkness at 5 °C until injection to the UHPLC system (no longer than 48 h).

Preparation of standard solutions

Accurately weighed quercetin-3-*O*-glucuronide was dissolved in dimethyl sulfoxide (DMSO) to obtain stock solution 1 mg/mL. Serial dilution of the standard stock solution with water:methanol (7:3, v/v) yielded the calibration standards at 10, 20, 40, 80, 120 and 140 μg/mL. After preparation each solution was stored in darkness at 5 °C for maximum 72 h. Then, 5 μL of each solution was injected into the UHPLC system (i.e. injecting 50–700 ng of standard).

Table 4. Validation parameters – accuracy, repeatability precision and recovery for quercetin-3-*O*-glucuronide

			Intermediate precision		Accuracy	
	Amount of standard injected to the column	Repeatability	Inter-day	Intra-day	Recovery	
	ng	%CV	%CV	%CV	Mean (%)	%CV
quercetin-3-*O*-glucuronide	50	4.17	4.76	5.49	103.12 ± 4.13	4.00
	100	0.11	3.52	4.24	—	—
	200	1.22	3.17	3.70	100.01 ± 3.28	3.28
	400	1.06	2.39	2.69	—	—
	600	3.02	2.84	3.12	95.60 ± 1.55	1.62
	700	2.48	2.62	2.74	—	—

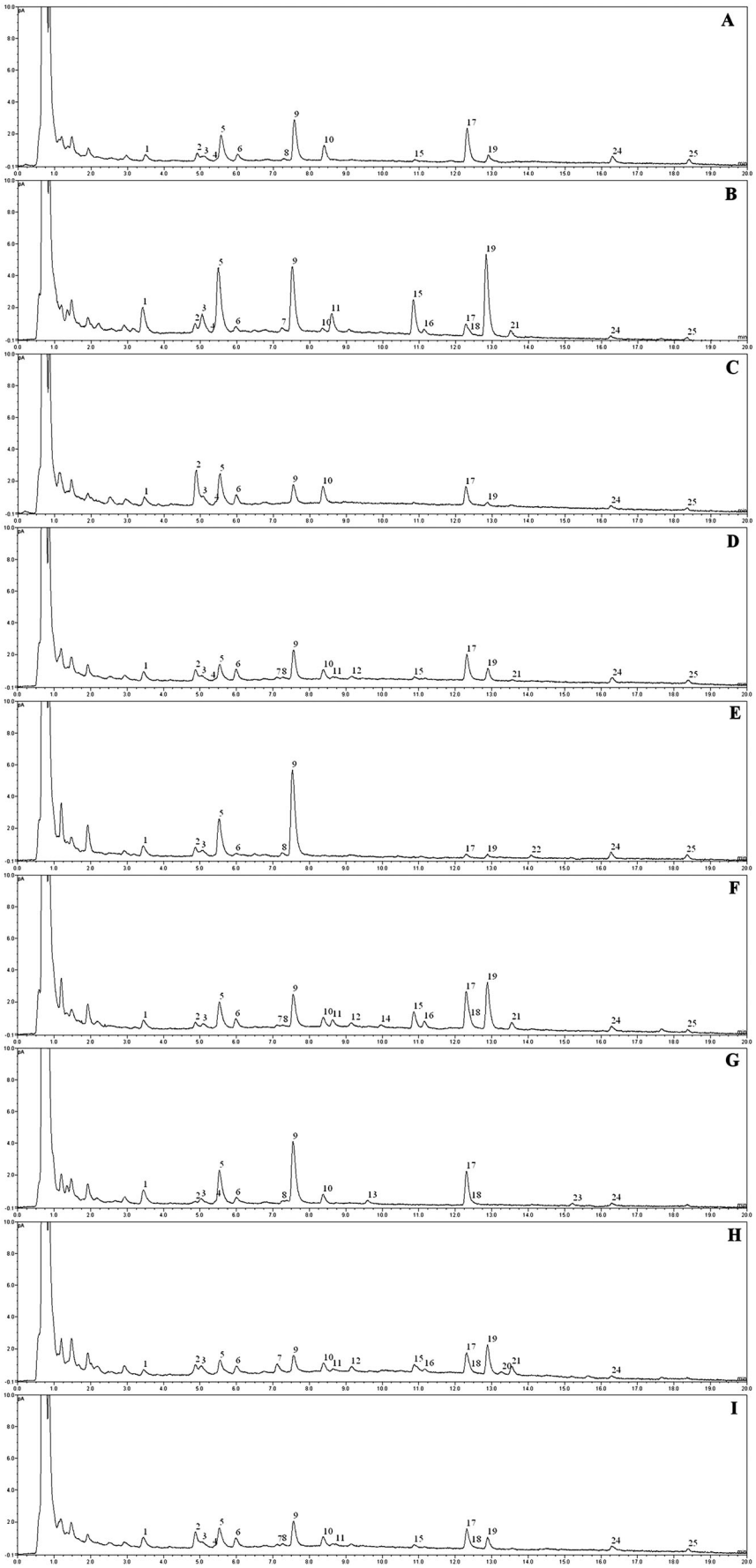

Figure 2. The UHPLC-CAD chromatograms of nine independent samples of *Polygonum aviculare* used in the present study.

Table 5. The quantitation results for compounds detected in *Polygonum aviculare* herb using UHPLC-CAD method

Sample	A				B				C				D				E			
Compound	Content (mg/g)			%CV	Content (mg/g)			%CV	Content (mg/g)			%CV	Content (mg/g)			%CV	Content (mg/g)			%CV
1	<LOQ	±	—	—	1.78	±	0.05	2.88	0.60	±	0.03	4.29	0.61	±	0.03	4.72	0.66	±	0.04	6.44
2	2.23	±	0.02	0.79	0.62	±	0.03	4.62	1.22	±	0.05	3.75	1.53	±	0.06	4.13	<LOQ	±	—	—
3	<LOQ	±	—	—	1.36	±	0.04	3.15	0.69	±	0.03	4.93	<LOQ	±	—	—	0.50	±	0.02	3.76
4	<LOQ	±	—	—	<LOQ	±	—	—	<LOQ	±	—	—	<LOQ	±	—	—	n.d.	±	—	—
5	1.94	±	0.10	5.20	4.93	±	0.17	3.49	2.33	±	0.08	3.44	1.15	±	0.04	3.08	2.75	±	0.11	3.94
6	<LOQ	±	—	—	<LOQ	±	—	—	0.60	±	0.03	4.53	0.61	±	0.03	4.47	<LOQ	±	—	—
7	n.d.	±	—	—	n.d.	±	—	—	n.d.	±	—	—	n.d.	±	—	—	<LOQ	±	—	—
8	<LOQ	±	—	—	<LOQ	±	—	—	n.d.	±	—	—	<LOQ	±	—	—	<LOQ	±	—	—
9	2.85	±	0.04	1.56	4.57	±	0.18	3.83	1.27	±	0.04	3.40	1.87	±	0.04	2.26	6.54	±	0.26	4.02
10	0.90	±	0.04	4.94	<LOQ	±	—	—	1.05	±	0.03	3.27	0.55	±	0.02	3.88	n.d.	±	—	—
11	n.d.	±	—	—	1.12	±	0.04	3.39	n.d.	±	—	—	<LOQ	±	—	—	n.d.	±	—	—
12	n.d.	±	—	—	n.d.	±	—	—	n.d.	±	—	—	<LOQ	±	—	—	n.d.	±	—	—
13	n.d.	±	—	—	n.d.	±	—	—	n.d.	±	—	—	n.d.	±	—	—	n.d.	±	—	—
14	n.d.	±	—	—	n.d.	±	—	—	n.d.	±	—	—	n.d.	±	—	—	n.d.	±	—	—
15	<LOQ	±	—	—	2.15	±	0.07	3.19	n.d.	±	—	—	<LOQ	±	—	—	n.d.	±	—	—
16	n.d.	±	—	—	<LOQ	±	—	—	n.d.	±	—	—	<LOQ	±	—	—	<LOQ	±	—	—
17	2.23	±	0.02	0.79	0.63	±	0.02	3.70	1.22	±	0.05	3.75	1.54	±	0.06	4.13	<LOQ	±	—	—
18	n.d.	±	—	—	<LOQ	±	—	—	n.d.	±	—	—	n.d.	±	—	—	n.d.	±	—	—
19	<LOQ	±	—	—	5.41	±	0.21	3.96	<LOQ	±	—	—	0.65	±	0.02	3.15	<LOQ	±	—	—
20	n.d.	±	—	—	n.d.	±	—	—	n.d.	±	—	—	n.d.	±	—	—	n.d.	±	—	—
21	n.d.	±	—	—	<LOQ	±	—	—	<LOQ	±	—	—	n.d.	±	—	—	n.d.	±	—	—
22	n.d.	±	—	—	n.d.	±	—	—	n.d.	±	—	—	n.d.	±	—	—	<LOQ	±	—	—
23	n.d.	±	—	—	n.d.	±	—	—	n.d.	±	—	—	n.d.	±	—	—	n.d.	±	—	—
24	<LOQ	±	—	—	<LOQ	±	—	—	<LOQ	±	—	—	<LOQ	±	—	—	<LOQ	±	—	—
25	<LOQ	±	—	—	<LOQ	±	—	—	<LOQ	±	—	—	<LOQ	±	—	—	<LOQ	±	—	—

Sample	F				G				H				I			
Compound	Content (mg/g)			%CV	Content (mg/g)			%CV	Content (mg/g)			%CV	Content (mg/g)			%CV
1	0.60	±	0.02	3.63	1.08	±	0.03	2.39	<LOQ	±	—	—	0.69	±	0.03	4.45
2	2.78	±	0.06	2.11	2.48	±	0.07	2.80	1.50	±	0.06	3.69	1.33	±	0.07	5.05
3	<LOQ	±	—	—	<LOQ	±	—	—	0.89	±	0.02	2.01	<LOQ	±	—	—
4	n.d.	±	—	—	<LOQ	±	—	—	n.d.	±	—	—	<LOQ	±	—	—
5	1.99	±	0.06	2.81	2.62	±	0.10	3.78	1.23	±	0.03	2.77	1.47	±	0.03	1.93
6	0.59	±	0.02	3.17	<LOQ	±	—	—	0.61	±	0.03	5.53	0.65	±	0.02	3.24
7	n.d.	±	—	—	n.d.	±	—	—	n.d.	±	—	—	n.d.	±	—	—
8	<LOQ	±	—	—	<LOQ	±	—	—	n.d.	±	—	—	<LOQ	±	—	—
9	2.39	±	0.07	2.94	5.32	±	0.14	2.72	1.30	±	0.06	4.42	1.70	±	0.07	3.99
10	0.58	±	0.03	4.37	0.59	±	0.02	2.73	0.53	±	0.03	5.35	0.57	±	0.02	3.66
11	<LOQ	±	—	—	n.d.	±	—	—	<LOQ	±	—	—	<LOQ	±	—	—
12	<LOQ	±	—	—	n.d.	±	—	—	<LOQ	±	—	—	n.d.	±	—	—

(Continues)

Table 5. (Continued)

Sample	F			G			H			I		
Compound	Content (mg/g)		%CV	Content (mg/g)		%CV	Content (mg/g)		%CV	Content (mg/g)		%CV
13	n.d.	±	—	<LOQ	±	—	n.d.	±	—	n.d.	±	—
14	<LOQ	±	—	n.d.	±	—	n.d.	±	—	n.d.	±	—
15	1.13	±	0.04	n.d.	±	—	0.64	±	0.01	1.73	<LOQ	±	—	—
16	<LOQ	±	—	n.d.	±	—	<LOQ	±	—	—	n.d.	±	—	—
17	2.78	±	0.06	2.11	2.38	±	0.10	4.26	1.50	±	0.06	3.69	1.33	±	0.07	5.05
18	<LOQ	±	—	—	<LOQ	±	—	—	<LOQ	±	—	—	<LOQ	±	—	—
19	3.22	±	0.06	1.90	n.d.	±	—	—	1.97	±	0.10	5.00	0.66	±	0.02	3.58
20	n.d.	±	—	—	n.d.	±	—	—	<LOQ	±	—	—	n.d.	±	—	—
21	<LOQ	±	—	—	n.d.	±	—	—	0.50	±	0.01	2.98	n.d.	±	—	—
22	n.d.	±	—	—	n.d.	±	—	—	n.d.	±	—	—	n.d.	±	—	—
23	n.d.	±	—	—	<LOQ	±	—	—	n.d.	±	—	—	n.d.	±	—	—
24	<LOQ	±	—	—	<LOQ	±	—	—	<LOQ	±	—	—	<LOQ	±	—	—
25	<LOQ	±	—	—	n.d.	±	—	—	n.d.	±	—	—	<LOQ	±	—	—
TFC (%)	1.33				1.20				0.92				0.71			

Note: n.d., not detected in analysed extract; TCF, total flavonoid content.

UHPLC analysis

The UHPLC-CAD and UHPLC-ESI-MS analysis were performed using an UHPLC-3000 RS system (Dionex, Idtstein, Germany) coupled with an Corona RS detector (Thermo Scientific, Waltham, MA, USA) or an AmaZon SL ion trap mass spectrometer with an ESI interface (Bruker Daltonik GmbH, Bremen, Germany). The quantitation of flavonoids in prepared material was carried out using a reversed-phase Kinetex XB-C_{18} analytical column (100 mm × 2.1 mm × 1.7 μm) (Phenomenex, Torrance, CA, USA) maintained at 25 °C. The mobile phase (A) was water:trifluoroacetic acid (99.9:0.1, v/v) and the mobile phase (B) was MeCN:trifluoroacetic acid (99.9:0.1, v/v). A two step gradient system was used: 0–20 min 15-35% B, 20–23 min 95% B. The flow rate was 0.4 mL/min. The column was equilibrated for 7 min between injections. The eluate was introduced directly to the CAD or into the ESI interface of mass detector. The CAD filter was set at medium, the range was set to 100 pA full scale. The CAD was supplied with compressed air with flow adjusted to 35 psi. The nebuliser pressure of the ESI interface of the mass detector was 50 psi; drying gas flow 10 L/min; drying temperature 300 °C and capillary voltage 4.5 kV. The MS spectra were recorded in positive ion mode. Furthermore, 10 or 7 μL of extract and 5 μL of standard were injected into the UHPLC column. The mass detector was used for selectivity studies and identification of quantitated compounds in all extracts. Quantitative assays and validation parameters refer to CAD data recorded by Corona RS detector.

Method validation

The selectivity was assessed by monitoring MS spectra for quantitated compounds in order to confirm or exclude the co-elution of other compounds in chosen conditions. The calibration curve was established at six concentration levels 50–700 ng per injection (10–140 μg/mL). The linearity of calibration curve was tested by *F*-test ($\alpha = 0.01$). The precision and the repeatability of the method were determined based on the calibration curve by calculating the coefficient of variation (%CV) at all six levels covering the whole calibration range. The accuracy was examined as recovery studies at three concentration levels, i.e. 50 ng per injection (low), 200 ng per injection (medium) and 600 ng per injection (high). Sample E was chosen for the recovery study. Limit of detection (LOD) was calculated as signal-to-noise ratio of 3:1 based on experimental data, according to the ICH guidelines (ICH, 2005). Limit of quantitation (LOQ) is given as the lowest level of the established calibration curve.

Results and discussion

UHPLC separation: selection of column and mobile phase modifier

In order to obtain the best separation of analytes four different UHPLC columns, namely Zorbax SB-C_{18} (100 mm × 2.1 mm × 1.9 μm, Agilent Technologies), Kinetex XB-C_{18} (100 mm × 2.1 mm × 1.7 μm, Phenomenex), Kinetex C_8 (100 mm × 2.1 mm × 1.7 μm, Phenomenex) and Hypersil Gold C_{18} (100 mm × 2.1 mm × 1.7 μm, Phenomenex) were tested. Sample F was chosen for the separation optimisation as it contained the largest number of compounds. The best UHPLC separation was achieved using Kintex XB-C_{18} column (Fig. 1). Formic acid used at the concentration of 0.1% added to both mobile phases was chosen at first but it turned out that better results were obtained with 0.1% TFA, which is also suitable for CAD detection if used at low concentrations.

Qualitative analysis of Polygoni Avicularis Herba

The qualitative UHPLC-ESI-MS survey of nine samples of *Polygonum aviculare* aerial parts revealed the presence of 25 major constituents (numbered from **1** to **25**). Most compounds were

identified or tentatively identified based on a comparison of their MS/MS (MS^2) profiles (Table 2) with available chemical standards and literature reports (Table 2) (Tsimogiannis *et al.,* 2007; Granica *et al.,* 2013b, 2013c).

MS^2 fragmentation of compounds **3–5**, **7**, **14**, **15** and **22** resulted in the production of an aglycone ion at *m/z* 303 Da, which was subjected to MS^3 fragmentation leading to the ion pattern characteristic for quercetin (Tsimogiannis *et al.,* 2007). The monitoring of neutral loss in MS^2 spectra revealed that compounds **3** and **4** are quercetin hexosides, compound **5** is quercetin glucuronide, compound **7** displayed neutral loss characteristic for pentoside and compounds **14** and **15** have acetyluronic acid moieties. Based on comparison of retention times with authentic samples compounds were identified as hyperoside (**3**), isoquercitrin (**4**), quercetin-3-*O*-glucuronide (**5**), quercetin-3-*O*-arabofuranoside (avicularin, **7**) and two isomeric quercetin-3″ or 2″-*O*-acetyl-3-*O*-glucuronides (**14** and **15**). Compound **22** was partially identified as a quercetin derivative but the data were insufficient to allow assigning of any particular structure.

Compounds **8**, **9**, **12**, **13**, **18** and **19** were identified as kaempferol glycosides showing an aglycone ion in their fragmentation spectra at *m/z* 287 Da (Tsimogiannis *et al.,* 2007). Based on detection of characteristic neutral loss in MS spectra of each constituent and by comparison with proper chemical standards they were identified as kaempferol-3-*O*-glucoside (astragalin, **8**), kaempferol-3-*O*-glucuronide (**9**), kaempferol-3-*O*-rhamnoside (**13**) and two isomeric kaempferol-3″ or 2″-*O*-acetyl-3-*O*-glucuronides (**18** and **19**). Due to the lack of a proper standard compound **12** was described as a kaempferol-*O*-pentoside most probably an arabinoside or xyloside.

Compounds **10** and **21** displayed in their MS^2 spectra an aglycone ion at *m/z* 317 Da which, when subjected to MS^3, showed the fragmentation pattern characteristic for isorhamnetin (Granica *et al.,* 2013c). By comparison with authentic standards they were identified as isorhamnetin-3-*O*-glucuronide (**10**) and isorhamnetin-2″-*O*-acetyl-3-*O*-glucuronide (**21**).

Compounds **1** and **11** were assigned as myricetin derivatives based on MS^2 and MS^3 fragmentation patterns (Granica *et al.,* 2013c). The fragmentation pattern of both compounds revealed the neutral loss of 176 Da for compound **1** and 218 Da for compound **11**. Compound **1** was identified as myricetin-3-*O*-glucuronide by comparison with an authentic standard. Compound **11** was tentatively assigned as myricetin-*O*-acetyl-3-*O*-glucuronide based on MS spectra and taking into account the chemical structures of other compounds present in the analysed plant material.

Compounds **6** and **16** were assigned as mearsetin (3′-methoxymyricetin) derivatives (Granica *et al.,* 2013c). The fragmentation of both compounds resulted in the production of an aglycone moiety ion at *m/z* 333 Da. The monitoring of neutral loss showed that compound **6** has an uronic acid in its structure and compound **16** has acetyluronic acid as a sugar moiety. By comparison of retention time with a standard compound **6** was unequivocally identified as mearsetin-3-*O*-glucuronide. Compound **16** based on its fragmentation pattern was described as mearsetin-*O*-acetyl-3-*O*-glucuronide.

Compounds **17** and **25** showed in their MS^2 spectra the ion at *m/z* 301 Da which, when subjected to MS^3 fragmentation, revealed the ion pattern characteristic for kaempferide (Granica *et al.,* 2013c). Thus both constituents were assigned as kaempferide glycosides. In the case of compound **17** the MS^2 led to the neutral loss of 176 Da corresponding to the cleavage of uronic acid moiety and identified as kaempferide-3-*O*-glucuronide by comparison with a standard. Compound **25** showed during MS^2 fragmentation the cleavage of an acetyluronic acid moiety. Compared to other compounds identified compound **25** was tentatively identified as kaempferide-*O*-acetyl-3-*O*-glucuronide.

Mass spectra recorded for compounds **2**, **20**, **23** and **24** showed protonated molecules $[M+H]^+$ at *m/z* 333, 795, 807 and 351 Da, respectively. MS^2 fragmentation data were insufficient to assign any particular chemical structure for detected compounds, thus in the present study they are described as unknown.

Most of the compounds were identified as flavonoids belonging to the group of *O*-glycosylated flavonols. The presence of compounds **2**, **16**, **20**, **22–25** was confirmed for the first time in the *Polygonum aviculare*. Compounds **11**, **16** and **25** were tentatively identified based on their MS^2 spectra, and taking into account the previous reports on the phytochemical composition of *P. aviculare*, have not been previously described. Therefore, the suggested structures need verification by the isolation of the compounds and unequivocal elucidation using NMR spectroscopy.

Despite the TLC method of standardisation recommended by the European Pharmacopeia relying on the detection of chlorogenic and caffeic acid, the present and previous HPLC studies (Granica *et al.,* 2013c) have not shown meaningful amounts of these compounds in *Polygonum aviculare*. Indeed, in the present study, these compounds were not observed using the TLC method (data not shown) and were only observed in trace amounts using extracted ion chromatograms displaying *m/z* 335 or 181 for the protonated molecules of chlorogenic acid and caffeic acid, respectively. Most previously reported results on HPLC analysis of flavonoid glycosides and their aglycones occurring in *P. aviculare* are significantly different from those described in the present study (Smolarz, 2002; Waksmundzka-Hajnos *et al.,* 2008; Nugroho *et al.,* 2014). These mismatches may be explained as the analyses were performed with simpler HPLC instruments and the identification of compounds was mainly based on their retention times that might sometimes lead to incorrect identification of analytes. The other issue is that at least several reports existing in the literature describe the occurrence of flavone glycosides (mainly apigenin and luteolin derivaties) in the herb of *P. aviculare* (Kawasaki *et al.,* 1986; Sun *et al.,* 2002; Nikolaeva *et al.,* 2009). The presence of those compounds was confirmed neither in the previous study (Granica *et al.,* 2013c) nor in the present paper. This could be explained by the fact that previously detected/isolated compounds may occur as minor constituents which are not detectable in raw extract or that their production depends strongly on ecological conditions.

Method validation

The CAD response is known to be non-linear (Blazewicz *et al.,* 2010; Crafts *et al.,* 2011), in particular over a wide concentration range, but as shown in previous studies the linear fit might be successfully used if the quantitation range of amount of compound injected to the UHPLC column is narrow enough (Crafts *et al.,* 2011; Granica *et al.,* 2014, 2015). Validation parameters are shown in Tables 3 and 4.

Quantitation of compounds in Polygoni Avicularis Herba samples

Twelve major constituents were quantitated in nine samples of raw material obtained from commercial sources or from wild harvesting

(Fig. 2, Table 5). Compounds **1–3**, **5**, **9** and **17** were major constituents and could be quantitated in almost all nine analysed samples (the content varied from 0.50 to 4.57 mg/g). In the case of samples B, D, F, H and I significant amounts of compound **19** (identified as kaempferol-2″-*O*-acetyl-3-*O*-glucuronide) were detected, i.e. 0.65 to 5.41 mg/g. In order to check if analysed samples fulfilled the requirements of the pharmacopoeial monograph with respect to total flavonoid content (TFC), the sum of all quantitated compounds was calculated as TFC expressed as percentage of dry raw plant material (Table 5). The TFC varied from 0.70 to 2.20% and showed that it may be assumed that all study samples would fulfil the requirement if analysed by the method given in the pharmacopoeia. On this basis all samples could be considered as valid medicinal plant material but as none of them passed the pharmacopoeial TLC authentication they are not valid according to the monograph for Polygoni Avicularis Herba. Flavononol glucuronides were shown to be major constituents in all of the samples in contrast to existing reports suggesting that avicularin and other simple flavonoid glycosides (glucosides, galactosides, rhamnosides etc.) occur in *Polygonum aviculare* in high quantities (Nugroho *et al.,* 2014). It must be noted that meaningful amounts of compound **3** were detected and quantitated but the identity of this constituent remains unknown. A qualitative and quantitative variability of chemical composition was also observed. The diversity in the composition within examined samples and divergence from results of other studies may be at least partially explained by ecological conditions or by the fact that samples come from plants belonging to different taxa within *P. aviculare s. l.* In order to confirm this thesis further studies using fully identified samples coming from regions and different ecological habitats should be planned and conducted.

The present research showed that none of the analysed samples would pass the TLC authentication required by European Pharmacopoeia although all samples were confirmed as *Polygonum aviculare* based on botanical and phytochemical profiles. This may be explained by the fact that chlorogenic acid and caffeic acid are not good phytochemical markers for Polygoni Avicularis Herba. Both compounds could be detected in some of analysed samples in trace amounts, which seem to be not enough for the less sensitive method such as TLC. Thus it is suggested that at least a part of the current monograph should be revised accordingly. The presented problem could be solved by the introduction of a simple HPLC method to the monograph basing the detection on one of the major compounds occurring in *P. aviculare* such as quercetin-3-*O*-glucuronide or kaempferol-3-*O*-glucuronide. The new HPLC method could also be used for the standardisation of this plant material instead of quantification of total flavonoid content.

Acknowledgements

This project was carried out with the use of CePT infrastructure financed by the European Regional Development Fund within the Operational Programme "Innovative economy" for 2007–2013. The project was financially supported by the Polish Ministry of Science through Iuventus Plus project nr 9006/IP1/2014/72. The author would like to thank the Foundation for Polish Science for the scholarship for young scientists "START" received in 2014. The author would also like to thank Barbara Żyżyńska-Granica PhD for proof reading the manuscript.

References

Blazewicz A, Fijalek Z, Warowna-Grzeskiewicz M, Jadach M. 2010. Determination of atracurium, cisatracurium and mivacurium with their impurities in pharmaceutical preparations by liquid chromatography with charged aerosol detection. *J Chromatogr A* **1217**: 1266–1272.

Crafts C, Bailey B, Plante M, Acworth I. 2011. http://www.dionex.com/en-us/webdocs/110512-PO-HPLC-ValidateAnalyticalMethods-CAD-31Oct2011-LPN2949-01.pdf [5 January 2015].

Eom HY, Park SY, Kim MK, Suh JH, Yeom H, Min JW, Kim U, Lee J, Youm JR, Han SB. 2010. Comparison between evaporative light scattering detection and charged aerosol detection for the analysis of saikosaponins. *J Chromatogr A* **1217**: 4347–4354.

European Pharmacopoeia. 2013. https://www.edqm.eu/en/european-pharmacopoeia-8th-edition-1563.html [20 April 2015].

Górecki T, Lynen F, Szucs R, Sandra P. 2006. Universal response in liquid chromatography using charged aerosol detection. *Anal Chem* **78**: 3186–3192.

Granica S, Krupa K, Klebowska A, Kiss AK. 2013a. Development and validation of HPLC-DAD-CAD-MS^3 method for qualitative and quantitative standardization of polyphenols in *Agrimoniae eupatoriae herba* (Ph. Eur). *J Pharmaceut Biomed* **86**: 112–122.

Granica S, Czerwinska ME, Zyzynska-Granica B, Kiss AK. 2013b. Antioxidant and anti-inflammatory flavonol glucuronides from *Polygonum aviculare* L. *Fitoterapia* **91**: 180–188.

Granica S, Piwowarski JP, Poplawska M, Jakubowska M, Borzym J, Kiss AK. 2013c. Novel insight into qualitative standardization of *Polygoni avicularis herba* (Ph. Eur.). *J Pharmaceut Biomed* **72**: 216–222.

Granica S, Piwowarski JP, Kiss AK. 2014. Determination of *C*-glucosidic ellagitannins in *Lythri salicariae herba* by ultra-high performance liquid chromatography coupled with charged aerosol detector: method development and validation. *Phytochem Anal* **25**: 201–206.

Granica S, Lohwasser U, Jöhrer K, Zidorn C. 2015. Qualitative and quantitative analyses of secondary metabolites in aerial and subaerial of *Scorzonera hispanica* L. (black salsify). *Food Chem* **173**: 321–331.

Hansel R, Keller K, Rimpler H, Greiner S, Schneider G. 1994. *Drogen*. Springer-Verlag: Berlin.

ICH. 2005. http://www.ich.org/fileadmin/Public_Web_Site/ICH_Products/Guidelines/Quality/Q2_R1/Step4/Q2_R1__Guideline.pdf [5 January 2015].

Kawasaki M, Kanomata T, Yoshitama K. 1986. Flavonoids in the leaves of twenty-eight polygonaceous plants. *Bot Mag Tokyo* **99**: 63–74.

Nikolaeva GG, Lavrent'eva MV, Nikolaeva IG. 2009. Phenolic compounds from several *Polygonum* species. *Chem Nat Compnd* **45**: 735–736.

Nugroho A, Kim EJ, Choi JS, Park HJ. 2014. Simultaneous quantification and peroxynitrite-scavenging activities of flavonoids in *Polygonum aviculare* L. herb. *J Pharmaceut Biomed* **89**: 93–98.

Rutkowski L. 2014. *Klucz do oznaczania roślin naczyniowych Polski niżowej*. Wydawnictwo Naukowe PWN: Warszawa; 108–109.

Smolarz HD. 2002. Flavonoid glycosides in nine *Polygonum* L. taxons. *Acta Soc Bot Pol* **71**: 29–33.

Strzelecka H, Kowalski J. 2000. *Encyklopedia zielarstwa i ziołolecznictwa*. Wydawnictwo Naukowe PWN: Warszawa.

Sun LP, Zheng SZ, Wang JX, Shen XW, Zheng XD. 2002. The flavonoids from *Polygonum aviculare*. *Indian J Chem B* **41**: 1319–1320.

The Plant List. 2014. http://www.theplantlist.org/ [15 December 2014].

Thomas D, Bailey B, Plante M, Acworth I. 2014. http://www.thermoscientific.com/content/dam/tfs/ATG/CMD/cmd-documents/sci-res/posters/ms/events/AOAC-2014/PN-70990-AOAC2014-Charged-Aerosol-Detection-PN70990-EN.pdf [5 March 2015].

Tsimogiannis D, Samiotaki M, Panayotou G, Oreopoulou V. 2007. Characterization of flavonoid subgroups and hydroxy substitution by HPLC-MS/MS. *Molecules* **12**: 593–606.

van Wyk BE, Wink M. 2004. *Rośliny lecznicze świata*. MedPharm Polska: Warszawa.

Waksmundzka-Hajnos M, Wianowska D, Oniszczuk A, Dawidowicz AL. 2008. Effect of sample-preparation methods on the quantification of selected flavonoids in plant materials by high performance liquid chromatography. *Acta Chromatogr* **20**: 475–488.

Wichtl M. 2004. *Herbal drugs and phytopharmaceuticals. Brickmann JA, Lidenmaier MP, translator*. Medpharm Scientific Publishers: Wurzburg.

Wolfender JL. 2009. HPLC in natural product analysis: The detection issue. *Planta Med* **75**: 719–734.

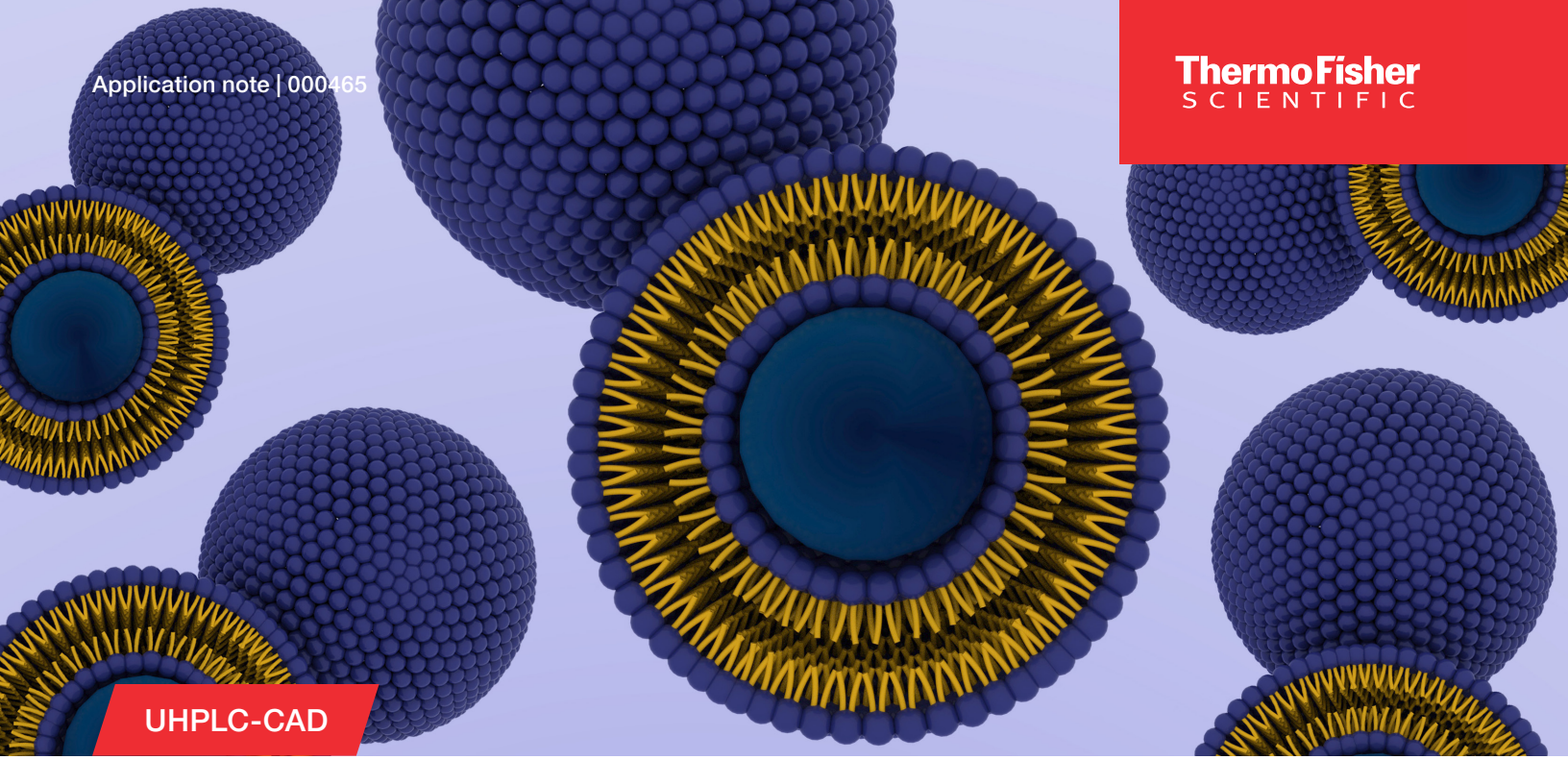

UHPLC-CAD

Characterization of lipid nanoparticle (LNP) composition using UHPLC-CAD

Authors

Sissi White[1], Ken Cook[2], Mark Netsch[3], Genia Verovskaya[4], Jason Potter[4], Min Du[5]

[1]Thermo Fisher Scientific, Franklin, MA, US; [2]Thermo Fisher Scientific, Hemel Hempstead, GB; [3]Thermo Fisher Scientific, Chelmsford, MA, US; [4]Thermo Fisher Scientific, Carlsbad, CA, US; [5]Thermo Fisher Scientific, Cambridge, MA, US

Keywords

Lipid nanoparticle (LNP), lipid analysis, charged aerosol detector (CAD), phospholipid, cationic lipids, Accucore C30 column

Application benefits

- Simple UHPLC method for characterization of the lipid components of LNPs
- Universal response shows relative amounts of each lipid compound in the formulation
- Low limits of detection even for cholesterol
- Wide linear range for all lipid compounds
- Baseline separation of components

Goal

Development of a simple UHPLC method for the characterization of the lipid content of LNP formulations. Implementation of the universal CAD detector to quantify large non-chromophoric lipids present in the LNP structure.

Introduction

Lipid nanoparticles (LNPs) have proven to be a preferred drug delivery system with the successful roll out of the mRNA vaccines during the COVID-19 pandemic. LNP-based therapies include antisense oligonucleotides (ASOs), siRNA therapies, and mRNA vaccines, all of which are growing in popularity. There are over 20 LNP-based therapeutics on the market with a rapidly growing number in development. At least four different lipid types are used in the LNP formulations, the exact composition of which is usually kept as proprietary information. Common constituents are as follows: cholesterol,

which keeps fluidity in the lipid bilayer; phospholipids, which are also normal constituents of cell membranes; PEGylated lipids, which generate a hydrophilic nature to the outer surface of the LNP; and an ionizable lipid, which is usually cationic and interacts with the negatively charged phosphate backbone of the encapsulated nucleic acid to aid stability. These cationic lipids are crucial components and are usually under patent protection. The composition of the LNP is an important aspect for function and so must be characterized in the formulation. As such, the identification, ratio, and purity of the lipids in the formulation are regarded as critical quality attributes for safety and efficacy. Lipids have no chromophore, so UV detection is not possible during the QC analysis of LNP.

Here we describe a UHPLC-based chromatography method for the lipid component analysis, utilizing the universal detection capabilities of the charged aerosol detector (CAD). This detection mechanism is applicable for virtually any non- or semi-volatile compound. The signal response is uniform for nonvolatile compounds, which makes this detection system ideal for compositional analysis, and the sensitivity is superior to alternative lipid detection systems such as refractive index or evaporative light scattering detectors (ELSD). The column used is a Thermo Scientific™ Accucore™ C30 column, which provides higher shape selectivity for long chain hydrophobic compounds such as lipids. The Thermo Scientific™ Vanquish™ Flex UHPLC system is totally biocompatible and has a metal-free flow path, which will not interact with the metal-chelating phosphate groups present on some of the lipids in the formulation. This ensures the sensitivity and recovery required for robust analysis.

Experimental

Chemicals	Part number
Lipid H, Cayman Chemical	33474
mPEG-DTA-2K, SINOPEG	1849616-42-7
DHA, SINOPEG	2036272-55-4
Cholesterol, Sigma-Aldrich	C1231
DOPE, Avanti polar lipids	850725P
PEG 5000, Avanti polar lipids	880210P
DSPC, Sigma-Aldrich	816944
Trifluoroacetic acid (TFA), Optima™ LC/MS grade, Fisher Chemical™	A11650
Formic acid (FA), Optima™ LC/MS grade, Fisher Chemical™	A11710X1AMP
Ethyl alcohol (EtOH), 200 proof, 99.5+%, Thermo Scientific™	61519-0010
Water, Optima™ LC/MS grade, Fisher Chemical™	W64
Isopropanol (IPA), Optima™ LC/MS grade, Fisher Chemical™	A461-4
Acetonitrile (ACN), Optima™ LC/MS grade, Fisher Chemical™	A955-4
Methanol, Optima™ LC/MS grade, Fisher Chemical™	A456-4
Autosampler inert vials and inserts, Thermo Scientific™ Chromacol™ GOLD-grade	13-622-351

Instrumentation	Part number
Vanquish Flex Binary system consisting of:	
Vanquish System Base	VH-S01-A
Vanquish Binary Pump F	VF-P10-A-01
Vanquish Sampler F	VF-A10-A
Vanquish Column Compartment H	VH-C10-A-02
Vanquish Charged Aerosol Detector H	VH-D20-A

Sample preparation

- It is recommended to use glass pipets to transfer lipids/LNPs in organic solvents.
- It is recommended to use glass inserts, vials, and bottles to store lipids and LNP samples.
- All lipids/LNPs were dissolved in 100% ethanol.
- Two different formulations are tested.

FA method

Column	Accucore C30, 3.0 × 100 mm, 2.6 µm, P/N 27826-103030		
Mobile phase A	0.1% FA in 50% ACN, 50% water		
Mobile phase B	0.1% FA in 60% IPA, 30% ACN, 10% water		
Gradient	Time (min)	A	B
	0.0	25	75
	1.0	25	75
	9.0	0	100
	10.0	0	100
	10.1	25	75
	12	25	75
Flow rate	0.9 mL/min		
Autosampler temperature	15 °C		
Column temperature	50 °C		
Post column cooler	40 °C		
Injection volume	1 µL		
Injection wash solvent	Mobile phase B		
CAD settings			
Power function	1.0		
Evaporator temperature	35 °C		
Gas resolution mode	Analytical		
Data rate	2 Hz		
Filter	3.6		

TFA method

Mobile phase A	0.1% TFA in 50% ACN, 50% water		
Mobile phase B	0.1% TFA in 70% IPA, 25% ACN, 5% water		
Gradient	Time (min)	A	B
	0.0	35	65
	1.0	35	65
	12.0	0	100
	13.0	0	100
	13.1	35	65
	16	35	65

Other conditions are the same as the FA method.

Chromatography Data System

The Thermo Scientific™ Chromeleon™ Chromatography Data System (CDS) software 7.2.10 ES was used for data acquisition and analysis.

Results and discussion

The individual lipid components of the LNP are quite different in their composition. They all still need to be separated in the chromatography.

A cationic lipid is required to interact with the phosphate backbone of the oligonucleotide to be encapsulated. An example of the structure of 4-hydroxybutyl)azanediyl)bis(hexane-6,1-diyl) bis(2-hexyldecanoate (DHA), which is used in LNP formulations.

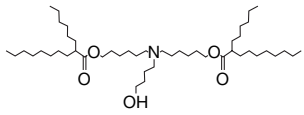

A phospholipid, such as 1,2-distearoyl-sn-glycero-3-phosphocholine (DSPC), is a naturally occurring phosphatidylcholine found in cell membranes.

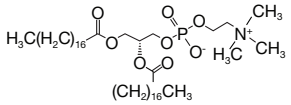

Cholesterol is also naturally occurring and found in cell membranes to add fluidity.

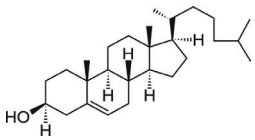

A synthetic PEGylated lipid is used to give the LNP surface hydrophilicity and low immunogenicity. Methoxypoly(ethylene glycol) ditetradecylacetamide (mPEG-DTA-2K) has been used in LNP formulations.

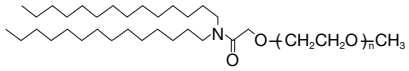

Long chain lipids are well separated on columns with a C30 functional group. The long hydrocarbon C30 chain lines up better with longer lipids to give good shape selectivity and impurity detection of these lipids. The Accucore columns are packed with solid core silica particles that give high separation power without high backpressures; this is important when using the more viscous eluents such as IPA. The Accucore columns have also been found to give extremely good recoveries for hydrophobic lipids. For these reasons, the Accucore C30 column was selected for this work.

The CAD detector gives close to a universal response for each lipid type in this formulation. This attribute makes the CAD ideal for compositional analysis of lipid formulations. The sensitivity is also greater than found with ELSD or refractive index detectors.[1] This is an attribute which aids in the detection of any low-level impurities in the formulation, which could come from any of the lipid components used in the LNP. Figure 1 shows the separation and compositional analysis of selected LNP lipids from formulation #1 injected at the same concentration. Baseline separation and detection of each lipid is obtained within 10 minutes.

All limits of detection were found to be around 10 µg/mL, which was targeted as the lower end of the calibration range. This is especially true for cholesterol (2.6 µg/mL), which is known to yield a diminished response with ELSD. The CAD, in contrast, gives a similar response for each lipid class. The detection is almost linear from 10 to 220 µg/mL. For CAD, it is possible to use either PFV optimization or nonlinear fits. Here a nonlinear fit (quadratic fit) was used in detection up to 220 µg/mL. The calibration curves are shown in Figure 2. The carryover from each injection was negligible using this workflow (not shown).

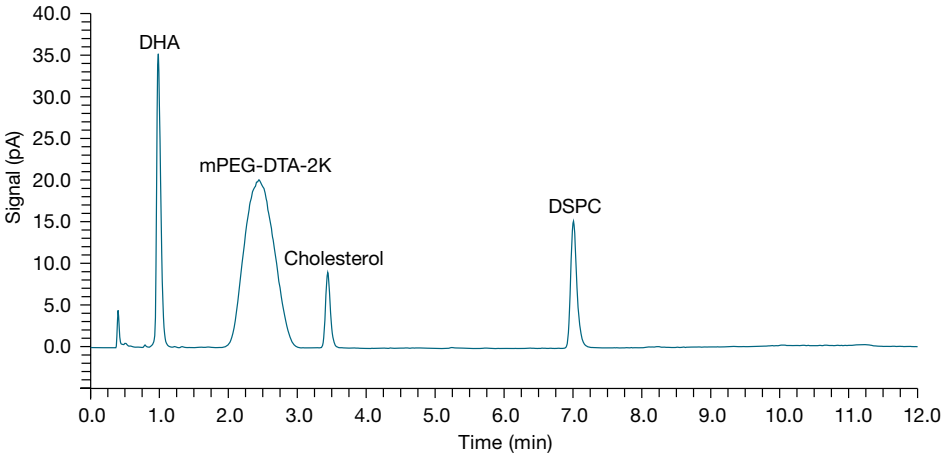

Figure 1. Separation of LNP formulation #1 using the FA method

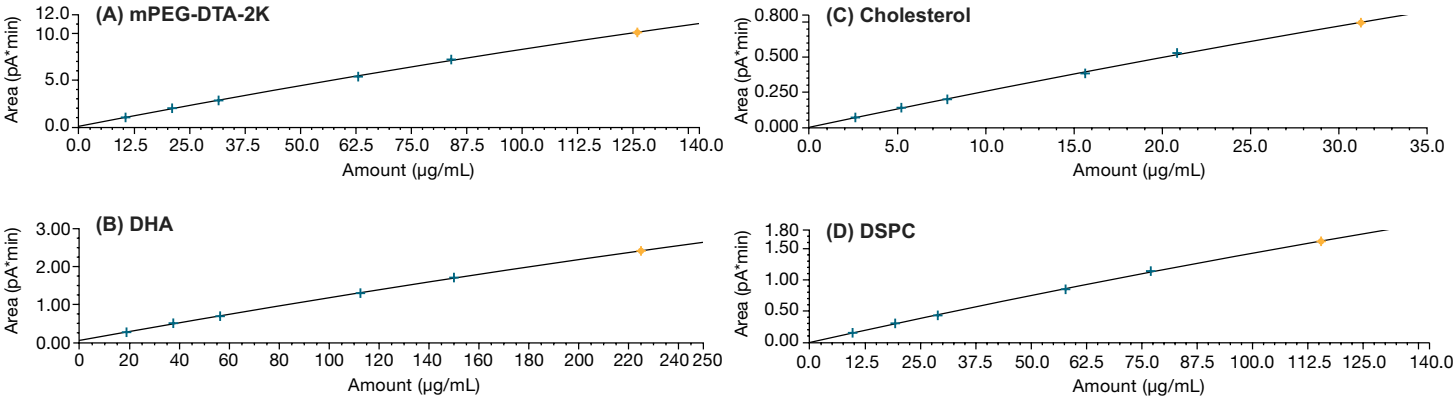

Figure 2. Calibration curves for the individual lipid components

All lipid components are separated well with good quadratic calibration curves for accurate quantitation. The calibration curves for all lipids show a calibration coefficient of 0.999 (Table 1).

In the overlay of all calibration standards, all peaks show good resolution and reproducibility using FA (Figure 3).

Figure 4 shows the separation of LNP formulation #1 using TFA. The elution order of mPEG-DTA-2K and DHA has changed. The sensitivity of the CAD allows small impurities to be observed in the baseline around the main peaks. Again, baseline separation can be achieved in 10 minutes.

Table 1. Calibration results

Peak no.	Peak name	Ret. time (min)	Cal. type	Eval. type	Number of points	Rel. std. dev. %	Coeff. of determination	C0 (offset)	C1 (slope)	C2 (curve)
1	DHA	0.983	Quad, WithOffset	Area	6	1.3619	0.99978	0.0501	0.0119	0.0000
2	mPEG-DTA-2K	2.442	Quad, WithOffset	Area	6	1.8382	0.99962	0.0634	0.0918	-0.0001
3	Cholestrol	3.442	Quad, WithOffset	Area	6	2.9175	0.9991	-0.0004	0.0266	-0.0001
4	DSPC	7.008	Quad, WithOffset	Area	6	1.7888	0.99966	-0.0038	0.0158	0.0000
Maximum						2.9175	0.99978			
Minimum						1.3619	0.9991			

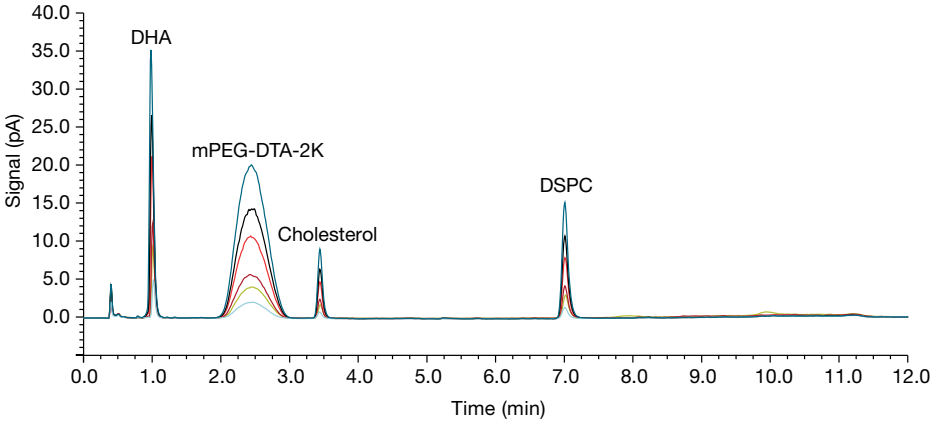

Figure 3. Overlaid chromatograms of calibration standards using the FA method

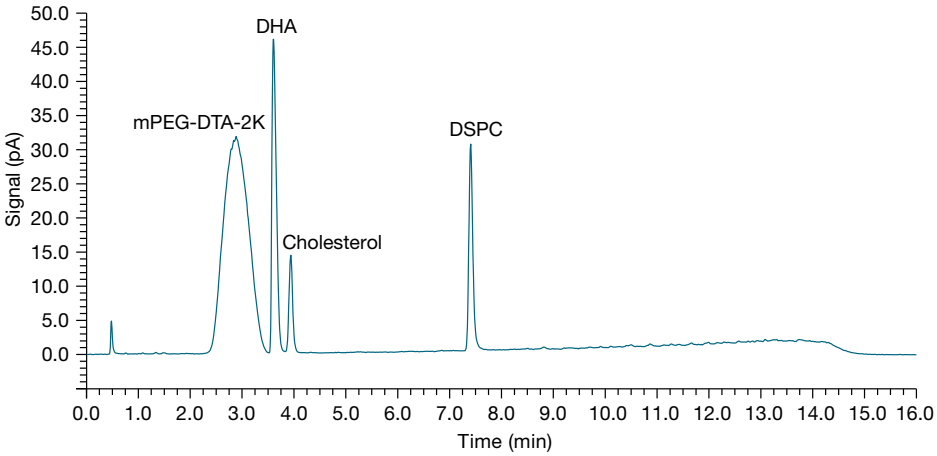

Figure 4. Separation of LNP formulation #1 using the TFA method

In comparing TFA and FA methods using the lowest concentration standard from the calibration plot, the TFA method showed higher sensitivity than the FA method but the FA method showed better separation (Figure 5).

The separation of LNP formulation #2 containing four different lipids using the TFA method is shown in Figure 6. Some impurities are present before and after the PEG 5000 peak. Baseline separation and detection of each lipid is obtained within 5 minutes. The FA separation with LNP formulation #2 did not provide the required resolution (not shown).

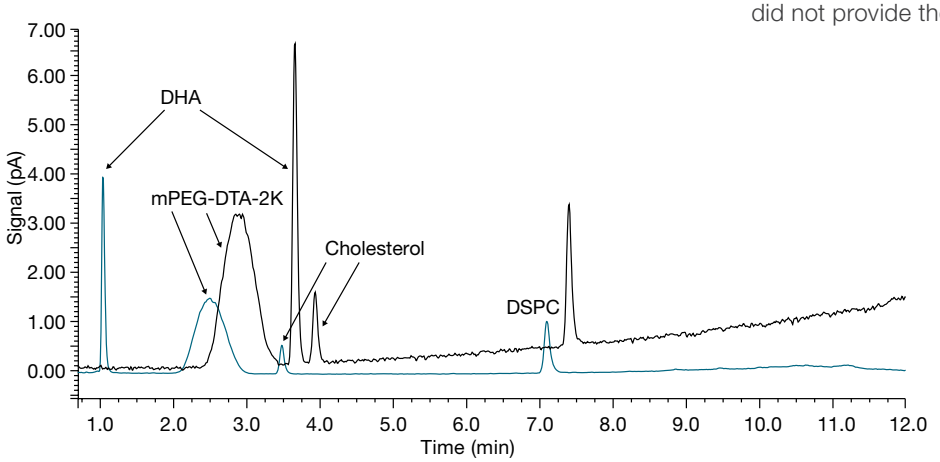

Figure 5. Comparison of separation of LNP formulation #1 using the TFA and FA methods.
Black Trace: TFA method; Blue Trace: FA method.

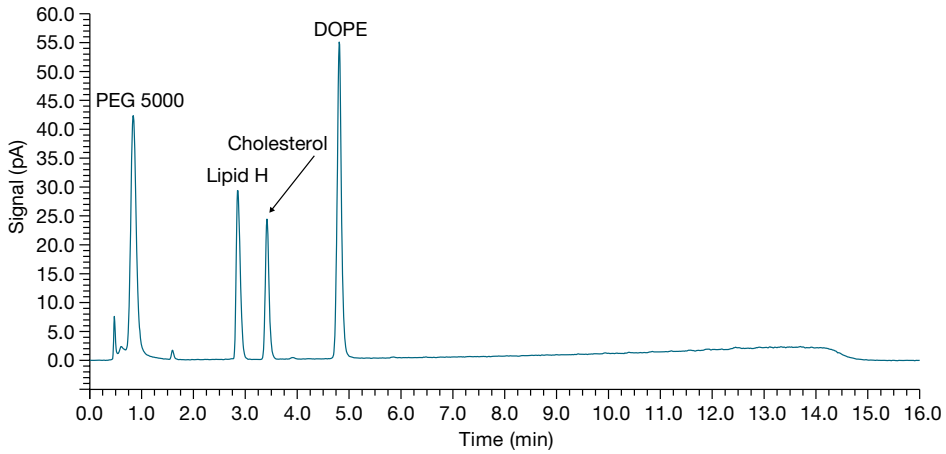

Figure 6. Separation of LNP formulation #2 using the TFA method. PEG5000: 1,2-dimyristoyl-sn-glycero-3-phosphoethanolamine-N-[methoxy(polyethylene glycol)-5000] (ammonium salt).
Lipid H: 8-[(2-hydroxyethyl)[6-oxo-6-(undecyloxy)hexyl]amino]-octanoic acid, 1-octylnonyl ester.
Cholesterol: Plant-derived. DOPE: 1,2-dioleoyl-sn-glycero-3-phosphoethanolamine.

Conclusion

- Two fast, robust methods for the characterization of the lipid components in the lipid nanoparticles used in oligonucleotide therapeutics have been described. Formulation #1 has better separation using the FA method, whereas formulation #2 has better separation using the TFA method.
- Separation of several components from each LNP class was achieved on the Accucore C30 column in 10 minutes.
- The CAD has low limits of detection for all the components, including cholesterol. The high sensitivity of the CAD allows any trace impurities to be monitored.
- The calibration curves for all lipids show a calibration coefficient of better than 0.999.

References

1. Kinsey, C.; Lu, T.; Deiss, A.; Vuolo, K.; Klein, L.; Rustandi, R.R.; Loughney, J.W. Determination of lipid content and stability in lipid nanoparticles using ultra high-performance liquid chromatography in combination with a Corona Charged Aerosol Detector, *Electrophoresis* **2021**, 1–24. https://doi.org/10.1002/elps.202100244
2. Tracy, M.; Hillbeck, D. Thermo Scientific Application Note 20663 – Comparative analysis of cooking oils using a solid core HPLC column. https://assets.thermofisher.com/TFS-Assets/CMD/Application-Notes/AN20663-Comparative-Cooking-Oils-HPLC-EN.pdf
3. Criscuolo, A.; Zeller, M.; Cook, K.; Angelidou, G.; Fedorova, M. Rational selection of reverse phase columns for high throughput LC–MS. *Chemistry and Physics of Lipids* **2019**, *221*, 120-127.

HPLC & UHPLC

List of compendial methods

Thermo Scientific Charged Aerosol Detectors

Charged aerosol detection is a reliable technology that will change the way you view every sample. The Charged Aerosol Detector (CAD) can detect all non-volatile, and many semi-volatile analytes, with uniform response. Charged aerosol detection can be used for the analysis of pharmaceuticals (large and small molecule), biomolecules, foods and beverages, specialty chemicals, and polymers.

In the following tables are examples of standardized methods—for example, American Society for Testing and Materials (ASTM International), Chinese Pharmacopeia (CP), European Pharmacopeia (EP), International Organization for Standardization (ISO), and United States Pharmacopeia (USP)—using charged aerosol detection technology.

General chapter information on Charged Aerosol Detectors

Chinese Pharmacopoeia

"*The latest HPLC developments and application progress are fully detailed. Information about multidimensional HPLC, charged aerosol detection, adjusted chromatographic conditions, and common qualitative analysis methods was added.*" 2020 edition.

European Pharmacopoeia

"Ultraviolet/visible (UV/Vis) spectrophotometers (including diode array detectors) (2.2.25), are the most commonly employed detectors. Fluorescence spectrophotometers, differential refractometers (RI), electrochemical detectors (ECD), light scattering detectors, charged aerosol detectors (CAD), mass spectrometers (MS) (2.2.43), radioactivity detectors, multi-angle light scattering (MALS) detectors or other detectors may be used."

thermo scientific

Specific monographs using Charged Aerosol Detector

Organ-ization	Analytes	Method Reference	Matrix	Column	Mobile Phase	Gradient or Isocratic	Status Additional Information
ASTM	**Lipids**	ASTM E3297-21 Standard Test Method for Lipid Quantitation in Liposomal Formulations	Liposomal Formulation	RP C18	Aqueous acetonitrile/ methanol	Gradient	Active **Additional info:** AppsLab Library
EP	**API and counterions**	Validation and application of an HPLC-CAD-TOF/ MS method for identification and quantification of pharmaceutical counterions. Pharmeuropa bio & scientific notes 2014, 81-91	None	Mixed mode Thermo Scientific™ Acclaim™ Trinity P1, 3.0 × 50 mm, 3 µm (P/N 071388)	A) 0.2 M ammonium formate in water (pH 4.0) B) water C) acetonitrile	Gradient	Published for consideration **Additional info:** AppsLab Library Mixed-mode HPLC columns
EP	**Aspartic acid**	Aspartic acid Pharmeuropa 22.4, October 2010	None	RP C18, 4.6 × 150 mm, 5 µm	4% 0.36 g/L perfluoroheptanoic acid (PFHPA) in methanol 96% 0.36 g/L (PFHPA) in water (%/% v/v)	Isocratic	In process/under consideration **Additional info:** AppsLab Library
EP	**Gadobutrol monohydrate**	Gadobutrol Monohydrate–Ph. Eur. 9.0 07/2016:1215	None	RP end-capped phenylhexylsilyl silica gel, 4.6 × 250 mm, 3 µm	A) 0.5% acetonitrile and 99.5% water pH 3.6 adjusted with formic acid B) acetonitrile	Gradient	In official text
EP	**Ibandronate sodium monohydrate**	Ibandronate Pharmeuropa 22.4, October 2010	None	RP octadecylsilyl silica gel with embedded strong anion exchange groups, 4.6 × 150 mm, 2.7 µm	A) water B) 150 mL acetonitrile plus 150 mL of 11.4 g/L trifluoroacetic acid, filled to 1 L with water	Gradient	In process/under consideration
EP	**Topiramate**	Topiramate Pharmeuropa 27.4, October 2015	None	RP solid core pentafluorophenylsilyl silica gel, 4.6 × 100 mm, 2.6 µm	A) 1.93 g/L ammonium acetate, pH 3.5 B) acetonitrile	Gradient	Adopted for next version
EP	**Valine and impurities**	Determination of the purity of valine by isocratic liquid chromatography coupled with charged aerosol detection Pharmeuropa bio & scientific notes. 2015; 2015, 11-18	None	RP C18, 4.0 × 150 mm, 3 µm	20 mM Perfluorobutyric acid in acetonitrile/ water (10:90 v/v)	Isocratic	Published for consideration **Additional info:** AppsLab Library
EP	**Vigabatrin**	Vigabatrin Pharmeuropa 30.2, April 2018.	None	RP end-capped solid core phenylhexylsilyl silica gel, 4.6 × 100 mm, 2.7 µm	19.5% methanol, 80.5% water (v/v) with 2.1 g/L perfluoroheptanoic acid (PFHPA)	Isocratic	Adopted for next version

Organ-ization	Analytes	Method Reference	Matrix	Column	Mobile Phase	Gradient or Isocratic	Status Additional Information
ISO	PEG with molecular mass greater than 400 g/mol	ISO 16560:2015(en) Surface active agents—Determination of polyethylene glycol content in nonionic ethoxylated surfactants—HPLC method	Nonionic ethoxylated surfactants that are soluble in methanol or methanol/water/H_2O and have [PEG]>0.1%	Reversed phase (RP) C18, 4.6 × 250 mm, 5 µm	A) water B) methanol	Gradient	In official text **Additional info:** Surfactants Application Notebook
ISO	Triton X-100, octylphenol ethoxylates (CAS 9002-93-1) IGEPAL CO-630, nonylphenol ethoxylates (CAS 68412-54-4)	ISO 18254-2:2018 Method for the detection and determination of alkylphenol ethoxylates (APEO)—Part 2: Method using NPLC	Textiles	Normal phase (NP) applying two columns: 1) C18 column, 4.6 × 50 mm, 1.7 µm 2) hydrogen bond adsorption, 4.6 × 150 mm, 3 µm	A) acetonitrile with 0.1% formic acid B) methanol with 0.1% formic acid and 0.01% ammonium formate	Gradient	In official text **Additional info:** AppsLab Library
USP	Deoxycholic acid powder	Deoxycholic (desoxycholic) acid—since USP 40 NF 35 S1	None	Type L1, Thermo Scientific™ Acclaim™ 120 C18, 4.6 × 150 mm, 3 µm (P/N 059133)	A) 0.1% formic acid in water B) 0.1% formic acid in acetonitrile	Gradient	In official text **Additional info:** AppsLab Library Application Note Poster
USP	Metoprolol succinate powder	Content of metoprolol related compound H and metoprolol related compound I, USP 41(3) In-Process Revision: Metoprolol succinate. Proposed change to United States Pharmacopeia and National Formulary USP 38-NF33;	None	Hydrophilic interaction liquid chromatography (HILIC) solid core silica gel with five hydroxyl bonded ligands, 4.6 × 150 mm, 5 µm	85% acetonitrile 15% 0.1 M ammonium formate in water, pH 3.2	Isocratic	In process/under consideration **Additional info:** AppsLab Library Application Note Poster

For more references download the Charged Aerosol Detection bibliography highlighting the breadth and scope of different analytical methods found in the literature, click **here**.

Learn more at **thermofisher.com/CAD**

thermo scientific